Irradiation Effects on the Mechanical Properties of Zirconium and Dilute Zirconium Alloys: A Review

P. J. Pankaskie

July 15, 1976

BN-SA-618

Battelle
Pacific Northwest Laboratories

LEGAL NOTICE

This report was prepared by Battelle as an account of sponsored research activities. Neither Sponsor nor Battelle nor any person acting on behalf of either: (a) Makes any warranty or representation, express or implied, with respect to the accuracy, completeness, or usefulness of the information contained in this report, or that the use of any information, apparatus, process, or composition disclosed in this report may not infringe privately owned rights; or (b) Assumes any liabilities with respect to the use of, or for damages resulting from the use of, any information, apparatus, process, or composition disclosed in this report.

The information in this report has been compiled for publication by the American Society for Metals in the forthcoming Volume 1 of the ninth edition of the Metals Handbook.

BN-SA-618

IRRADIATION EFFECTS ON THE MECHANICAL PROPERTIES OF ZIRCONIUM AND DILUTE ZIRCONIUM ALLOYS: A REVIEW

P. J. Pankaskie

July 15, 1976

Battelle
Pacific Northwest Laboratories
Richland, Washington 99352

TABLE OF CONTENTS

LIST OF FIGURES

LIST OF TABLES

IRRADIATION EFFECTS ON MECHANICAL PROPERTIES

GENERAL

Of the radiation environments, wherein zirconium and dilute zirconium alloys may be used, only "fast" ($\sim 0.1 < E < \sim 15$ Mev) neutrons possess energies sufficient to significantly affect the microstructure and those mechanical properties which are structure sensitive. Other radiation sources such as gamma rays, ion bombardment, etc., are capable of altering the atomic structure (e.g., ionization) and/or microstructure but generally are incapable of any significant penetration of metallic materials and are therefore of little practical importance with regard to altering mechanical behavior. For these reasons, this review is limited to the effects of fast flux ($E \gtrsim 1$ Mev) neutron irradiation.

It has been "fairly well" established through electron microscopy and thermal activation studies[1-5] that fast flux neutron irradiation "strenghtening", in pure fcc metals, is at least qualitatively attributable to two types of "defect clusters" produced by a momentum exchange between high energy neutrons and the lattice atoms. The two types of "defects" which are believed to be the result of the momentum exchange are:

- large interstitial loops whose density tends to saturate at a low fluence (i.e., fast flux x time).
- small, variably sized "planar" vacancy clusters whose density continues to increase approximately linearly with fluence.

It is generally supposed[1] that the irradiation "strenghtening" mechanism in bcc and hcp metals is similar to that in fcc metals but with the added complication that diffusion of interstitial impurity atoms to the irradiation "defect clusters" can strengthen and stabilize

them as obstacles to dislocation motion. The diffusion of interstitial impurity atoms can occur either during irradiation and/or after irradiation depending upon temperatures. This phenomenon has been observed in post-irradiation-evaluation (PIE) annealing studies on niobium.[1]

The mechanical behavior of hcp Zr and dilute Zr alloys is complex due to inherent crystallographic anisotropy and dynamic strain aging characteristics.[6,7] Veevers et al[7] have shown that, for Zr-2, strain aging occurs at temperatures ranging from about 200°C through about 450°C (see Figure 1a). The 300°C strain aging peak has been attributed to interstitital oxygen[7] and has a significant effect on creep strength (see Figure 1b). Within the strain aging temperature range, the mechanical behavior tends to be athermal and somewhat unpredictable.[6] After irradiation to a fluence of about 5E19 nvt or greater, the oxygen strain aging appears to be effectively suppressed (see Figure 1c) presumably because the oxygen is trapped at irradiation "defect clusters."[7] In PIE annealing tests, an increase in yield strength is observed when annealed at temperatures above the irradiation temperatures (see Figure 1d). Although this phenomenon has not been investigated systematically, these data appear to provide some basis to question whether or not PIE mechanical behavior is fully characteristic of the in-flux mechanical behavior of Zr and those dilute Zr alloys susceptible to oxygen strain aging.

ELASTIC CONSTANTS

For unirradiated Zr and dilute Zr alloys, the elastic and shear modulii have been obtained from tests employing both the static stress-strain and dynamic resonant frequency methods[6,8] (see Table 1). There have been no specific in-flux or PIE tests undertaken on the elastic and shear modulii. Based on PIE tensile data, irradiation appears to have no significant effect on the elastic constants. There are only a few instances[8-12] wherein contractile/extension strain (Poisson's Ratio) measurements were obtained on either irradiated or unirradiated Zr and/or dilute Zr alloys. In those few instances the

test material from one data set to the next differed significantly (anisotropy in particular). For this reason pre-postirradiation comparisons cannot be made.

STRENGTH AND DUCTILITY

The effects of fast flux neutron irradiation on the yield and ultimate strength and ductility of Zr and the dilute Zr alloys have, with one notable exception,[13] been determined from PIE tests. Data are available from PIE uniaxial tensile tests on coupon bars and tubing and from biaxial tensile tests on tubing stressed by internal pressurization (see Tables 2 through 14). There are no data from PIE tests employing compressive stress states. The data listed in Tables 2 through 14 include the effects of cold work,[14-20,26] heat treatment[14,15,17,19,20,23,26,27] and PIE test temperature.[11,16,19,20,24] Data for evaluating the effect of the irradiation temperature[2,4,14,18,27] and strain rate[12,13,28] are limited. Data relating to in-flux tensile behavior[13] are very limited.

Based on PIE data, the general effects of fast flux ($E \gtrsim 1$ Mev) neutron irradiation on the tensile properties of Zr and dilute Zr alloys are:

- a very substantial increase in yield strength and which tends to approach a saturation value
- a smaller but significant increase in ultimate strenth
- a drastic reduction in uniform (pre-maximum load elongations) strain
- the yield strength tends to approach the ultimate strength. The small difference in yield and ultimate strength and the reduction in uniform strain signal a substantial reduction in strain hardenability.
- the reduction in area, accompanying a tensile failure is essentially unchanged. The reduction in the total tensile elongation essentially reflects only the reduction in uniform strain.

The increase in yield and ultimate strength, as determined from PIE tests, is dependent upon the prior metallurgical condition. Zr and dilute Zr alloys, which have been recrystallization annealed prior to irradiation tend to sustain significantly greater increases in strength than the same alloy[3] which had been cold worked prior to irradiation at the same temperature and fluence. In general, the PIE yield and ultimate strength tend to approach a pseudo-saturation strength at relatively high fluences ($\phi t \gtrsim$ 1E21 n/cm^2) and which is essentially independent of the prior metallurgical condition. Although the effects of irradiation temperature have not been systematically studied, there is experimental evidence[2,4,14,17,27] (see also Tables 2, 12 and 14) that the pseudo-saturation strength diminishes with increasing irradiation temperature. PIE annealing experiments[14] tend to show that the irradiation strengthening, sustained from irradiation temperatures below about 280°C, is removed by annealing at temperatures ranging from about 250°C to 400°C. Irradiation of cold-worked Zr-2 showed[14] the extent of thermally activated recovery, during a 380°C irradiation, to be essentially identical to the extent of recovery occurring during an out-of-flux heat treatment for the same time at 380°C. Considering these data (see also Figures 2 and 3), it is expected that, in the temperature range of $\sim$375°C < T $\lesssim$ 475°C, thermally activated recovery mechanisms will effectively remove irradiation produced "defect clusters" and interstitital loops at about the rate they form or alternatively render them ineffective as obstacles to dislocation motion.

Although the effect of PIE test temperature has not been systematically studied, some data has been obtained.[11,16,18,19,23,24,25,27,28] As suggested by Makin,[1] interstitital impurity atoms may diffuse to irradiation produced "defect clusters" and strengthen and stabilize them as obstacles to dislocation motion either during and/or after irradiation. As shown in Figure 1d, the increase in yield strength suggests that there may have been some further interstitial impurity atom diffusion (i.e., thermal and/or strain aging) when annealed at temperatures above the irradiation temperature. Some of the PIE tensile data (see Tables 5-7, 10-14) show, for some tests, significant differences in the

normalization factor - $f(YS)/f(\phi t)$*- with testing temperature. These differences in the normalization factor also suggest that some thermal/strain aging may have occurred in these PIE tests. In some instances, prior metallurgical condition (e.g., alloying, texture, etc.) may have also been a factor in the relatively greater increase in the yield and ultimate strengths.

Only one set of in-flux tensile data was obtained (see Table 11). These data were obtained from uniaxial tests on rolled Zr-4 plate. All of the in-flux tests were done at slow strain rates (1.9E-4 to 5.0E-6 per hour) and which are not generally typical of the strain rates employed in the bulk of the PIE tests. A few PIE uniaxial tensile tests were done on the same material but not at identical strain rates. For this reason, exact comparisons of in-flux with PIE tensile behavior are not possible. Although the in-flux test results are variable, the apparent irradiation strengthening effect tends to be significantly less as compared with results from PIE tests. From these data, it cannot be determined whether the differences in irradiation strenthening may be attributable to fast flux and/or fluence differences or to thermal/strain aging effects during the slow strain rate PIE tests.

The effect of strain rate on the post-irradiation tensile behavior of Zr and dilute Zr alloys has not been systematically evaluated over any range of test temperatures. The data available are shown in Figure 4 and which were obtained from Zr-4 irradiated to a fluence estimated to range from 3.8 to 4.4E21 nvt.[2] Comparisons with strain rate effects on non-irradiated Zr-2[6] show that the strain rate effect on yield and ultimate strength is comparable. In contrast, however,

---

*$f(YS) = \Delta YS/YS$ where ΔYS is the difference in the irradiated and non-irradiated yield strength only.

$f(\phi t) = \sqrt[4]{1 - \exp(-B\phi t)}$ where ϕt = fluence.

the total elongation, as measured in the PIE tests, is a maximum at the minimum of the strain rates employed. The reason for this difference is as yet unknown but is probably due, in part at least, to the drastically reduced strain hardenability and tendency for strain localization* generally observed in PIE tensile tests. The uniform strain tends to be generally low over the entire range of strain rate employed.

The effect of irradiation superimposed upon cold work effects on the strain hardenability and strength coefficient for Zr-2, has been rather systematically evaluated at room temperature[3] (see Figures 5 and 6) but not at elevated temperatures. There are, however, considerable elevated temperature PIE data which, by the small differences between the yield and ultimate strength, show that irradiation drastically reduces the strain hardenability of the Zr and dilute Zr alloys. (As shown in Tables 14a and 15b, large strain hardenability values were reported.[27] When compared to the small differences between the PIE yield and ultimate strength, these reported strain hardenability values appear to be erroneous). As stated previously, irradiation at temperatures above about 375°C showed that thermally activated recovery occurred at a rate about equal to the rate of irradiation "strengthening".[14] Based on these observations, the strain hardenability, strain rate sensitivity, strength and ductility should approach the values for comparable non-irradiated material.

---

*The strain localization generally observed in PIE tensile tests have been referred to by some investigators[3,12] as "dislocation channelling." Transmission electron microscopy studies show the localized slip/shear bands, wherein failure ultimately occurs, to be essentially cleared of dislocations and irradiation produced "defect clusters".

There have been considerable efforts undertaken to analytically model or empirically account for the inherent anisotropy in the out-of-flux elastic and inelastic mechanical behavior observed in Zr and the dilute Zr alloys.[6,12,16] There have, however, been no specific and systematic efforts to determine whether or not there is anisotropy in the formation of irradiation produced "planar" vacancy clusters and interstitial loops or any accentuation of the anisotropy in the mechanical properties arising from the irradiation produced strengthening effect. Considering Makins'[1] hypothesis for irradiation "strengthening", it may be expected that there can also be some anisotrophy in irradiation effects inasmuch as the irradiation produced "interstitial loops" and "planar vacancy clusters" may form preferentially on favored crystallographic planes. Reiger and Lee[12] undertook a very limited effort to evaluate the effect of texture on the strength and ductility of irradiated and unirradiated Zr-2. From these limited data (see Table 8), it was concluded that the anisotropy in mechanical properties was not significantly altered by irradiation. It is doubtful whether the limited data, shown in Table 8, are adequate to make any generalized conclusion as to anisotropy in irradiation effects.

In summary, the effect of fast flux neutron irradiation on the PIE tensile behavior of Zr and dilute Zr alloys appears to be generally characterized by the following:

- At irradiation temperatures above about 375°C, thermally activated recovery mechanisms tend to operate at rates sufficient to effectively offset the strengthening effect of the irradiation produced "planar" vacancy clusters and interstitial loops.
- At irradiation temperatures below about 375°C:
  - o There is a substantial increase in the yield and a small but still significant increase in the ultimate strength. Both the yield and ultimate strength tend to approach saturation values at fluences estimated to be in the range of E21 to E22 n/cm^2 or perhaps even greater.

- o There is a drastic reduction in uniform strain and the yield tends to approach the ultimate strength. These changes signal a very substantial reduction in strain hardenability.
- o There is little or no decrease in the reduction in area and the decrease in tensile elongation essentially reflects the decrease in uniform strain.

- It as as yet unknown whether or not the inherent anisotropy in the hcp Zr and dilute Zr alloys results in anisotropy accentuation in either the formation of or strengthening effects from irradiation produced "planar" vanancy clusters and/or interstitial loops.
- Data from slow-strain rate in-flux tensile tests and PIE tensile tests at temperatures above the irradiation temperature provide some basis to question whether the tensile behavior observed in PIE tests are always and fully indicative of in-flux tensile behavior.

CREEP

The effect of fast flux ($E \gtrsim 1$ Mev) neutron irradiation on the creep behavior of Zr and dilute Zr alloys, has, in contrast with PIE tensile data, been determined, in all cases, from in-flux tensile creep tests. Data are available from in-flux uniaxial and biaxial tensile tests on coupon bars and tubing[29-37,43] and biaxial tensile tests on full component sized pressure tubes[42,45] (See Tables 15 and 16 and Figures 7-13, 17 and 18). Significant amounts of data have also been obtained from in-flux tensile stress-relaxation tests.[38-40,49-51] There are few data for evaluating the effect of pre-irradiation on the in-flux creep behavior and no reported PIE creep data. There are no reported data relating to the in-flux creep behavior for compressive stress states. There are limited amounts of PIE fuel rod profilometry measurements which may be used in a limited way to evaluate the effect of compressive stress states.

The effect of temperature on the in-flux creep behavior has not been systematically investigated. Nearly all in-flux creep and stress-relaxation data for Zr and the dilute Zr alloys were obtained at temperatures ranging

from about 250°C to 500°C.[29-51] Most of these data, however, were obtained at temperatures ranging from about 250°C to about 325°C which corresponds to the temperature range for pressure tube and fuel clad tubing service in water cooled nuclear power reactors. At temperatures below about 350°C, the creep behavior tends to be athermal for both irradiation and non-irradiation environments. In a non-irradiation environment and in about the 250°C to 325°C temperature range the creep rates may diminish markedly due to strain aging effects[30,32] (see also Figure 1b). In contrast, the in-flux creep rates always increase with increasing temperatures.[30] As temperatures increase, the effect of irradiation tends to diminish. At temperatures above about 325°C to 350°C, creep tends to be essentially thermally activated with little or no further activation by irradiation. The thermally activated, high temperature creep can be readily modelled by the Arrhenius type function - $\dot{\varepsilon} \propto \exp(-Q/RT)$ - where Q is approximately the activation energy for self diffusion. At temperatures below about 325°C-350°C, the in-flux creep rates tend to be increasingly activated by fast flux ($E \gtrsim 1$ Mev) irradiation with decreasing temperature. In effect, fast neutron irradiation appears to supplant the thermal activation of creep deformation mechanisms. The approach, generally used to date, to analytically model the "low" temperature, irradiation enhanced creep is to use the Arrhenius function - $\exp(-Q'/RT)$ with a low valued apparent thermal activation energy and a power function - $B\phi^n$ - to account for the fast neutron flux activation of creep mechanisms. This approach has been used with reasonable success in modelling the creep behavior of Zr-2 and Zr-4[41] (see Figure 20). The constitutive equations employed to model the thermally high temperature activated and the low temperature fast flux activated creep are:

- High temperature creep:

$$\dot{\varepsilon}_T = B_T[1 + \alpha k \exp(-kt)] \exp(-Q_T/RT) \cdot \sinh(S_T\sigma)$$

- Low temperature, irradiation activated creep:

$$\dot{\varepsilon}_I = B_I[1 + \alpha k \exp(-kt)] \phi^{0.85} \cdot \exp(-Q_I/RT) \cdot \sinh(S_I\sigma)$$

where:

B_T = 5.96 E14

B_I = 1.62 E-14

α = 3300

k = 4.4 E-3

Q_T = 63600 cal/mole °K

Q_I = (9500 - 0.038σ) cal/mole °K

S_T = 6.25 E-4

S_I = 1.0 E-5 - psi^{-1}

ϕ = fast flux - nvt ($E \gtrsim 1$ Mev)

σ = applied stress - psi

The effect of stress on the in-flux creep and stress-relaxation behavior of Zr and the dilute Zr alloys has been systematically evaluated over relatively small ranges of temperature and fast neutron flux[29-39, 42-46, 49-51] (see also Figure 11). As shown in Figure 11, the out-of-flux and thermal flux ($E \lesssim 1$ Mev) creep rate-stress dependency tends to be roughly linear. At low stresses, the in-flux creep rates tend to be significantly greater than for out-of-flux creep at otherwise comparable test conditions. With increasingly larger stress, the creep rate enhancement tends to diminish. At temperatures above about 350°C, any effect of irradiation on the creep rate-stress dependency may be expected to essentially disappear. In analytically modelling the effect of stress on the in-flux creep rate, power functions - σ^n - and a hyperbolic sine - $\sinh(k\sigma)$ - function have generally been used. The hyperbolic sine function, in effect, models a power function with a continuously changing exponent and therefore appears to provide a slightly better overall representation of the in-flux creep rate-stress dependency.

The effect of the intensity of the fast flux neutron irradiation on the creep behavior of Zr and the dilute Zr alloys has not been systematically investigated because the attainable range of fast flux, in any single irradiation facility, is not large. In all analytical modelling efforts, a power function - $B\phi^n$ - has generally been employed. In these modelling efforts,

the fast flux exponent ranged from 1.0[30-35,38-40,42] to as low as 0.5[29] when the effective creep rate was corrected for thermally activated creep as determined from out-of-flux creep tests. Considering the uncertainties in reported fast flux intensity and the variation in fast flux intensity over the period of creep observations, it appears that the fast flux exponent is probably greater than 0.5 and less than 1.0. Several correlation efforts suggest fast flux exponent values at about 0.6[30] to 0.85.[41,45] In general, Fidleris[30] reports that:

- in annealed Zr and dilute Zr alloys, the primary creep strains tend to decrease with increasing fast flux intensity whereas in cold worked materials, the fast flux intensity has little or no effect.
- creep rates tend to become constant after fluences ranging from about 1.0 to 5.0E 20 n/cm^2.

Ibrahim,[30] however, reports that the secondary creep rates continue to diminish with time but at a much slower rate as compared with creep rates for otherwise comparable out-of-flux conditions.

There are only a few in-flux creep tests which were done to evaluate the effect of pre-irradiation.[30,31] In general, pre-irradiation appeared to have little or no effect on material in the cold-worked condition while for material in the annealed condition, pre-irradiation, to fluences of about 1.0E 19 n/cm^2 or greater, tended to diminish the primary creep strains. At greater fluences (e.g. $\sim$ 3E20 n/cm^2) pre-irradiation tended to also diminish the primary strains for material in the cold-worked condition. When irradiated in a very high intensity fast neutron flux environment ($\phi \gtrsim$ E14 nv) the subsequent in-flux (E12 $\lesssim \phi \lesssim$ E14 nv) creep strains and rates were greater than for the in-flux creep strains and rates of comparable material which had not been pre-irradiated.

There have been considerable efforts undertaken to analytically model or empirically account for the inherent anisotropy in the in-flux creep behavior of Zr and the dilute Zr alloys.[6,30,32,33,35,40,41,48] There have, however, been no specific and systematic effort to determine whether

or not there is anisotropy in the formation of irradiation produced "planar" vacancy clusters and interstitial loops or any accentuation of the anisotropy in creep properties arising from irradiation activation and/or enhancement of creep mechanisms. Any effects, if such exist, are inseparably included in all of the reported creep data.

In summary, the effect of fast flux neutron irradiation on the in-flux tensile creep behavior of Zr and dilute Zr alloys appears to be generally characterized by the following:

- At irradiation temperatures above about 350°C, creep tends to be essentially controlled only by thermally activated mechanisms.
- At irradiation temperatures below about 350°C:
  - Cr[illegible] to be irradiation activated and enhanced over and above that for thermal activation at otherwise comparable conditions.
  - The extent of creep activation and enhancement by irradiation tends to be inversely proportional to the irradiation temperature.
  - At fluences greater than about 1 to 5 E20 n/cm^2, secondary creep rates tend to become constant or at least diminish at a much slower rate as compared with thermally activated creep at otherwise comparable conditions.
  - Pre-irradiation appears to have little, if any, effect on material in a cold-worked condition whereas for annealed material, pre-irradiation to fluences of about 1 E19 n/cm^2 or greater tends to diminish primary creep strains.
  - At creep strain rates, Zr-2 and Zr-4 tend to be somewhat superplastic.[6,41,47]
- If there is anisotropy in the activation and/or enhancement of creep deformation mechanisms by irradiation, any such effect is inseparably included in all of the reported creep data.

FATIGUE AND FRACTURE

The effect of fast flux neutron irradiation on the fatigue and fracture behavior of several dilute Zr alloys has been evaluated only in PIE tests. PIE fatigue data have been reported only for the Zr-2 and Zr-4 alloys. PIE fatigue data at temperatures to 400°C have been reported for low cycle fatigue in both the axial and bending mode [52,53] (See Figures 21 through 23) and moderate cycle (20 cpm), low stress loading in a tension mode on compact tension specimens from Zr-4 rolled plate.[54] (See Table 17). PIE fatigue crack growth data has been reported for Zr-4 rolled plate in moderate cycle (20 cpm) fatiguing in a tension-tension mode.[54] (See Figure 2a). As yet, all of the fatigue crack growth data reported for the Zr-2 and Zr-2.5Nb alloys has been obtained from large diameter unirradiated tubing.[55,56,56] PIE fracture data have been reported for Zr-4 rolled plate[54] and Zr-2 and Zr-2.5Nb alloy tubing[55-63] at temperatures to about 350°C. (See Tables 17-22 and Figures 25-27).

Data from axial mode, constant strain amplitude fatigue tests on the Zr-2 and Zr-4 alloys in the cold-rolled, recrystallization annealed and the as-welded conditions show no significant effect of either anisotropy or cold-worked substructure.[52] (See Figures 21 and 22). There appears, however, to be some effect of mean stress and strain amplitude (see Figure 22). As to an effect from prior irradiation, it was observed that both the Z-2 and Z-4 alloys, prior to irradiation, tended to strain harden under cyclic loading, whereas after irradiation, they tended to strain soften so that there was no essential difference in the cyclic stress-strain behavior.[53] The only significant effect of irradiation on ductility appears to reduce the allowable stress/strain amplitude.[52] When fatigue tested in the bending mode, the number of cycles to failure appear to be about one-third the number of cycles to failure in axial mode fatigue tests under otherwise comparable test conditions.[53] The bending mode fatigue data show significantly less scatter and appear to fit the Coffin-Manson equation rather well:

$$\Delta\varepsilon_p \, N_f^{\,n} = \text{constant}$$

where: $\Delta\varepsilon_p$ = inelastic strain amplitude

N_f = cycles to failure

n = exponent

In the bending mode, irradiation appears to decrease the allowable stress/strain amplitude at 20°C but had no significant effect at 300°C. Heat treatment of identical test material at 300 C for an equivalent test time, or longer, did not significantly alter the tensile yield strength or ductility. Based on these results, it is uncertain as to why there was an effect of irradiation on the bending mode fatigue behavior at 20°C but essentially none at 300°C.

The only reported fatigue crack growth data was obtained from moderate cycle (20 cpm), low stress fatiguing in a tension-tension mode on compact tension specimen from Zr-4 rolled plate.[54] (See Figure 24). The compact tension specimens were machined from rolled plate with the following orientations:

TW = crack plane normal to plate thickness and crack propagation parallel to plate width

RW = crack plane normal to rolling direction and crack propagation parallel to plate width

Pre-and-post irradiation fatigue crack growth was determined at 20°C for the Zr-4 alloy in both the hydrided and non-hydrided conditions and fluence to about 2.08 E21 n/cm^2 (see Table 17a). As shown in Figure 24, there is appreciable scatter in the PIE fatigue crack growth data. Considering the difficulties in PIE crack growth measurements, it is uncertain as to whether the data scatter is attributable to crack growth measuring difficulties, specimen orientation or both. Considering the rather minimal effect of irradiation observed in the low cycle fatigue behavior[52,53] the effect on fatigue crack growth is also expected to be minimal. Any effect, if it exists, is inseparable from the scatter in the available data.

The effect of fast flux neutron irradiation on the fracture behavior has been determined for only the Zr-2, Zr-4 and Zr-2.5Nb alloys at temperatures ranging from about -70°C to 315°C in both the hydrided and non-hydrided conditions.[54,57-63] (See Tables 17b-23 and Figures 24-27). In PIE

fracture tests, both compact tension specimens and internally pressurized tubular specimens have been used. In fracture tests on tubular specimens, the crack initiating defects employed, were axial slits produced by conventional or electro-discharge machining or pre-cracked by fatigue. In all of the tubular specimen PIE tests, a through-wall defect was employed so as to provide a test specimen analogous to a center-notched sheet fracture specimen. As yet, fracture testing of tubular specimens employing part-through-wall defects, machined and/or pre-cracked by fatigue, have been done only on the Zr-2 and Zr-2.5Nb alloys in the non-irradiated condition[55-57] (See Figure 25).

In PIE tests employing compact tension specimens from rolled Zr-4 plate, the fracture toughness-K_{IC}- for both the hydrided and non-hydrided conditions tended to increase with increasing temperature.[54] (See Table 17b).

The fracture toughness-K_C-as determined in PIE fracture tests on through-wall defected Zr-2 and Zr-2.5Nb alloy tubing in the hydrided condition, tends to undergo a transition with increasing temperatures which is analogous to the Charpy impact energy absorption transition. Based largely on data from non-irradiated tubing, the transition temperature ranges from about 100°C to about 150°C for hydrogen contents ranging from about 100ppm to 300ppm respectively.[55,57,61,63] There appears to be little or no effect of temperature on the fracture toughness of Zr-2 or Zr-2.5Nb alloy tubing in the non-hydrided condition as determined from PIE fracture tests on through-wall defected tubular specimen.[57-63] (See Tables 20,22, 23 and Figure 26).

There appears to be considerable variance in the observation of the effects of fluence on the fracture toughness of the Zr-2, Zr-4 and Zr-2.5Nb alloys as determined from compact tension specimens and through-wall defected tubing. As determined in PIE tests with compact tension specimens the fracture toughness tends to increase with increasing fluence even though irradiation, as determined from PIE tensile tests, produces a significant increase in yield strength and a drastic decrease in the strain hardenability. These two material properties are generally considered to be the principle sources of fracture toughness in metals. As determined from PIE fracture

tests on tubing with machined through-wall defects, there appears to be essentially no effect of fast flux neutron irradiation over the entire range of fluence investigated.[57,60-62] (See Figure 26). As determined from PIE fracture tests on tubing, pre-cracked by fatigue, the fracture toughness tends to be generally less than for tubing with machined through-wall defects and fracture toughness also tends to decrease with increasing fluence.[57,58] (See Figure 27).

In summary, the effect of fast flux neutron irradiation on the PIE fatigue crack growth and fracture behavior of several dilute Zr alloys appears to be generally characterized by the following:

- Data are not available to show whether irradiation has an effect on the fatigue crack growth and fracture behavior that is analogous to that observed for PIE tensile and in-flux creep behavior.
- There are conflicting observations as to the effect of fluence on the PIE fracture toughness. Considering the metallurgical sources of fracture toughness-modulus, yield strength, strain hardenability and true strain at fracture--it is anticipated that the fracture toughness will diminish with increasing fluence and tend to approach asymptotically a psuedo-saturation fracture toughness analogous to the psuedo-saturation in PIE yield strength.

IRRADIATION GROWTH

All Zr and dilute Zr alloys undergo small changes in dimensions during fast ($E \gtrsim 1$ Mev) neutron irradiations in the absence of any applied stress. These irradiation induced dimensional changes are generally referred to as "irradiation growth" and they tend to occur with essentially no change in density. In general, irradiation growth, in Zr and the dilute Zr alloys, is anisotropic and dependent upon both the crystallographic texture and the deformation substructure.[30]

There are anomalies in the observed irradiation growth of annealed zirconium single crystals.[30] In one experiment, expansion occurred along the "a" axis of the hcp Zr, and contracted along the "c" axis with no net volume change. In another experiment, expansion occurred predominantly along the "a" axis and with also a slight expansion along the "c" axis after irradiation to a fluence of about 7 E20 n/cm^2. In still another experiment, Fidleris[30] observed expansion predominantly along the "c" axis. After irradiation to a fluence of about 6 E19 n/cm^2, contraction along the "c" axis was observed to begin although there was still a net "c" axis growth after irradiation to a fluence of about 8 E19 n/cm^2. Irradiation growth experiments have not been done on plastically deformed single crystals.

Significant amounts of irradiation growth data have been obtained from polycrystalline Zr and dilute Zr alloys in both the annealed and cold worked condition.[30,64-71] (See Table 24 and Figures 28 through 30). These data show that irradiation growth and growth rates tend to be greater in material in the cold worked condition than in either the stress relieved or the annealed and recrystallized condition. (See Figures 29 through 31). All data show that the direction of irradiation growth tends to coincide with the principal direction of plastic deformation during cold working. Post-irradiation, recrystallization annealing experiments[30] show that irradiation growth strain recovery occurs and that the fractional strain recovery is inversely proportional to the degree of cold work. The maximum strain recovery, however, was insensitive to the degree of cold work. These observations and the anomalies observed in the growth of Zr single crystals, suggest that irradiation growth is as much or perhaps more dependent upon the cold work substructure as upon the crystallographic texture. In considering the crystallographic textures in cold-worked or cold-worked and recrystallization annealed material, irradiation growth appears to occur by expansion along the "c" axis and contraction along the "a" axis. In most investigations, however, dimensional change measurements were limited to one (i.e., plastic flow direction) or two (i.e., transverse to the direction of plastic flow) directions. For this reason, there is still considerable uncertainty as to the crystallographic directions of growth and whether or not there are net volume changes resulting from irradiation growth. Microscopy studies have not as yet disclosed any void formation associated with the irradiation growth phenomena.

The effect of fast neutron flux intensity or flux spectrum on growth has not been systematically investigated. Based on limited data[30] the irradiation growth rate appears to be directly proportional to the flux intensity in the range of 1 to 20 E13 n/cm^2 sec.[30] In general irradiation growth is analytically modeled by a power function:

$$\varepsilon_{growth} = \text{constant} \times (\phi t)^n$$

where:

ϕ = fast flux (E $\geq$ 1 Mev) n/cm^2 sec

t = time - hours

n = exponent.

Figures 28 and 29 show the range of exponent determined for the more common Zr alloy. Figure 30 shows the average for Zr-2 and Zr-4. Inasmuch as the growth rate appears to be directly proportional to the flux intensity,[30] it may be more appropriate to model growth as follows:

$$\varepsilon_g = \text{constant} \times \phi \times t^n$$

Measurements of dimensional changes due to irradiation have been obtained from irradiations at temperatures ranging from about 78°K (-195°C)[65] to as high as about 350°C.[68] (See also Figures 28 through 30.) Based on these data, and his own unpublished data, Fidleris[30] suggests a small irradiation growth-temperature dependence which may be represented by the Arrhenius function:

$$\dot{\varepsilon}_g \propto \exp(-Q_g/RT)$$

The activation energy - Q_g - was estimated to be about 4 kcal/mole°K in the temperature range of about 150°C to 300°C. Considering the data shown in Figures 28 through 30, and the observation that irradiation growth appears to be significantly greater in material in the cold worked condition than in a stress relieved or the recrystallization annealed condition, there appears

to be some uncertainty as to any irradiation growth-temperature dependence. Considering that the in-flux creep behavior, and to a lesser extent, the PIE tensile behavior appear to be inversely temperature dependent, an inverse growth-temperature dependence might also be expected.

In summary, the effect of fast flux irradiation on the unstressed growth behavior of Zr and dilute Zr alloys appears to be generally characterized by the following:

- There are no data from irradiations above about 350°C to 375°C to determine any irradiation-growth effect. Based on observations of the effect of irradiation on the PIE tensile and the in-flux creep behavior, it is anticipated that irradiation growth will be minimal or nonexistent.
- At irradiation temperatures below about 350°C to 375°C.
  - o Irradiation tends to produce dimensional changes in the absence of any applied loading.
  - o The anisotropy in irradiation growth appears to be dependent upon both the crystallographic texture and the cold worked substructure.
  - o The rate and magnitude of irradiation growth appear to be significantly greater in material in the cold worked condition than in a stress relief or the recrystallization annealed condition.
  - o The direction of irradiation growth tends to coincide with the direction of plastic flow during prior cold working.
  - o Irradiation growth, within at least a limited range of fast flux intensity, appears to be directly proportional to the fast flux intensity.
  - o Post-irradiation annealing appears to produce some recovery of irradiation produced growth strains. The magnitude of recoverable growth strains appears to be independent of the condition (e.g., degree of cold work, stress relief or recrystallization anneal) of the material.

  The available irradiation growth data appear to be inadequate to establish, with reasonable certainty, any irradiation growth-temperature dependence.

REFERENCES

1. M. J. Makin, "The Hardening of Metals by Irradiation," Irradiation Embrittlement and Creep in Fuel Cladding and Core Components, Proceeding of the Conference Organized by the British Nuclear Energy Society in London, November 9-10, 1972.

2. H. R. Higgy and F. H. Hammand, "Effect of Neutron Irradiation on the Tensile Properties of Zircaloy-2 and Zircaloy-4," Journal of Nuclear Materials, Vol. 44, pp. 215-227, 1972.

3. A. L. Bement, "Fundamental Materials Problems in Nuclear Reactors," Second International Conference on the Strength of Metals and Alloys, August 30 - September 9, 1970, Conference Proceedings, Vol. 2, American Society for Metals.

4. Z. M. Hammad, B. D. Sharma and P. Rodriquez, "Radiation Hardening of Zirconium," B.A.R.C-578, 1971, Bhaba Atomic Research Centre, Bombay, India.

5. D. O. Northwood and R. W. Gilbert, "Neutron Radiation Damage in Zirconium and It's Alloys," Radiation Effects, Vol. 22, 1974, pp. 139-140.

6. C. L. Mohr, P. J. Pankaskie and F. E. Panisko, "A State-of-the-Art Report on the Anisotropic Deformation and Analysis of Zircaloy," RP-251-1, 1976, (EPRI/MPC Zircaloy-LOCA Program).

7. K. Veevers, W. B. Rotsey, and K. U. Snowden, "The Effect of Neutron Irradiation and Cold Work on the Strain-Aging Behavior of Zircaloy-2." Applications Related Phenomena for Zirconium and It's Alloys, ASTM STP 458, 1969, pp. 194-209.

8. D. O. Northwood, I. M. London and L. E. Bahen, "Elastic Constants of Zirconium Alloys," Journal Nuclear Materials, Vol. 55, p. 299-310, 1975.

9. P. L. Rittenbouse and M. L. Picklesimer, "Research on the Anisotropy of Zircaloy-2," Electrochemical Technology, Vol. 4, no. 7-8, pp. 322-329, 1966.

10. C. R. Woods, Editor, Properties of Zircaloy-4 Tubing, WAPD-TM-585, 1966.

11. C. D. Williams, R. B. Adamson and K. D. Olshausen, "Effects of Boiling Water Reactor Irradiation on Tensile Properties of Zircaloy," European Conference on Irradiation Behavior of Fuel Cladding and Core Component Materials, Karlsruhe, 3-5 December, 1974, pp. 189-192.

12. G. F. Reiger and D. Lee, "Strength and Durability of Neutron Irradiated and Textured Zircaloy-2", Zirconium in Nuclear Applications, ASTM STP 551, 197, p. 355-369.

13. F. J. Azzarto, E. E. Baldwin, F. W. Wiesinger and D. M. Lewis, "Unirradiated, In-Pile and Post-Irradiation Low-Strain Rate Tensile Properties of Zircaloy-4", Journal of Nuclear Materials, Vol. 30, 1969, pp. 208-218.

14. L. M. Howe and W. R. Thomas, "The Effect of Neutron Irradiation on the Tensile Properties of Zircaloy-2", Journal of Nuclear Materials, Vol. 2, no. 3, 1960, pp. 248-260.

15. L. M. Howe, "The Annealing of Irradiation Damage in Zircaloy-2 and the Effect of High Temperature Irradiation on the Tensile Properties of Zircaloy-2", CR Met-922, April 1960,

16. A. L. Bement Jr., "Effects of Cold Work and Irradiation on the Tensile Properties of Zircaloy-2", HW-74955, April 1963.

17. J. E. Irvin, "Effects of Irradiation and Environment on the Mechanical Properties and Hydrogen Pickup of Zircaloy", Electrochemical Technology, Vol. 4, no. 5-6, May-June, 1966, pp. 240-249.

18. M. Kangiloski, "The Effects of Neutron Radiation on Structural Materials", N68-16876, June 30, 1967, Battelle Memorial Institute, Columbus, Ohio.

19. D. G. Hardy, "The Effects of Neutron Irradiation on the Mechanical Properties of Zirconium Alloy Fuel Cladding in Uniaxial and Biaxial Tests", Irradiation Effects on Structural Alloy for Nuclear Reactor Applications, ASTM, STP484, 1970, pp. 215-258.

20. D. G, Hardy, "Burst Testing of Zircaloy Cladding from Irradiated Pickering-Type Fuel Bundles", Effects of Radiation on Substructure and Mechanical Properties of Metals and Alloys, ASTM, STP 529, 1973, pp. 415-434.

21. D. L. Hagrman, "Irradiation and Cold Work Effect on Zircaloy Cladding Mechanical Properties", SRD-42-76, January 1976.

22. C. J. Baroch, A. V. Munin, and E. N. Harbinson, "Effects of Irradiation in a Thermal Reactor on the Tensile Properties of Zircaloy-2 and 4 and Borated Stainless Steel", Irradiation Effects on Structural Alloys for Nuclear Reactor Applications, ASTM, STP 484, 1970, pp. 176-193.

23. C. E. Ells and V. Fidleris, "Effect of Neutron Irradiation on Tensile Properties of the Zirconium-2.5 Weight Percent Niobium Alloy". Electrochemical Technology, Vol. 4, no. 5-6, May-June 1966, pp. 268-274.

24. F. H. Megerth, "Zircaloy Clad-UO_2 Fuel Rod Evaluation Program", GEAP 10070, July 1969.

25. W. R. Smalley, "Saxton Plutonium Program, Semiannual Progress Report for the Period Ending December 31, 1969, WCAP-3385-22, March 1970.

26. W. R. Smalley, "Effects of Irradiation on Mechanical Properties of CVTR Pressure Tube Material", CVNA-159, September 1962.

27. B. A. Cheadle, C. E. Ellis, and J. van der Kuur, "Plastic Instability in Irradiated Zircaloy-Sn and Zircaloy-Nb Alloys", Zirconium in Nuclear Applications, ASTM, STP 551, 1974, pp. 370-384.

28 A. A. Bauer, et al., Unpublished Data, Battelle Memorial Institute.

29. E. R. Gilbert, "In-Reactor Creep of Reactor Materials", Reactor Technology, vol. 14, no. 3, Fall 1971, pp. 258-285.

30. V. Fidleris, "Summary of Experimental Results on In-Reactor Creep and Irradiation Growth of Zirconium Alloys", Atomic Energy Review, vol. 13, no. 1, 1975, pp. 51-80.

31. V. Fidleris, "Uniaxial In-Reactor Creep of Zirconium Alloys", Journal of Nuclear Materials, vol. 26, no. 1, 1968, pp. 51-76.

32. V. Fidleris, "The Effect of Texture and Strain Aging on Creep of Zircaloy-2", Application-Related Phenomena for Zirconium and Its Alloys, ASTM, STP 458, 1968, pp. 1-17.

33. E. F. Ibrahim, "In-Reactor Creep of Zirconium-Alloy Tubes and Its Correlation with Uniaxial Data", Applications-Related Phenomena for Zirconium and Its Alloys, ASTM, STP 458, 1968, pp. 18-36.

34. E. F. Ibrahim, "In-Reactor Creep of Zircaloy-2.5% Nb. Tubes at 570°K", Zirconium in Nuclear Applications, ASTM, STP 551, 1974, pp. 249-261.

35. E. F. Ibrahim, "In-Reactor Tubular Creep of Zircaloy-2 at 260 to 300°C", Journal of Nuclear Materials, vol. 46, 1973, pp. 169-182.

36. J. J. Holmes, J. A. Williams, D. H. Nyman and J. C. Tobin, "In-Reactor Creep of Cold Worked Zircaloy-2", Flow and Fracture of Metals in Nuclear Environments, ASTM, STP 380, 1964, pp. 385-394.

37. E. R. Gilbert and N. E. Harding, "Comparison on In-Reactor Creep and Postirradiation Creep Tests of Structural Materials for Nuclear Applications", Irradiation Effects in Structural Alloys for Thermal and Fast Reactors, ASTM, STP 457, 1969.

38. D. E. Fraser, P. A. Ross Ross, and A. R. Causey, "The Relation Between Stress-Relaxation and Creep for Some Zirconium Alloys During Neutron Irradiation", Journal of Nuclear Materials, vol. 46, 1973, pp. 381-392.

39. C. E. Coleman and E. F. Ibrahim, "In-Reactor Creep Ductility of Zirconium Alloys," Unpublished Data transmitted to PNL under AECL/USNRR information exchange, June 1975.

40. P. A. Ross Ross, V. Fidleris and D.E. Frazer, "Anisotropic Creep Behaviour of Zirconium Alloys in A Fast Neutron Flux," Canadian Metallurgical Quarterly, Vol. II, No. 1. 1972, pp. 101-111 (also AECL-4237)

41. P. J. Pankaskie, "BUCKLE, An Analytical Computer Code for Calculating Creep Buckling of in Initially Oval Tube," BNWL-1784, May 1974.

42. P. A. Ross Ross and C. E. L. Hunt, "The In-Reactor Creep of Cold Worked Zircaloy-2 and Zirconium 2.5 wt % Niobium Pressure Tubes," Journal of Nuclear Materials, Vol. 26, no. 1, 1968, pp. 2-17.

43. E. R. Gilbert, "In-Reactor Creep of Zr-2.5 wt % Nb," Journal Nuclear Materials, Vol. 26, no. 1, 1968, pp. 105-111.

44. P. H. Kreyns and M. W. Burkart, "Radiation Enhanced Relaxation in Zircaloy-4 and in A Zirconium + 2.5 w/o Niobium + 0.5 w/o Copper Alloy," Journal of Nuclear Materials, Vol. 26, no. 1, 1968, pp. 87-104.

45. B. Watkins and D. S. Wood, "The Significance of Irradiation Induced Creep on Reactor Performance of A Zircaloy-2 Pressure Tube," Applications-Related Phenomena For Zirconium And Its Alloys, ASTM STP 458, 1969, pp. 18-36.

46. V. Fidleris, "The Stress Dependence of The In-Reactor Creep Rate of Heat Treated Zr-2.5 wt % Nb and Cold Worked Zircaloy-2," Journal of Nuclear Materials, Vol. 36, 1970, pp. 343-346.

47. D. S. Wood and B. Watkins, "A Creep Limit Approach to the Design of Zircaloy-2 Reactor Pressure Tubes at 275°B," Journal of Nuclear Materials, Vol. 41, 1971, pp. 327-340.

48. P. A. Ross Ross and V. Fidleris, "Design Basis for Creep of Zirconium Alloy Components in a Fast Neutron Flux," Paper C216/73, International Conference on Creep and Fatigue in Elevated Temperature Application," Instn Mech Engrs. Conference Publication 13, 1973.

49. A. R. Causey, "In-Reactor Stress Relaxation of Zirconium Alloys," Zirconium in Nuclear Applications ASTM STP 551, 1973, pp. 263-273.

50. C. C. Dollins and R. P. Tucker, "Irradiation-Induced Primary Creep," Journal of Nuclear Materials, Vol. 52, 1974, pp. 277-288.

51. A. R. Causey, "In-Reactor Creep of Zircaloy-2, Zircaloy-4 and Zr-1.15 wt % Cr-0.1 wt % Fe at 568K Derived from Their Stress-Relaxation Behaviour," Journal of Nuclear Materials, Vol. 54, 1974, pp. 64-72.

52. W. J. O'Donnell and B. F. Langer, "Fatigue Design Basis for Zircaloy Components," Nuclear Science and Engineering 20, 1964, pp. 1-12.

53. Kjell Pettersson, "Low Cycle Fatigue Properties of Zircaloy-2 Cladding," Journal of Nuclear Materials, Vol. 56, 1957, pp. 91-102.

54. T. J. Walker and J. N. Kass, "Variation of Zircaloy Fracture Toughness in Irradiation," Zirconium in Nuclear Applications, ASTM STP 551, 1974, pp. 328-354.

55. S. Kusumoto, A. Nishioba, H. Maki, S. Usami, K. Hayashi, and Y. Ando, "Effects of Hydrogen Content, Temperature, and Crack Configuration on Fatigue Crack Propagation and Unstable Fracture Behavior of Zr-2.5 Nb Pressure Tube," Conf - 7309 A2 - P2.

56. P. J. Pankaskie, "Fatigue-Crack Growth and Propagation in 2.5 Nb Zirconium Alloy Pressure Tubing," Application-Related Phenomena for Zirconium and its Alloys, ASTM, STP 458, 1969, pp. 129-140.

57. P. J. Pankaskie, Unpublished Data.

58. P. A. Carlson, A. Russell, and J. P. Schmidt, "Zircaloy-2 Pressure Tube Experience at the N Reactor," Transactions of the American Nuclear Society, Vol. 16, Annual Meeting, Chicago 10-14 June 1973.

59. L. A. James and T. R. Ostrum, "Fracture Behavior of Flawed Zircaloy-2 Pressure Tubes," Nuclear Engineering and Design, 1970.

60. W. J. Langford and L. E. J. Mooder, "Metallurgical Properties of Irradiated Cold-Worked Zr-2.5 wt % Nb Pressure Tubes," Journal of Nuclear Materials, Vol. 39, 1971, pp. 292-302.

61. A. Cowan and W. J. Langford, "Effect of Hydrogen and Neutron Irradiation on the Failure of Flawed Zircaloy-2 Pressure Tubes," Journal of Nuclear Materials, Vol. 30, 1969, pp. 271-281.

62. W. J. Langford, "Metallurgical Properties of Cold-Worked Zircaloy-2 Pressure Tubes Irradiated under CANDU-PHW Power Reactor Conditions," ASTM STP 484, 1970, pp. 259-286.

63. M. C. Frazer, Postirradiation Evaluation of Zircaloy-2 PRTR Pressure Tubes - Part III," BNWL-5, January 1965.

64. R. V. Hesketh, J. E. Harbottle, N. A. Waterman and R. C. Lobb, "Irradiation Growth and Creep in Zircaloy-2," Proceeding of the Symposium on Radiation Damage in Reactor Materials, Vol. 1, 1969, International Atomic Energy Agency, Vienna.

65. J. E. Harbottle, "The Temperature and Neutron Dose Dependence of Irradiation Growth in Zircaloy-2," Irradiation Effects on Structural Alloys for Nuclear Reactor Applications, ASTM STP 484, 1970, pp. 287-299.

66. V. Fidleris, "The Effect of Cold-Work and Stress-Relieving on the Irradiation Growth Behavior of Zirconium Alloys," Journal of Nuclear Materials, Vol. 46, 1973, pp. 356-360.

67. E. F. Ibrahim and J. E. Winegar, "Dimensional Changes of Unstressed Zircaloy-2 and Zr-2.5 wt % Nb Specimens in a Fast Flux," Journal of Nuclear Materials, Vol. 45, 1972/3 pp. 335-338.

68. R. N. Duncan, N. Fuhrman, J. C. LaVake, H. Knaab, and R. Manzel, "Dimensional Stability of Water Reactor Fuel," 75-CNA/ANS-100, Proceedings of the Joint Topical Meeting on Commercial Nuclear Fuel Technology Today, April 28-30, 1975, Toronto.

69. G. J. C. Carpenter and D. O. Northwood, "The Contribution of Dislocation Loops to Radiation Growth and Creep of Zircaloy-2," Journal of Nuclear Materials, Vol. 56, 1975, pp. 260-266.

70. R. V. Hesketh, "Non-Linear Growth in Zircaloy-4," Journal of Nuclear Materials, Vol. 30, 1969, pp. 219-221.

71. S. N. Buckley, "Irradiation Growth and Irradiation Enhanced Creep in F. C. C. and B. C. C. Metals," UKAEA Report AERE-R5944, Vol. II., pp. 547-565.

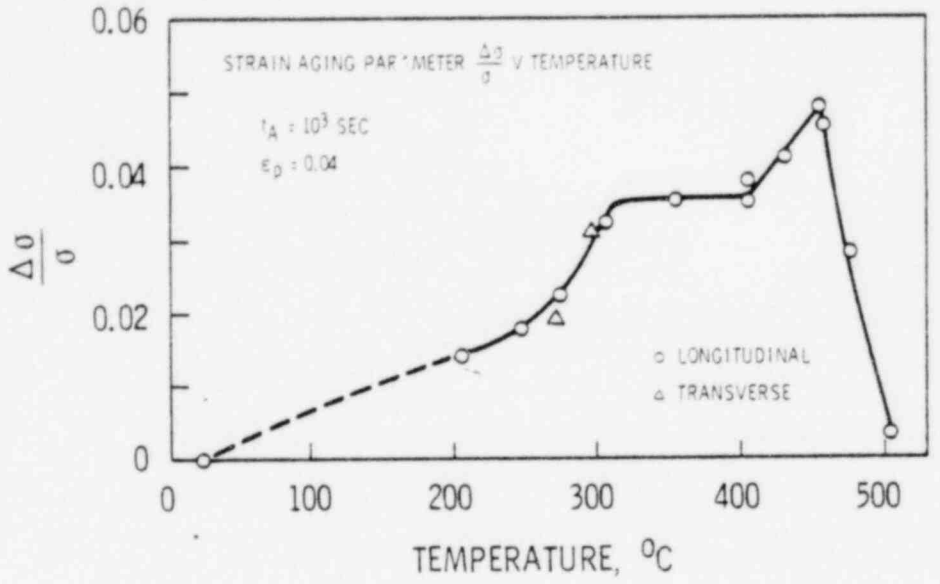

FIGURE 1a. Strain Aging Verus Temperature for Zircaloy-2 (From Reference 7)

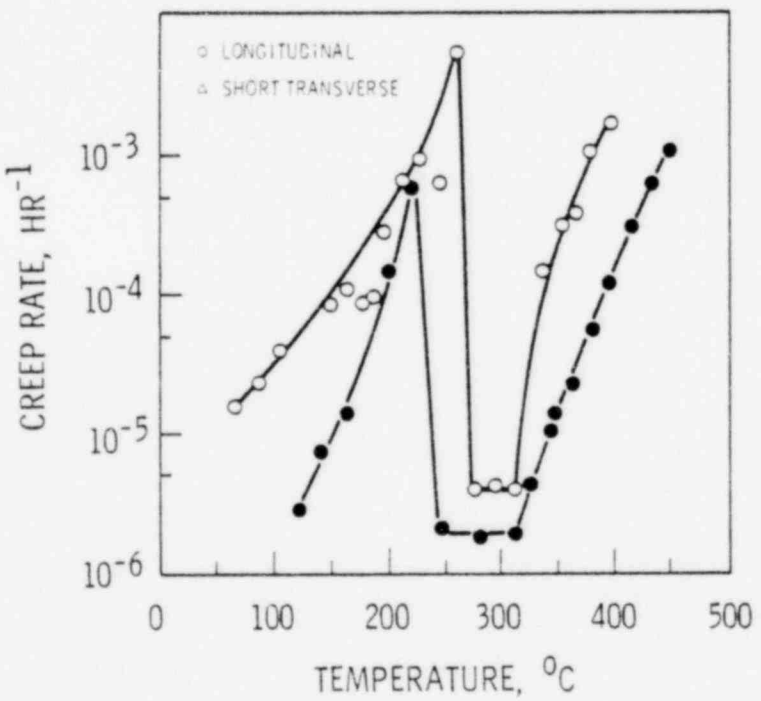

FIGURE 1b. Variation of Creep Rate of Annealed Zircaloy-2 with Temperature at a Stress of 20 ksi (From Reference 7)

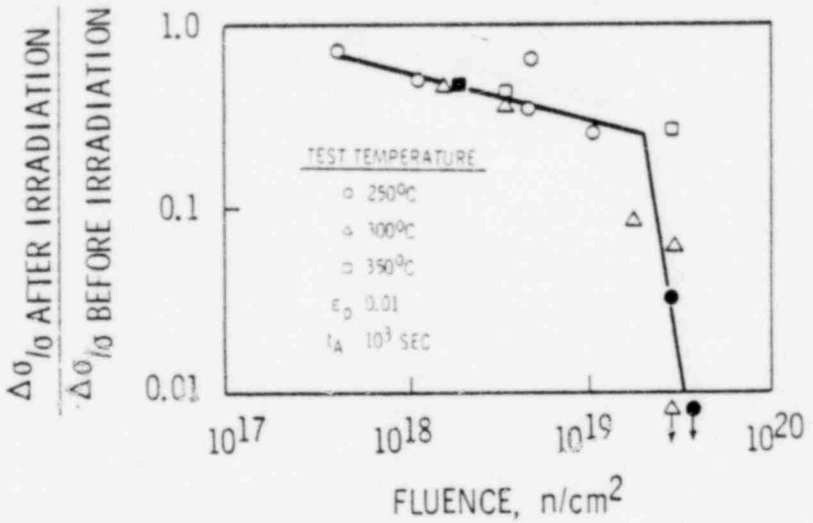

FIGURE 1c. Suppression of Strain Aging by Irradiation at a Fluence Greater than 5 E 19 n/cm^2 (From Reference 7)

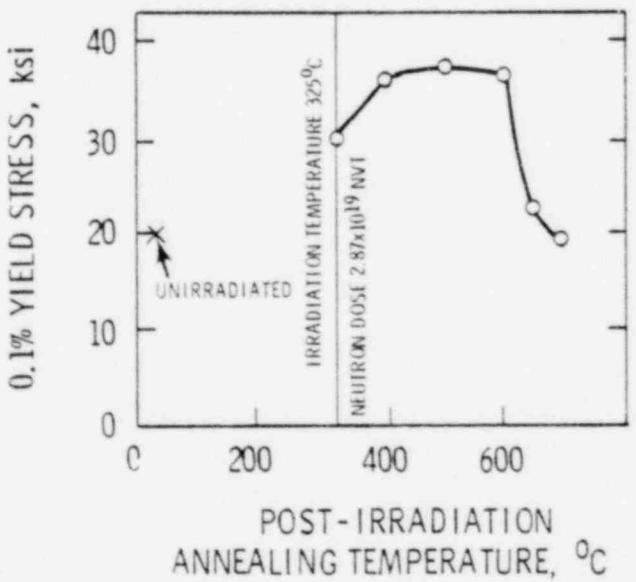

FIGURE 1d. Curve Showing 0.1% Yield Stress of Zircaloy-2 after Postirradiation Annealing for one Hour (From Reference 7)

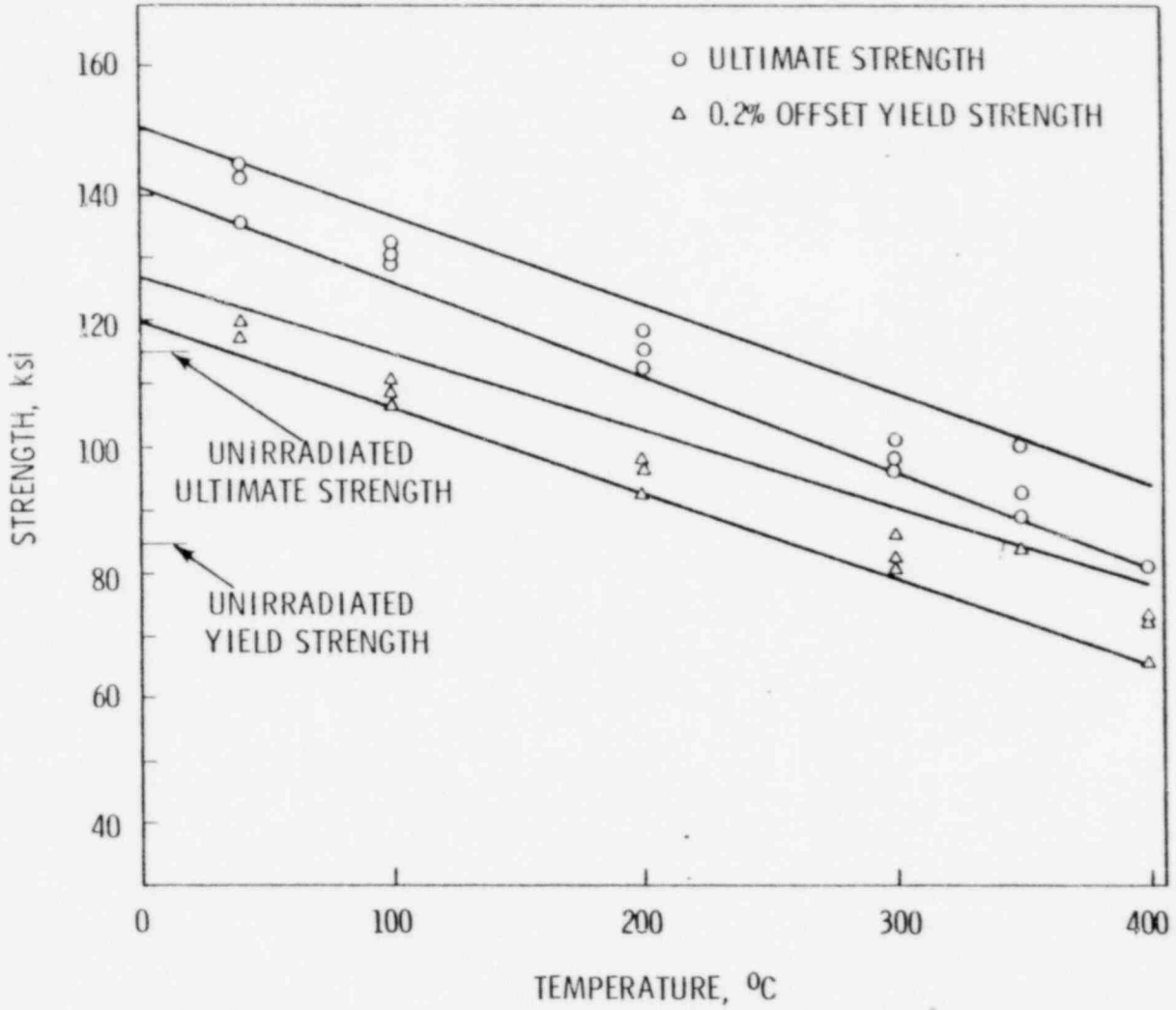

FIGURE 2. Effect of Temperature on the Strength of Irradiated Zircaloy Fuel-Rod Tubing (From Reference 28)

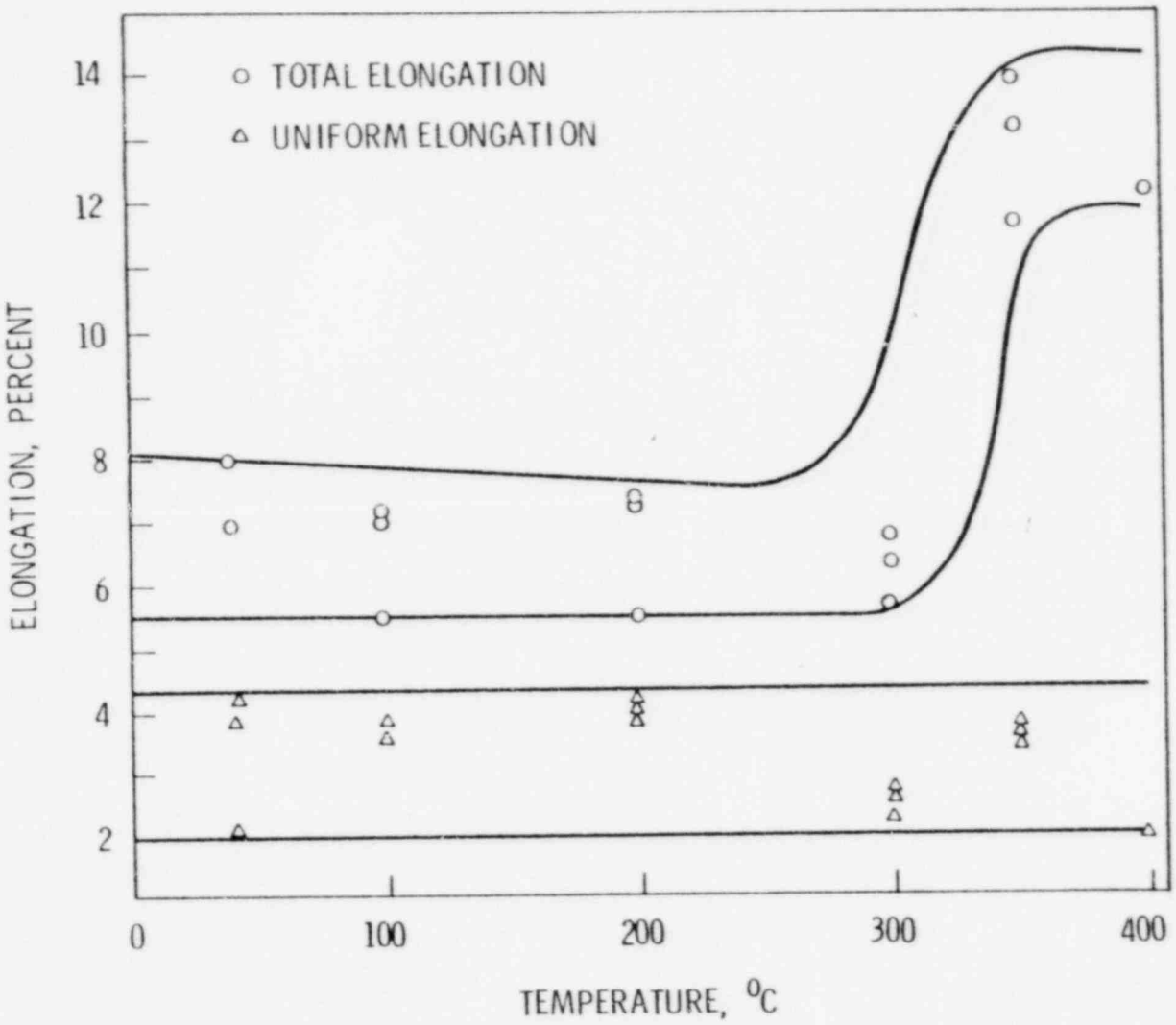

FIGURE 3. Effect of Temperature on the Ductility of Irradiated Zircaloy Fuel-Rod Tubing (From Reference 28)

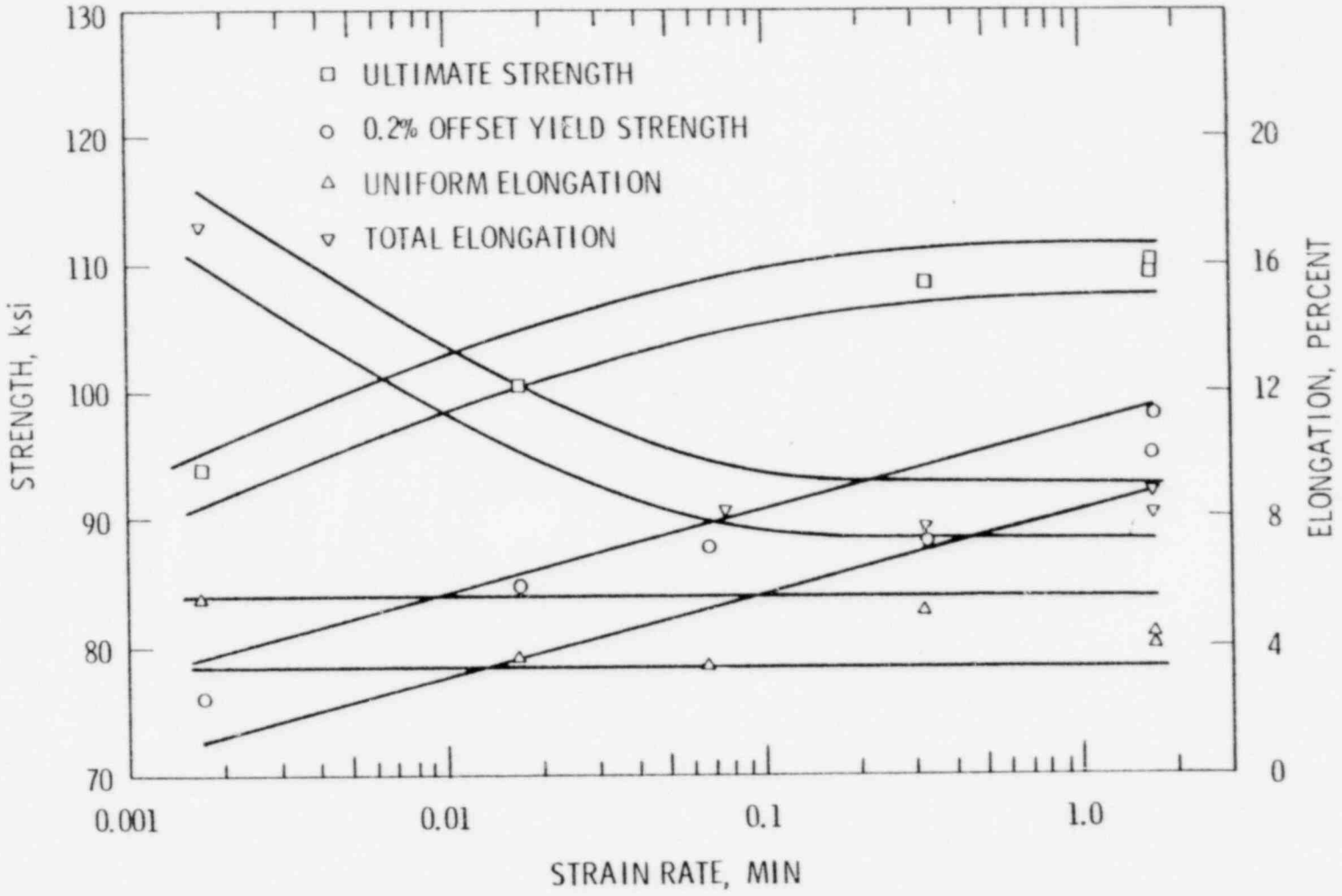

FIGURE 4. Effect of Strain Rate at 370°C on the Tensile Properties of Irradiated Zircaloy Fuel-Rod Tubing (From Reference 28)

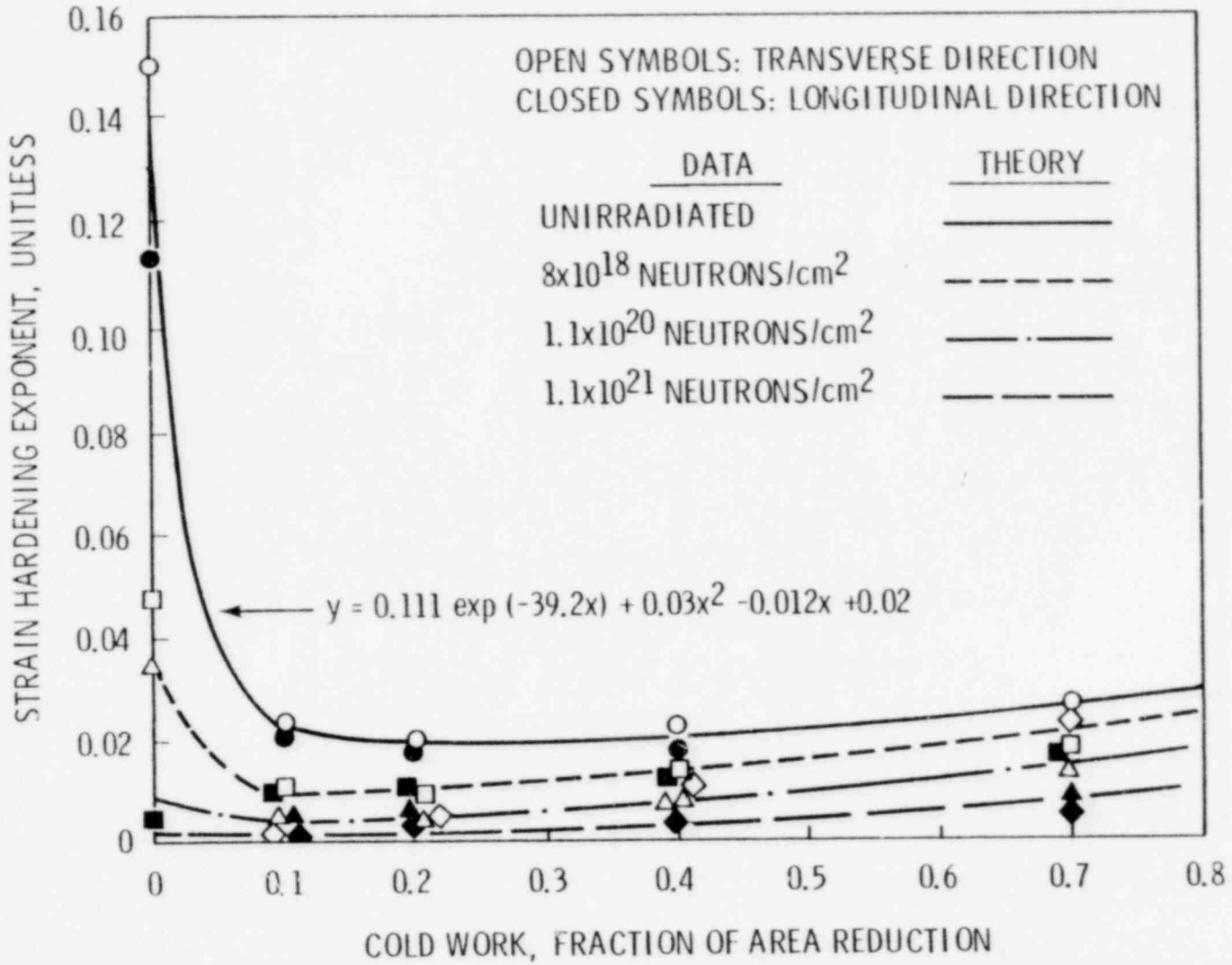

FIGURE 5. Data and Analytical Functions for Strain Hardening Coefficient as a Function of Cold Work and Irradiation at Room Temperature (From Reference 21)

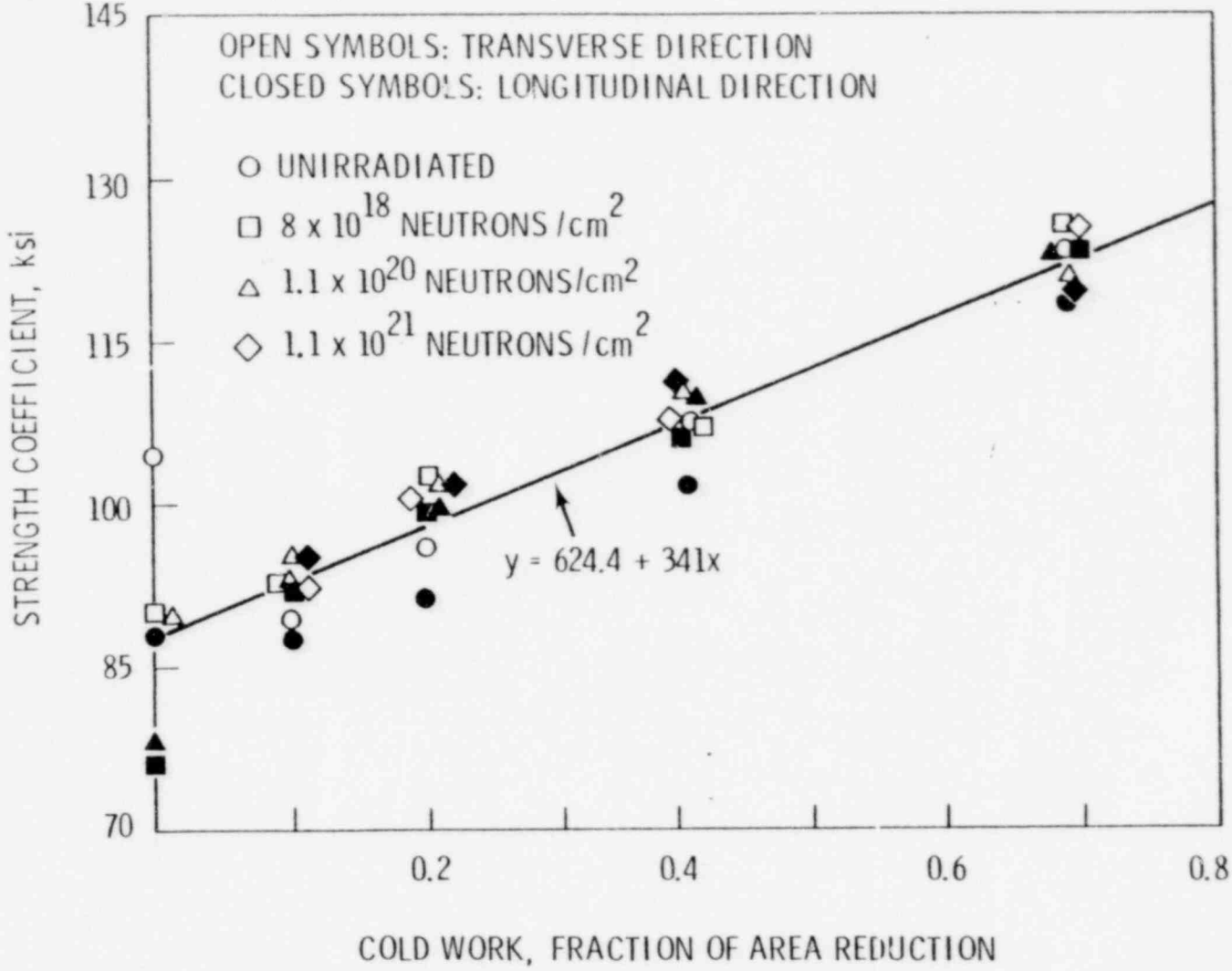

FIGURE 6. Strength Coefficient for Zircaloy-2 as a Function of Cold Work and Fluence (From Reference 21)

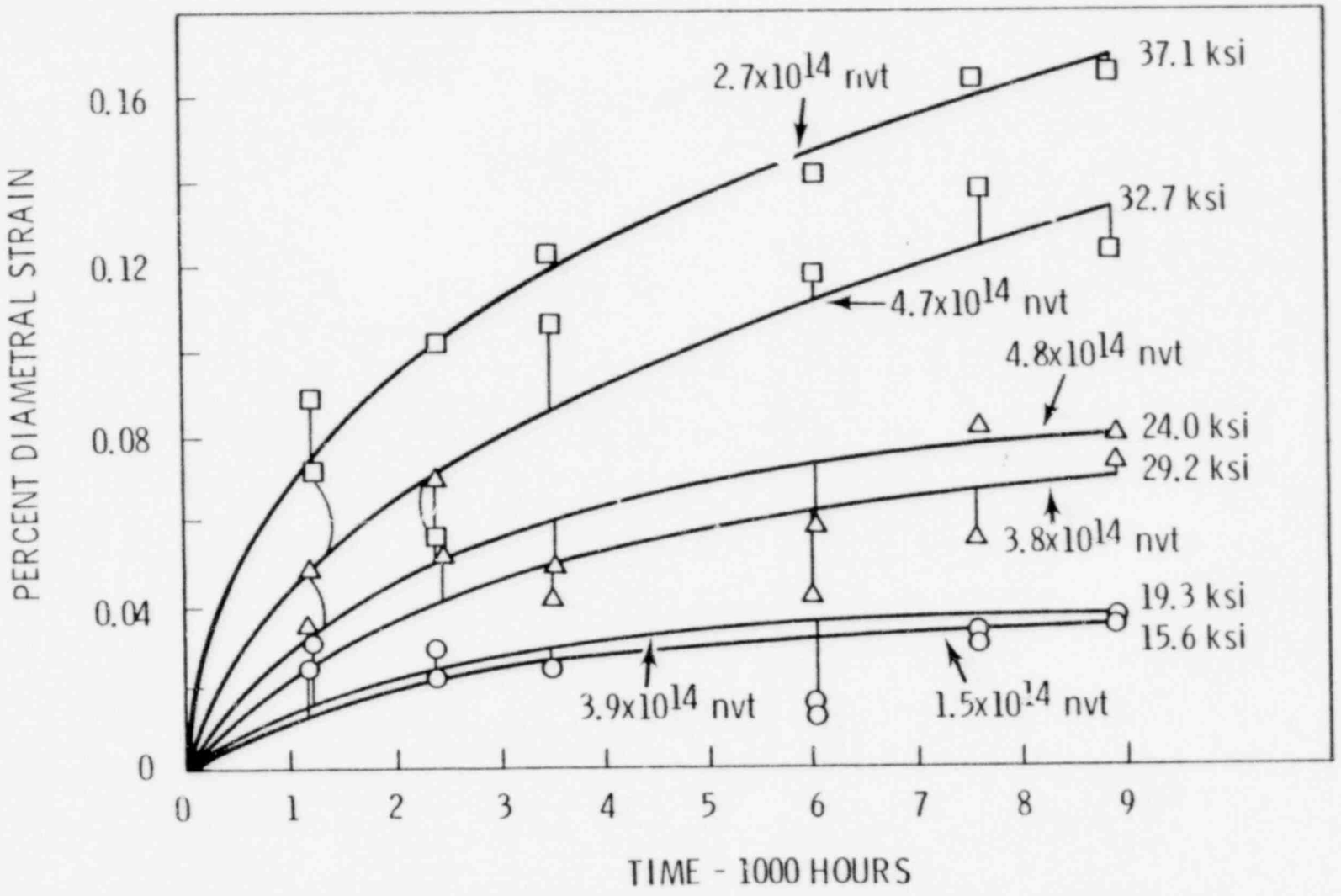

FIGURE 7. Creep Curves for Diametral Creep of Zircaloy-2 Tubes in Thermal Neutron Flux of 1.4 E13 to 1.5 E14 n/cm^2 s at 258^{o}C (From Reference 33)

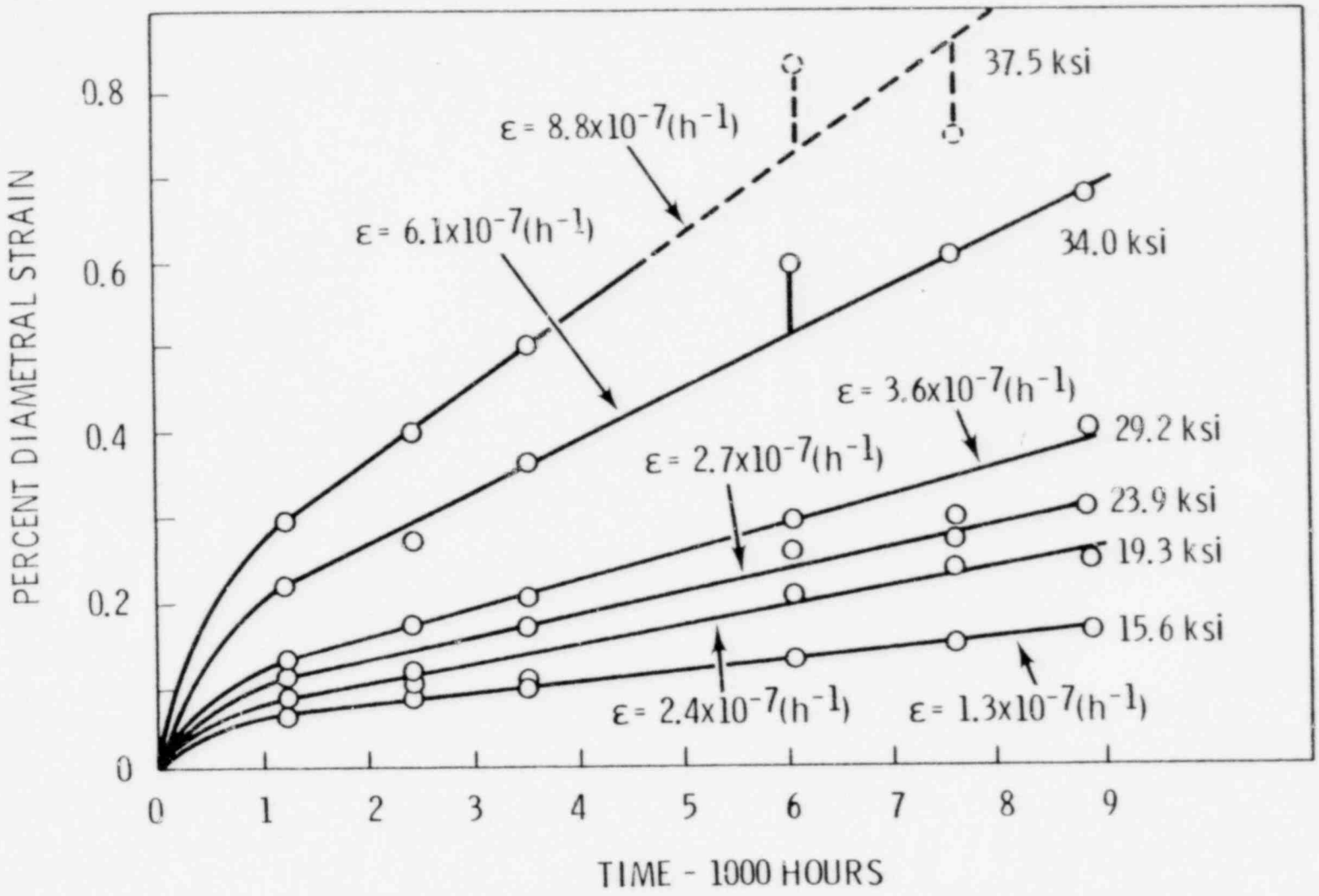

FIGURE 8. Creep Curves for Diametral Creep of Zircaloy-2 Tubes in a Fast-Flux of 2.56 E13 n/cm^2 s at 258^{o}C (From Reference 33)

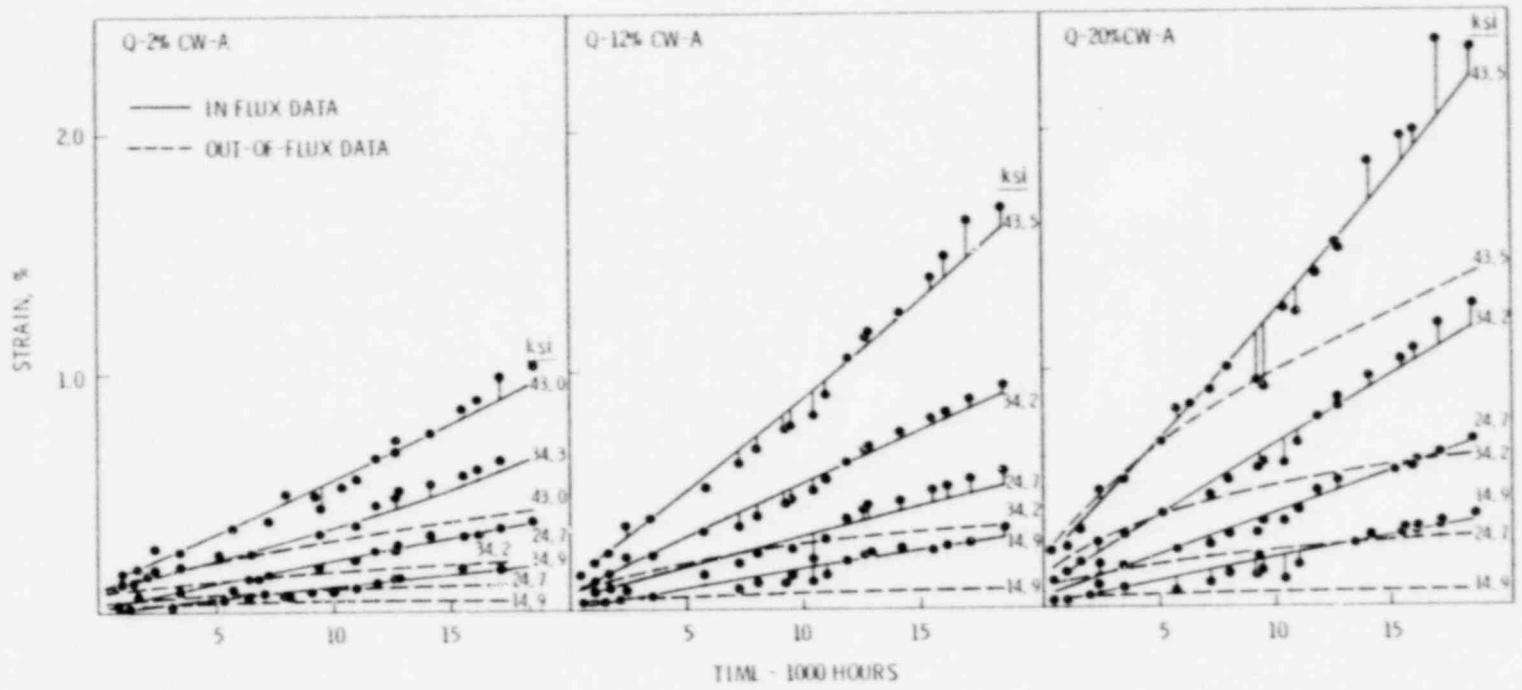

FIGURE 9. Curves for Diametral Creep of Quenched, Cold-Drawn and Aged Zr-2.5% Nb, Out-of-Flux and in a Fast Neutron Flux (2.3 E13 n/cm^2 sec) 1 MeV at 295^{o}C (From Reference 34)

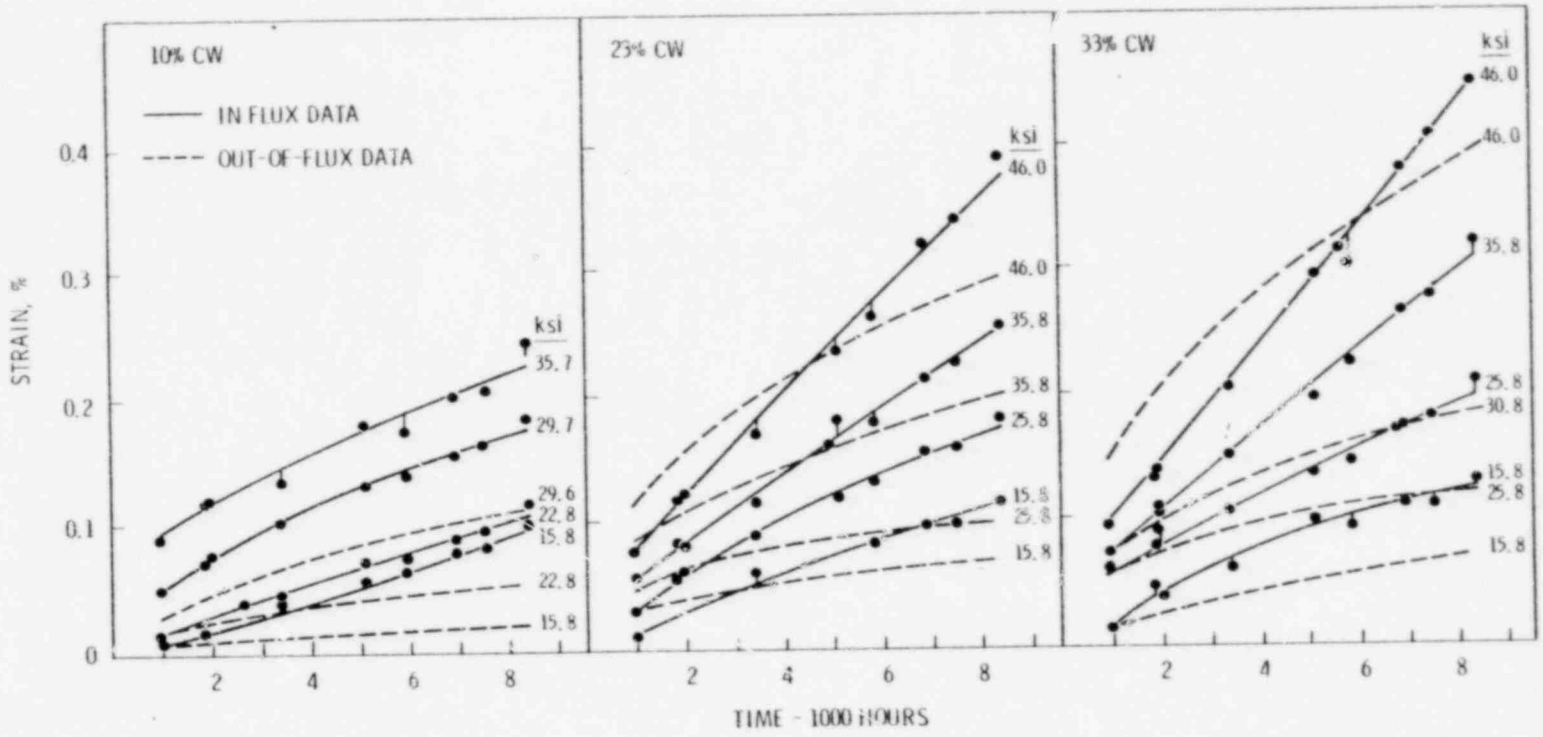

FIGURE 10. Curves for Diametral Creep of Cold Drawn Zr-2.5% Nb, Out-of-Flux and in a Fast Neutron Flux (1.9 E13 n/cm^2 sec) 1 MeV at 295°C (From Reference 34)

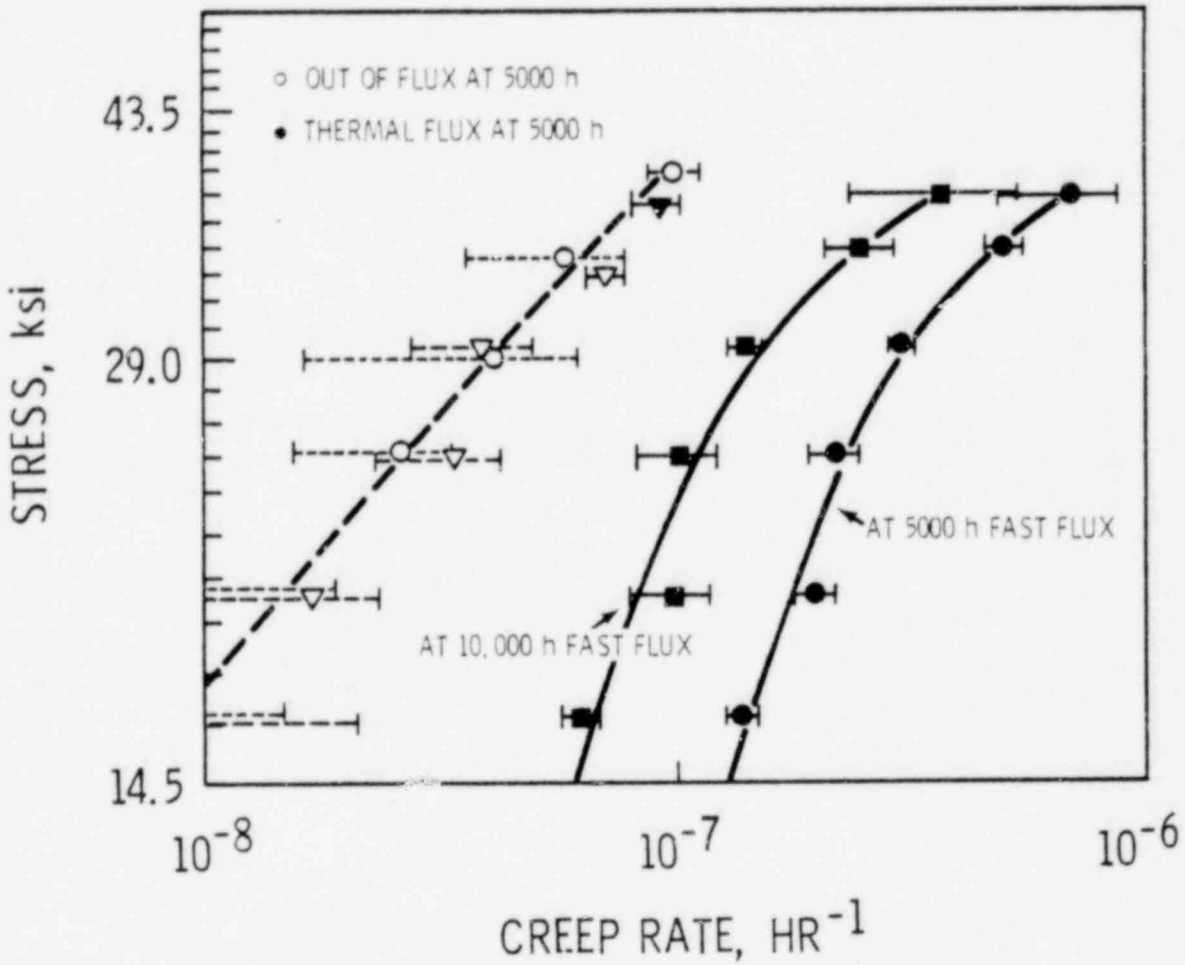

FIGURE 11. Creep Rates of 20% Cold Drawn Zircaloy-2 Specimens at 263°C in-and out-of-Neutron Fluxes (From Reference 35)

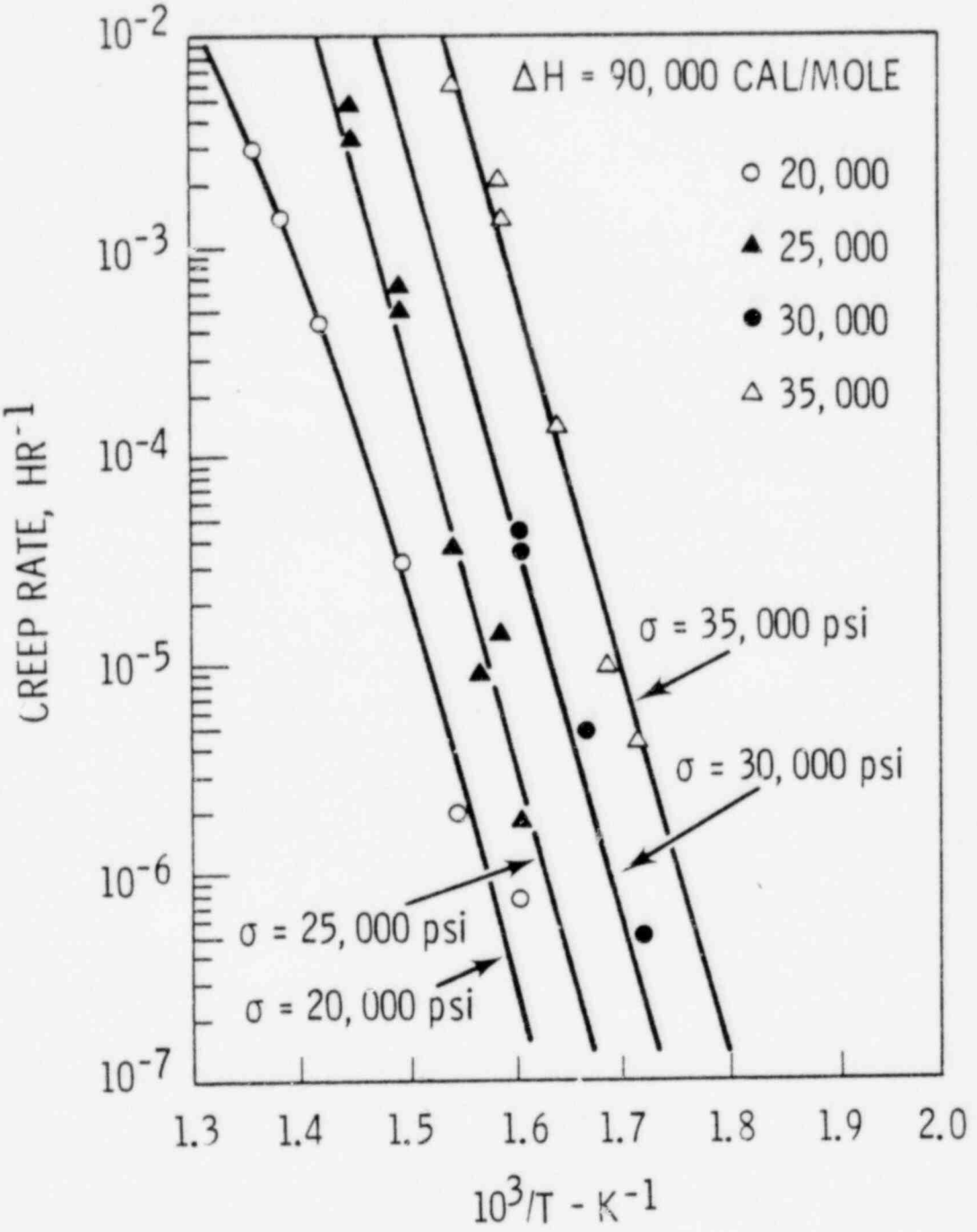

FIGURE 12. Arrhenius Plot of In-Reactor Creep Data (From Reference 36)

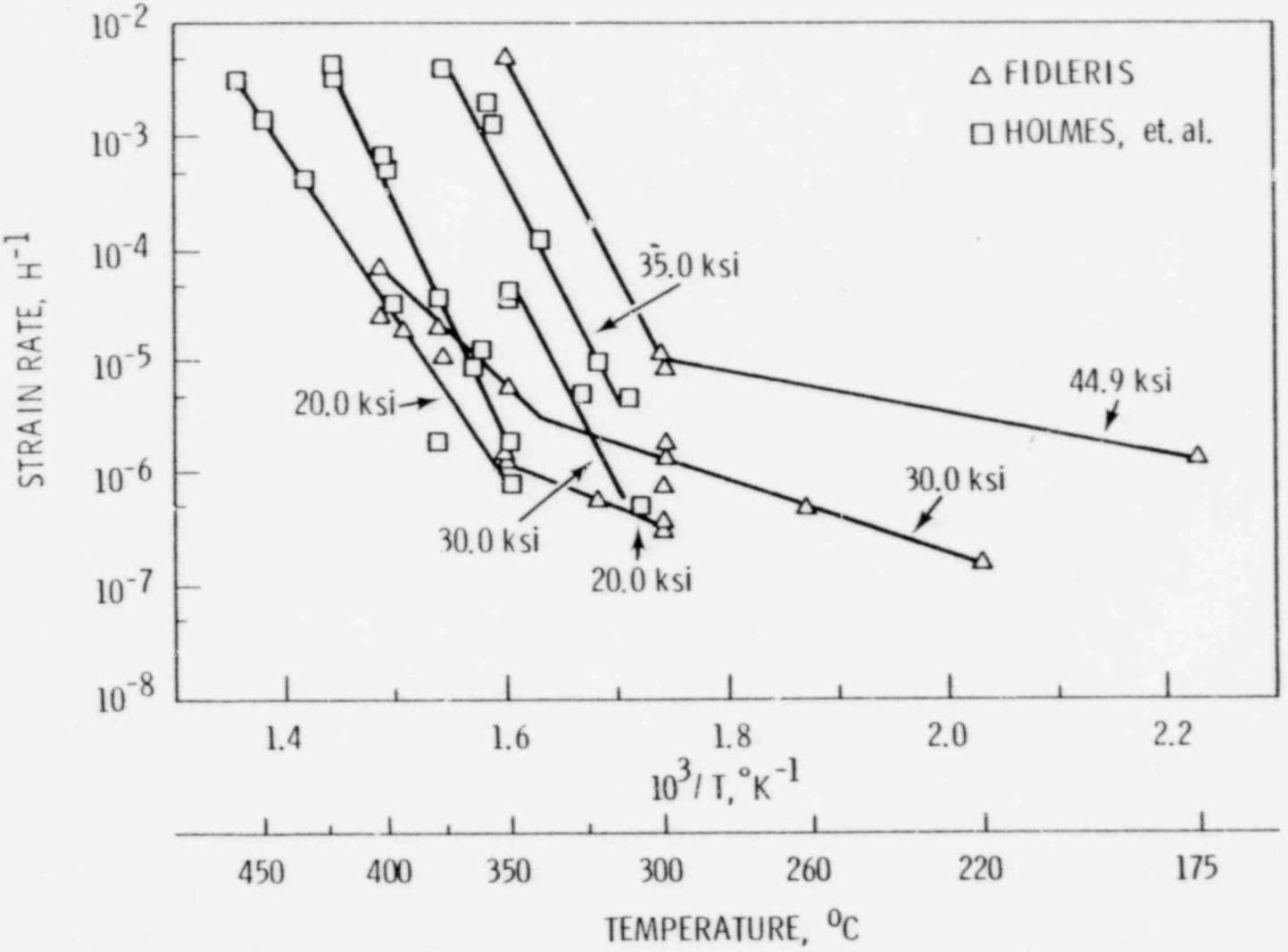

FIGURE 13. In-Reactor Creep of Cold-Worked Zircaloy-2 Showing the Effect of Temperature on Creep Rate (From Reference 37)

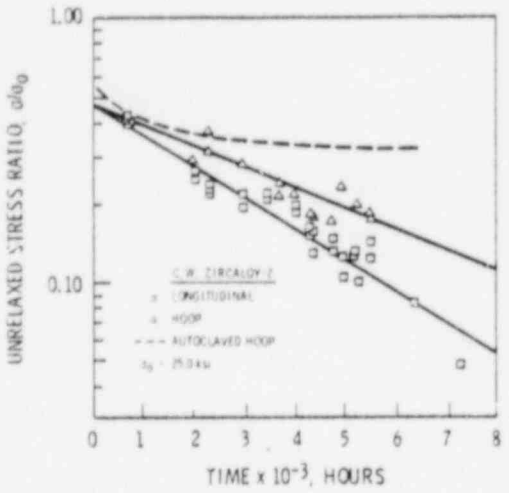

FIGURE 14a. Unrelaxed Stress Ratio as a Function of Time for Cold-Worked Zircaloy-2 Showing the Behavior of Longitudinal and Hoop Specimens In-Reactor at 239°C and Comparing the Data for Hoop Specimens with Those from AutoClave Tests at 300°C (From Reference 38)

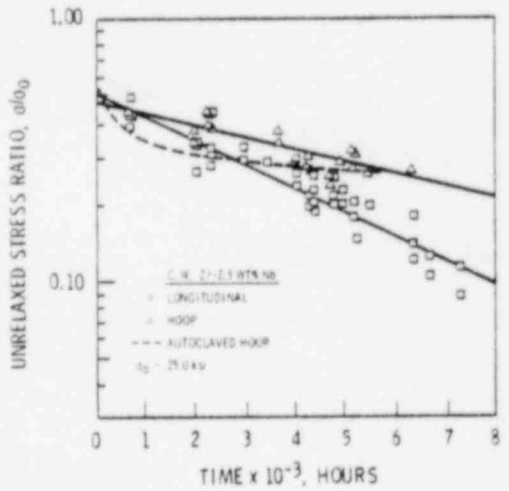

FIGURE 14b. Unrelaxed Stress Ratio as a Function of Time for Cold-Worked Zr-2.5 wt% Nb Showing the Behavior of Longitudinal and Hoop Specimens In-Reactor at 293°C and Comparing the Data for Hoop Specimens with Those from Autoclave Tests at 300°C (From Reference 37)

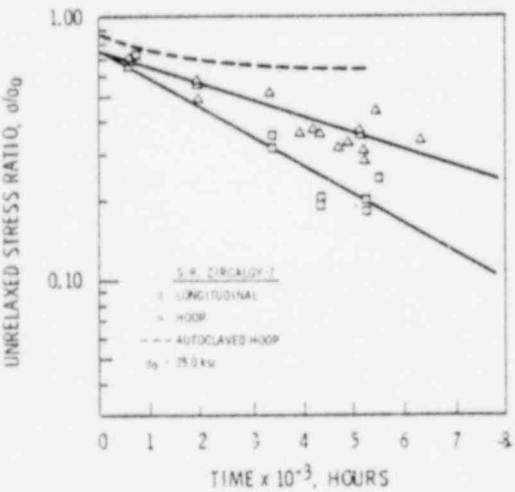

FIGURE 14c. Unrelaxed Stress Ratio as a Function of Time for Stress-Relieved Zircaloy-2 Showing the Behavior of Longitudinal and Hoop Specimens In-Reactor at 293°C and Comparing the Data for Hoop Specimens with Those from Autoclave Tests at 300°C (From Reference 38)

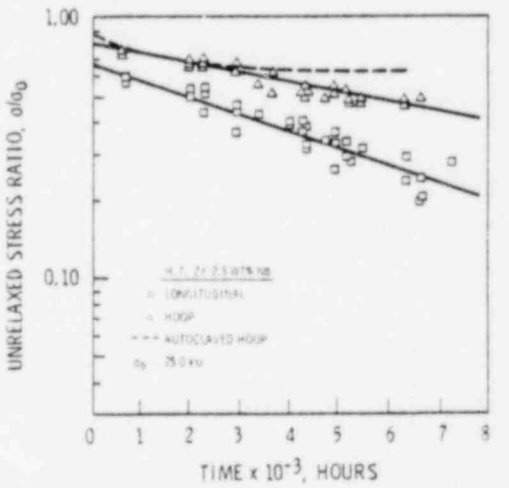

FIGURE 14d. Unrelaxed Stress Ratio as a Function of Time for Heat-Treated Zr-2.5 wt% Nb Showing the Behavior of Longitudinal and Hoop Specimens In-Reactor at 293°C and Comparing the Data for Hoop Specimens with Those from Autoclave Tests at 300°C (From Reference 38)

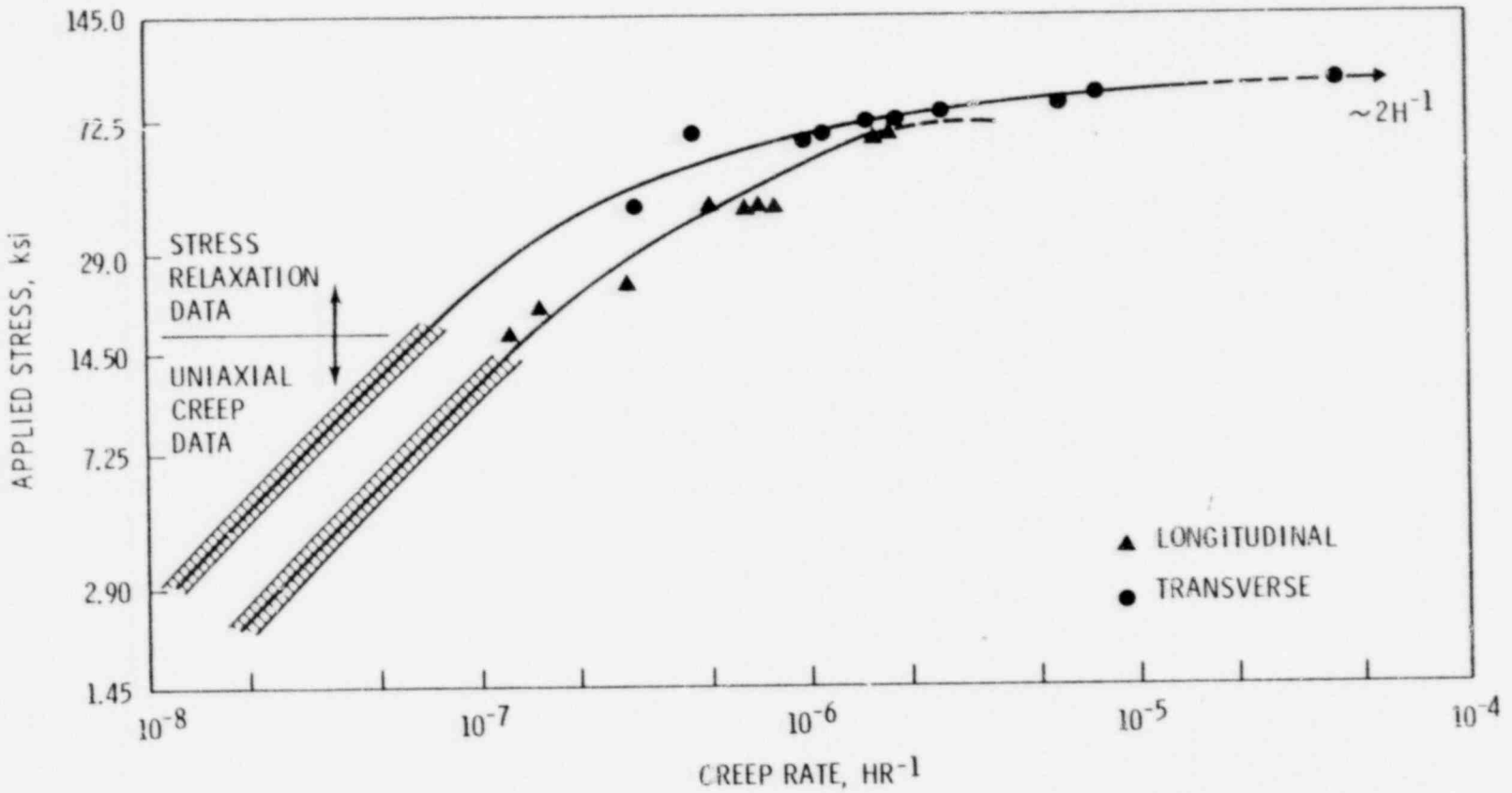

FIGURE 15. Stress Dependence of the In-Flux Creep Rate for Cold-Worked Zr 2.5 wt% Nb (From Reference 39)

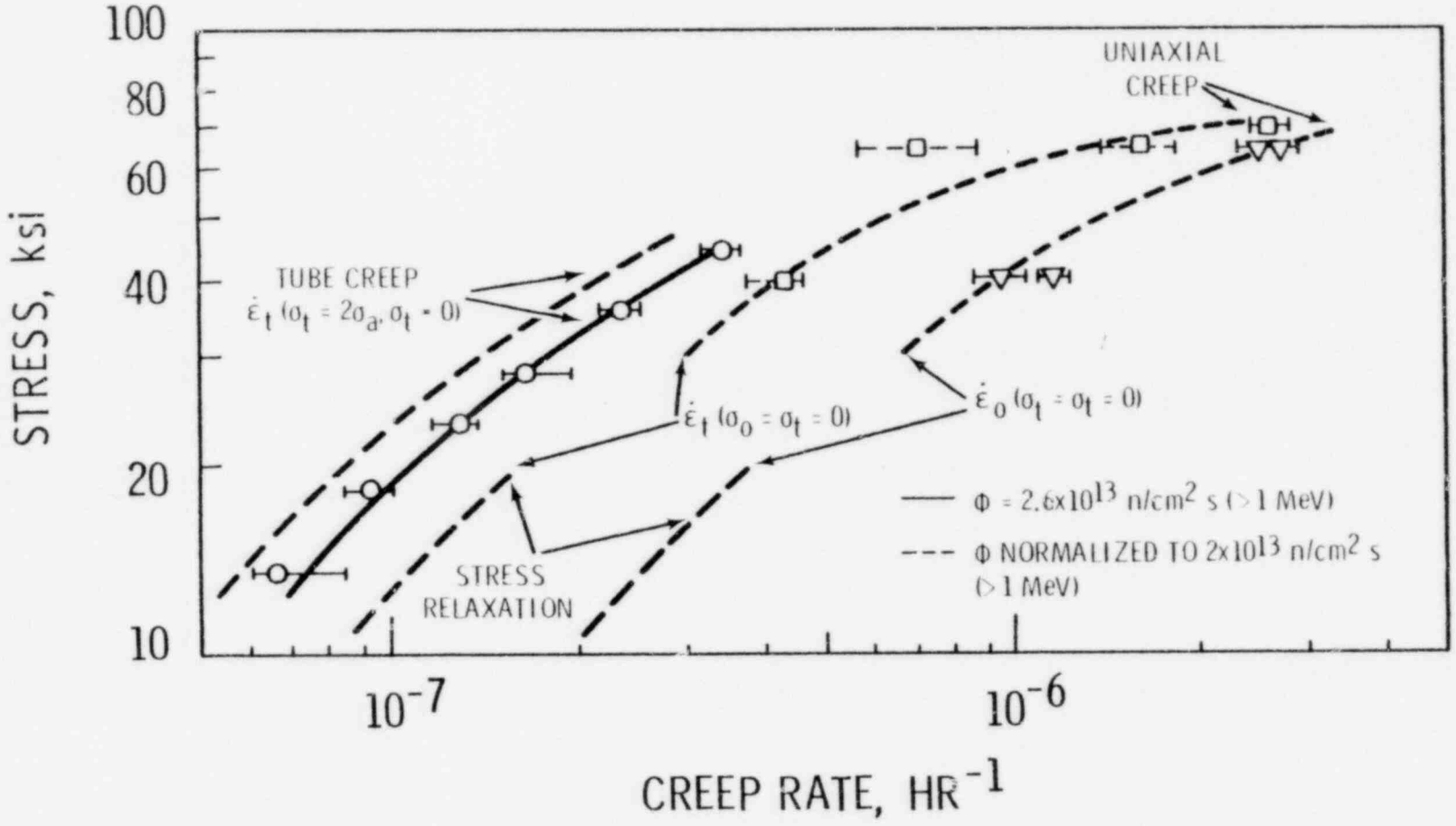

FIGURE 16. Stress Versus Creep Rate Results for Zr-2.5 wt% Nb from Stress-Relaxation, Uniaxial Creep and Tube Tests at 285°C (From Reference 40)

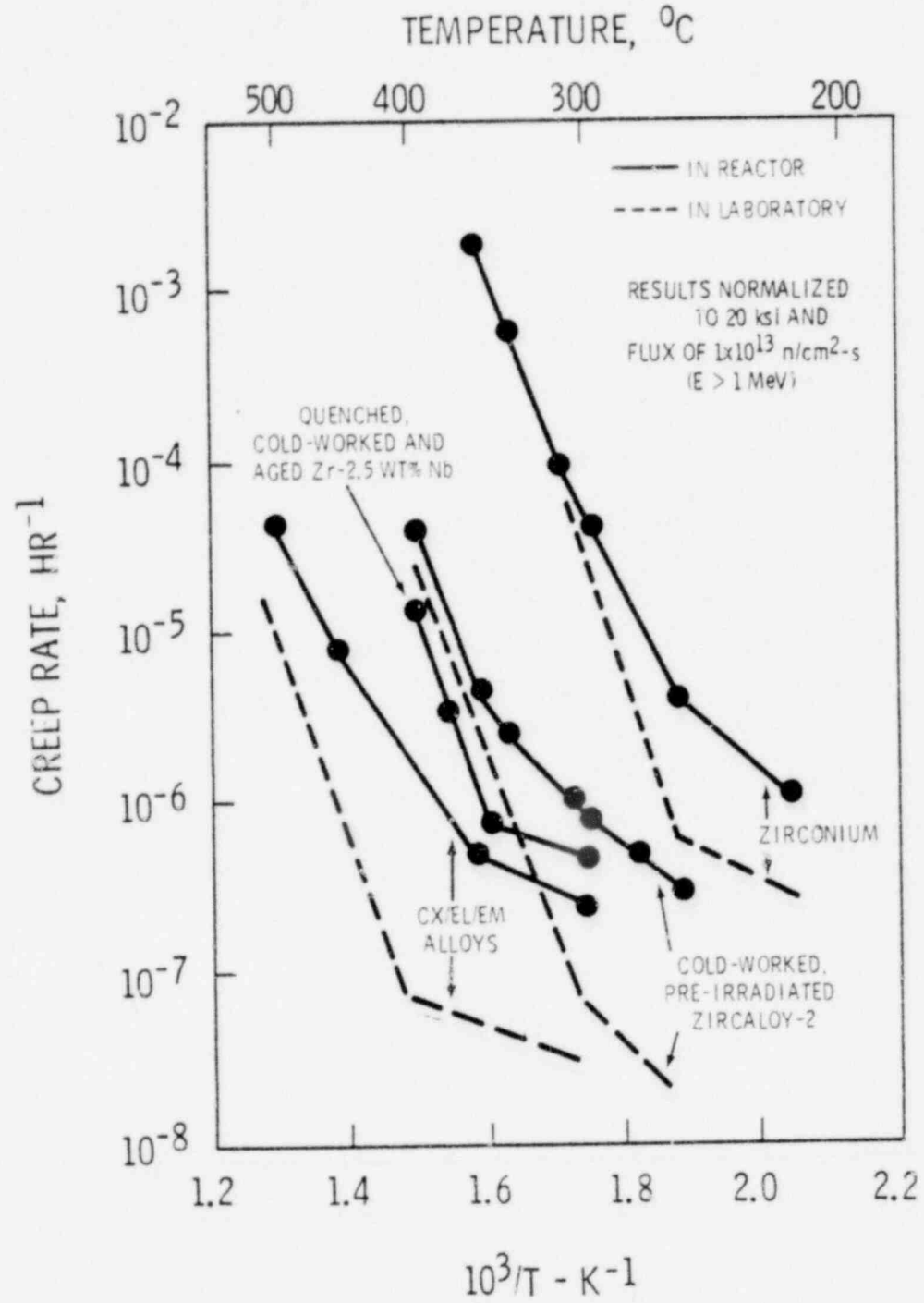

FIGURE 17. Effect of Alloying on In-Reactor Creep (From Reference 30)

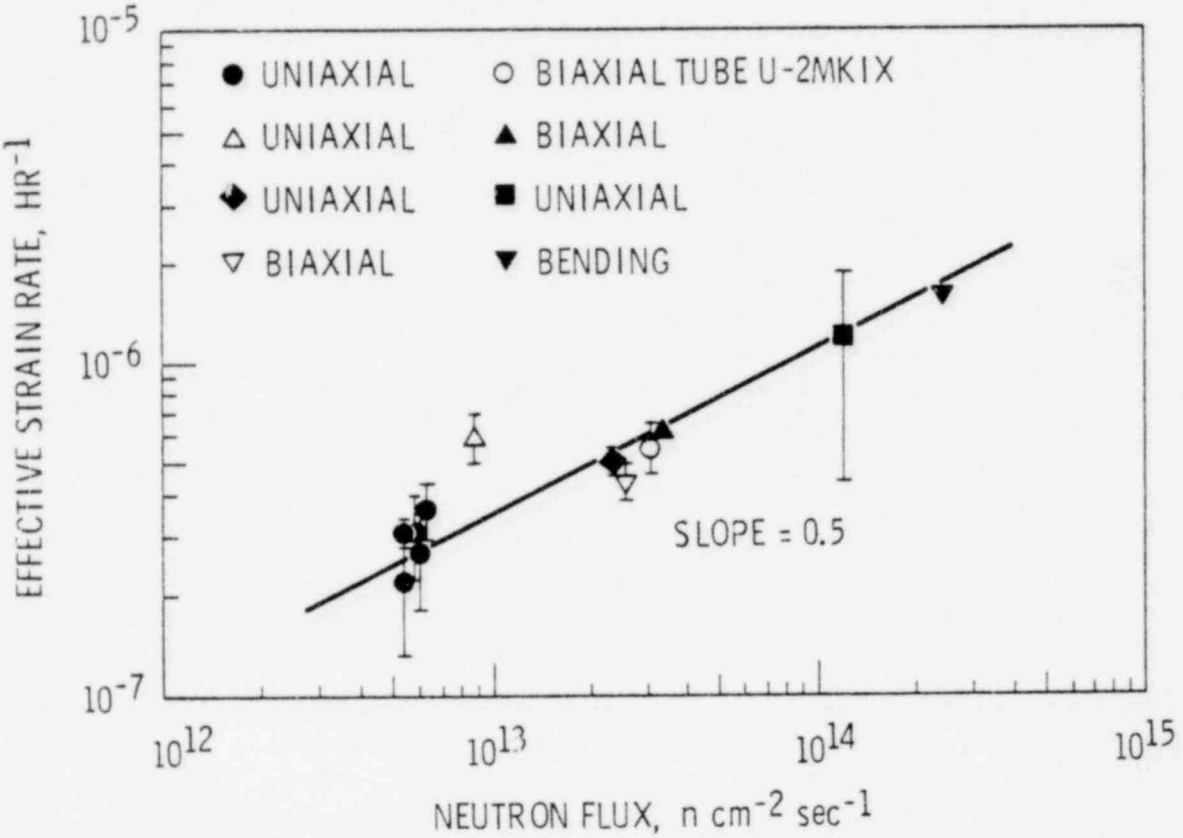

FIGURE 18. Effect of Neutron Flux on Creep Rate of Cold-Worked Zircaloy Normalized to an Effective Stress of 20,000 psi and 300°C. The Creep Rates Plotted Represent the Total Effective Creep Rate Less the Effective Creep Rate Measured in Tests on Unirradiated Specimens (From Reference 29)

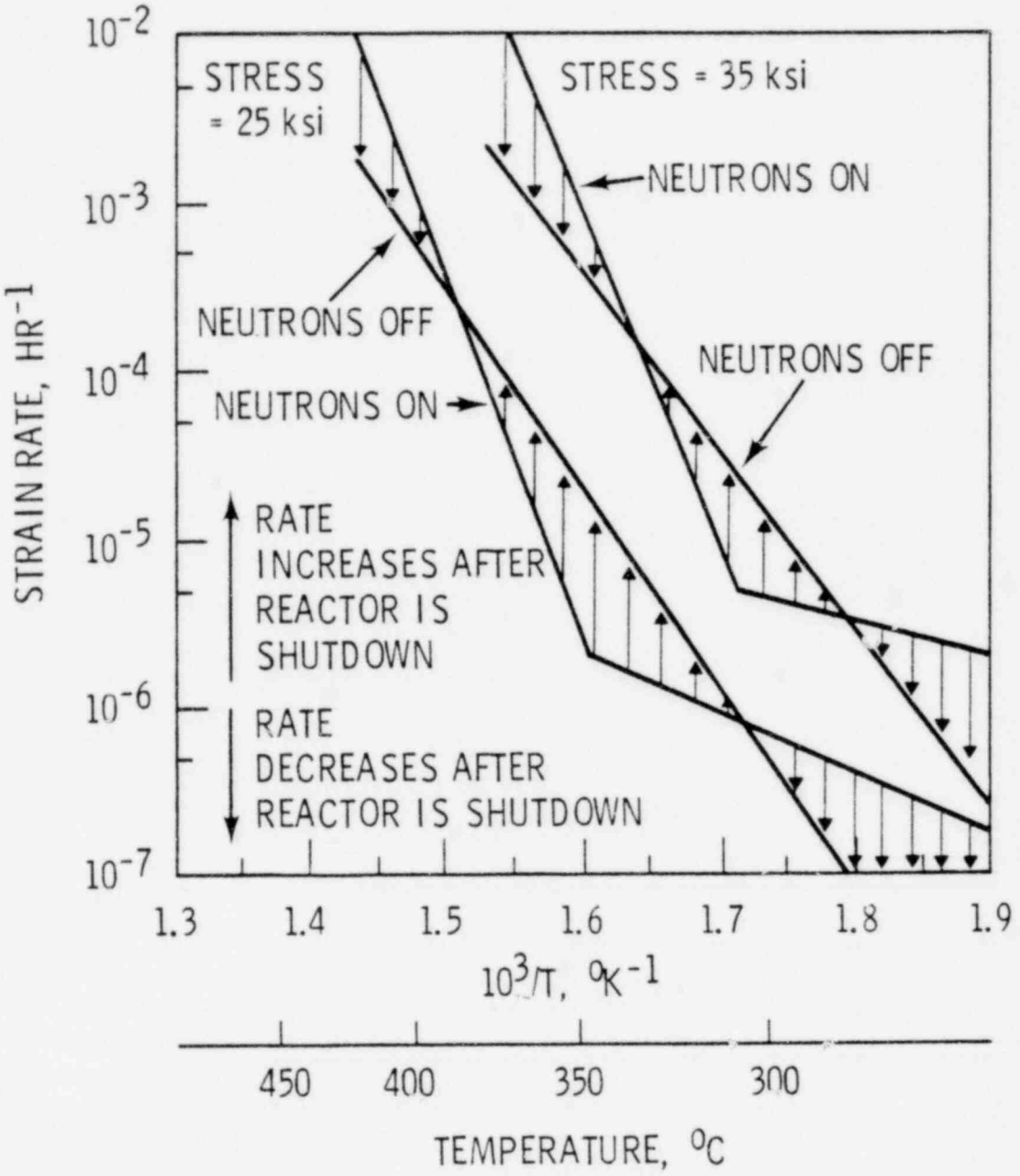

FIGURE 19. In-Reactor Creep of Cold-Worked Zircaloy-2 Showing Effect of Fast Neutron Flux on Creep Rate (From Reference 29, 37)

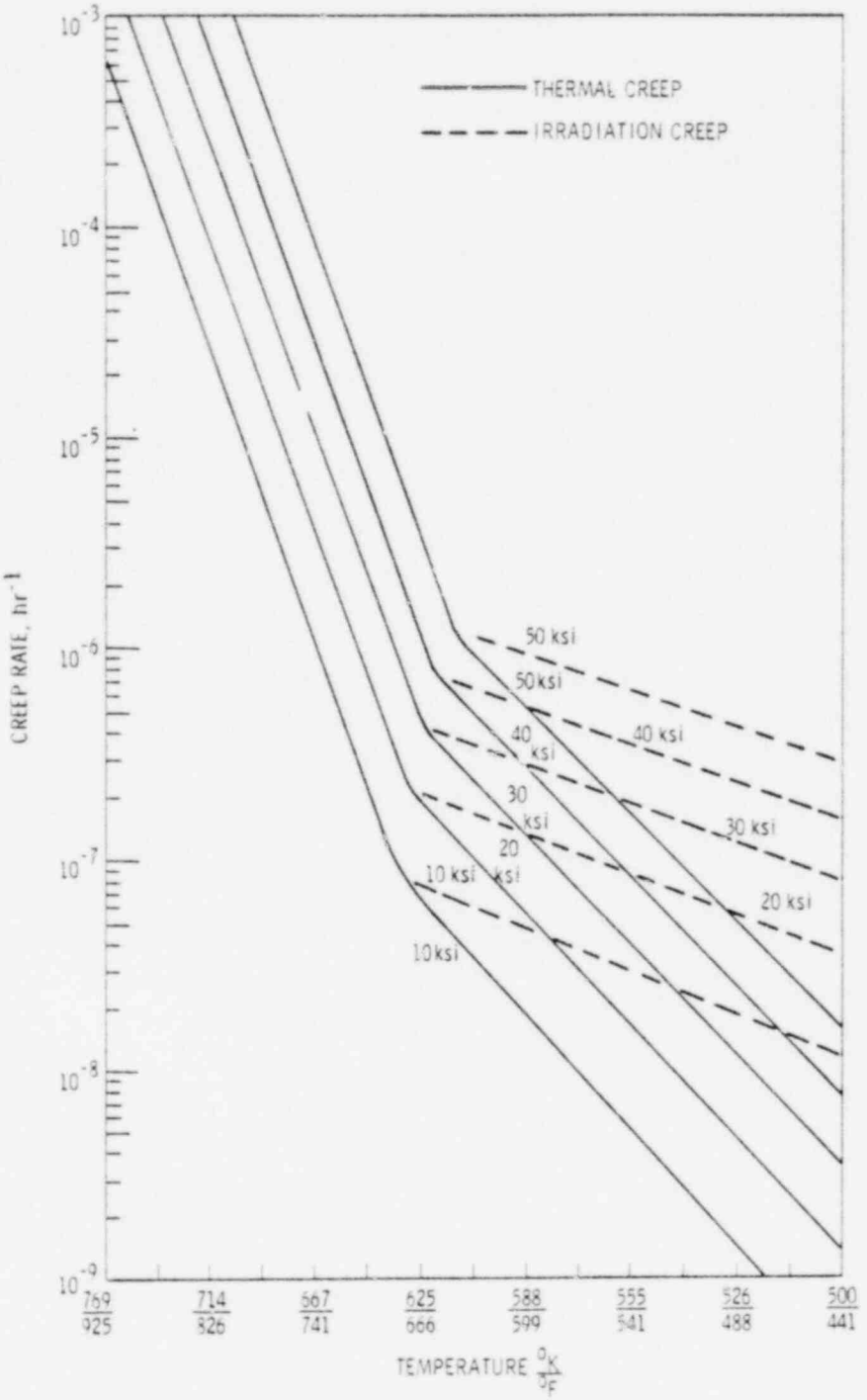

FIGURE 20. Calculated Creep Rate as a Function of Irradiation Temperature for a Flux of 6.0 E12 n/cm^{2}s (From Reference 41)

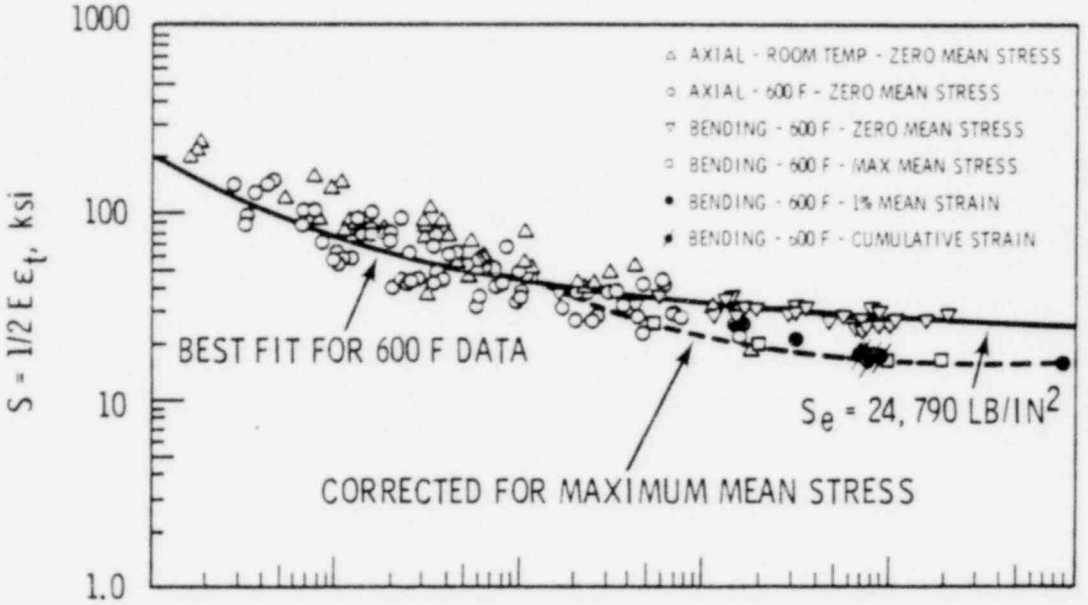

FIGURE 21a. Fatigue Data on Unirradiated Zircaloy-2 (From Reference 52)

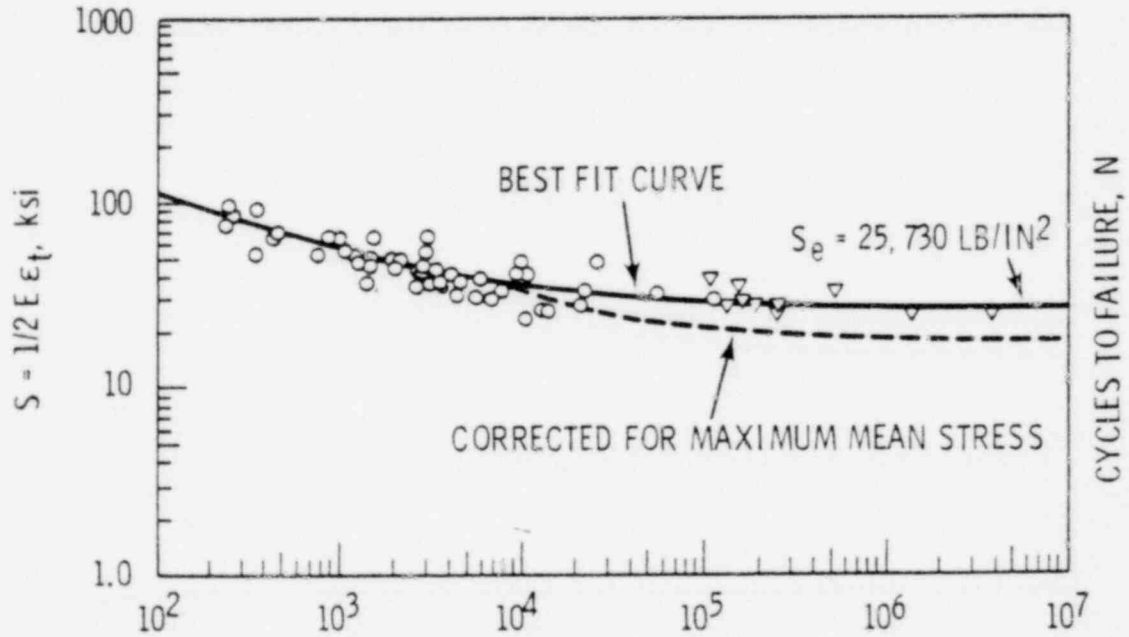

FIGURE 21b. Fatigue Data on Irradiated Zircaloy-2 (1.5 x E21 to 5.5 x E21 n/cm^2 s > 0.625 MeV) (From Reference 52)

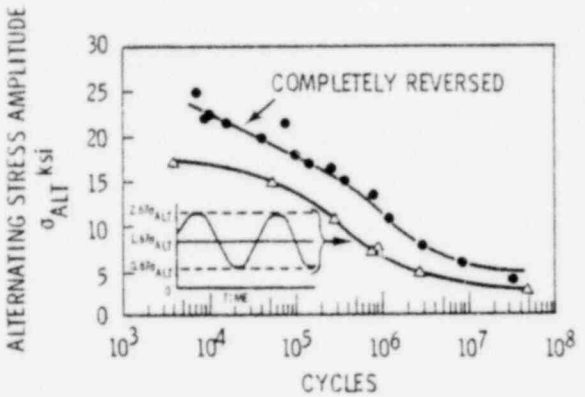

FIGURE 22a. Effect of Mean Stress on Fatigue Life (From Reference 52)

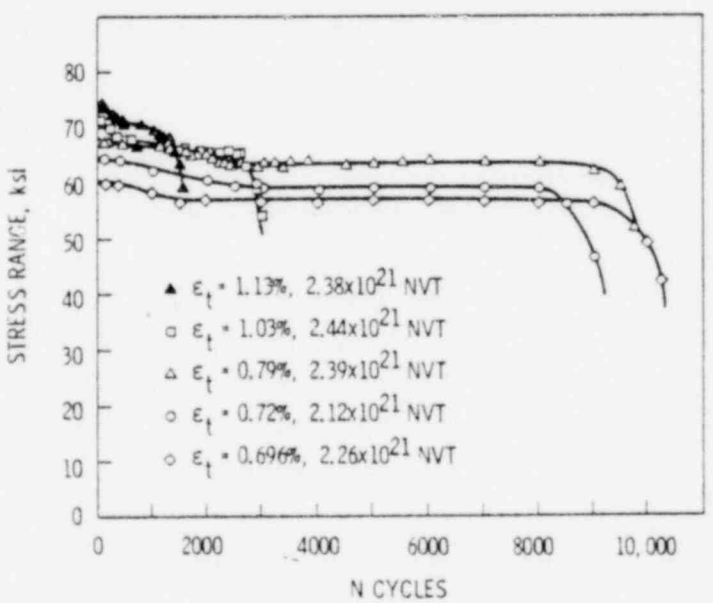

FIGURE 22b. Axial Strain Fatigue Data for Irradiated Alpha-Annealed Zircaloy-2 at 315°C (Longitudinal Direction) (From Reference 52)

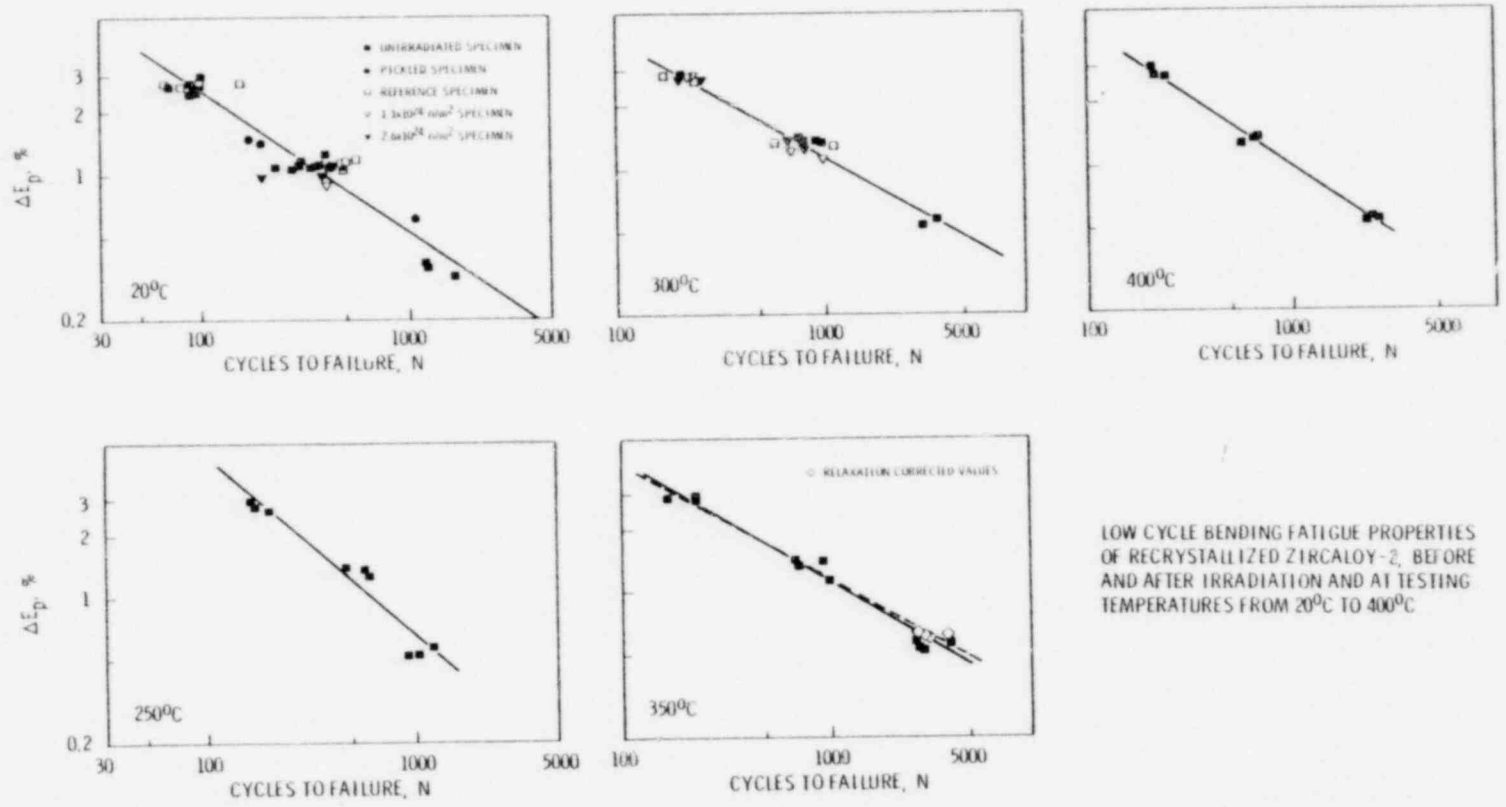

LOW CYCLE BENDING FATIGUE PROPERTIES OF RECRYSTALLIZED ZIRCALOY-2, BEFORE AND AFTER IRRADIATION AND AT TESTING TEMPERATURES FROM 20°C TO 400°C

FIGURE 23. Low Cycle Bending Fatigue Properties of Recrystallized Zircaloy-2, Before and After Irradiation and at Testing Temperatures from 20°C to 400°C (From Reference 59)

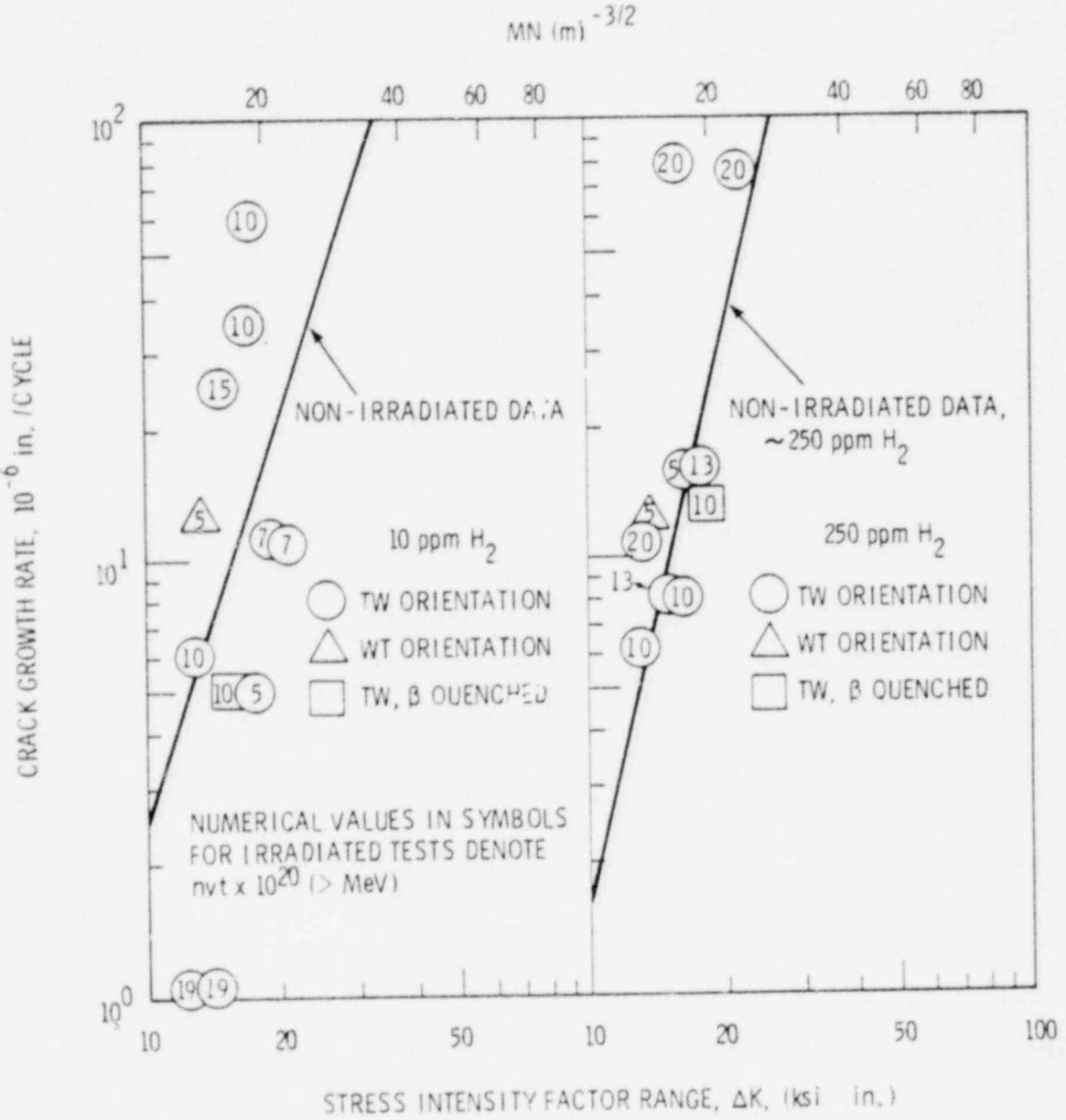

FIGURE 24. Fatigue Crack Growth Rate for Irradiated and Non-Irradiated Zircaloy-A Rolled Plate (From Reference 54)

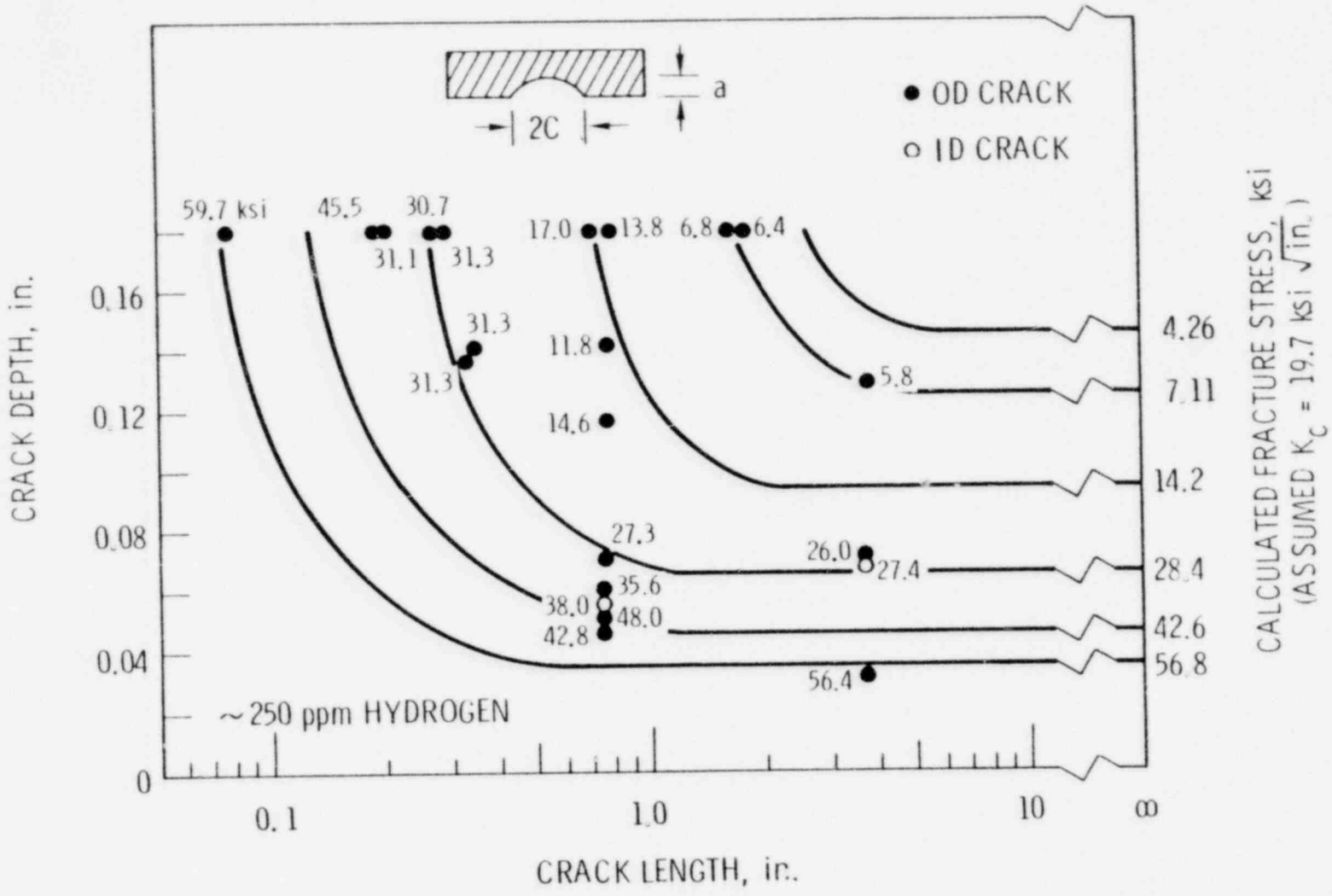

FIGURE 25. Effect of Crack Depth and Length on the Fracture Strength of Hydrided Zr-2.5 Nb Tubing at 20°C and Stressed by Internal Pressurization. Numbers Adjoint to Data Points Indicate Actual Fracture Stress. Solid Curves Indicate Calculated Fracture Stress Based on an Assumed K_C=19.7 ksi $\sqrt{in.}$ (From Reference 55)

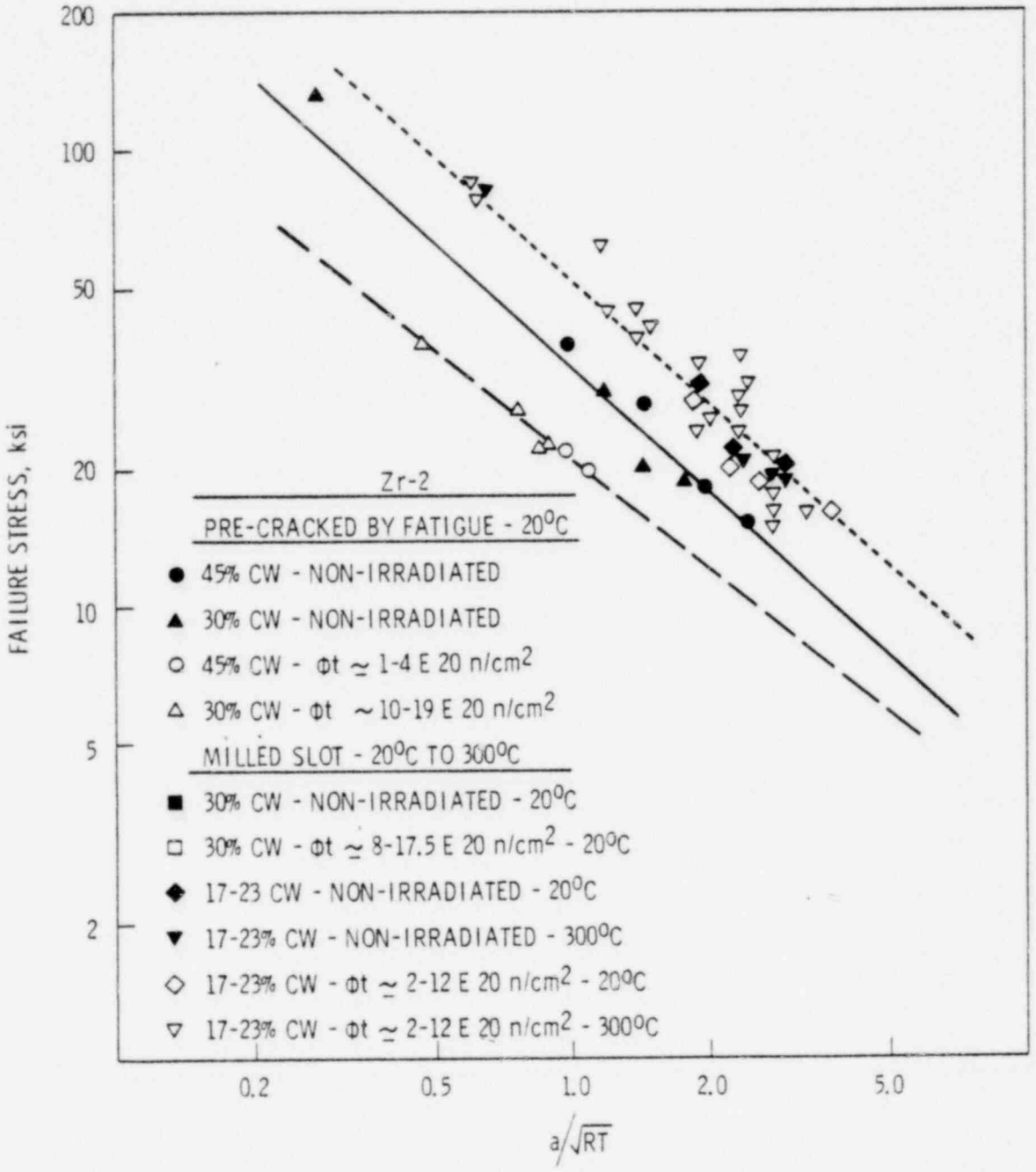

FIGURE 26. Failure Stress as a Function of the Parameter $a/\sqrt{RT}$ for Irradiated and Nonirradiated Zircaloy-2 Tubes Defected by Machined Slits or Pre-Cracked by Fatigue (From Reference 57 through 63)

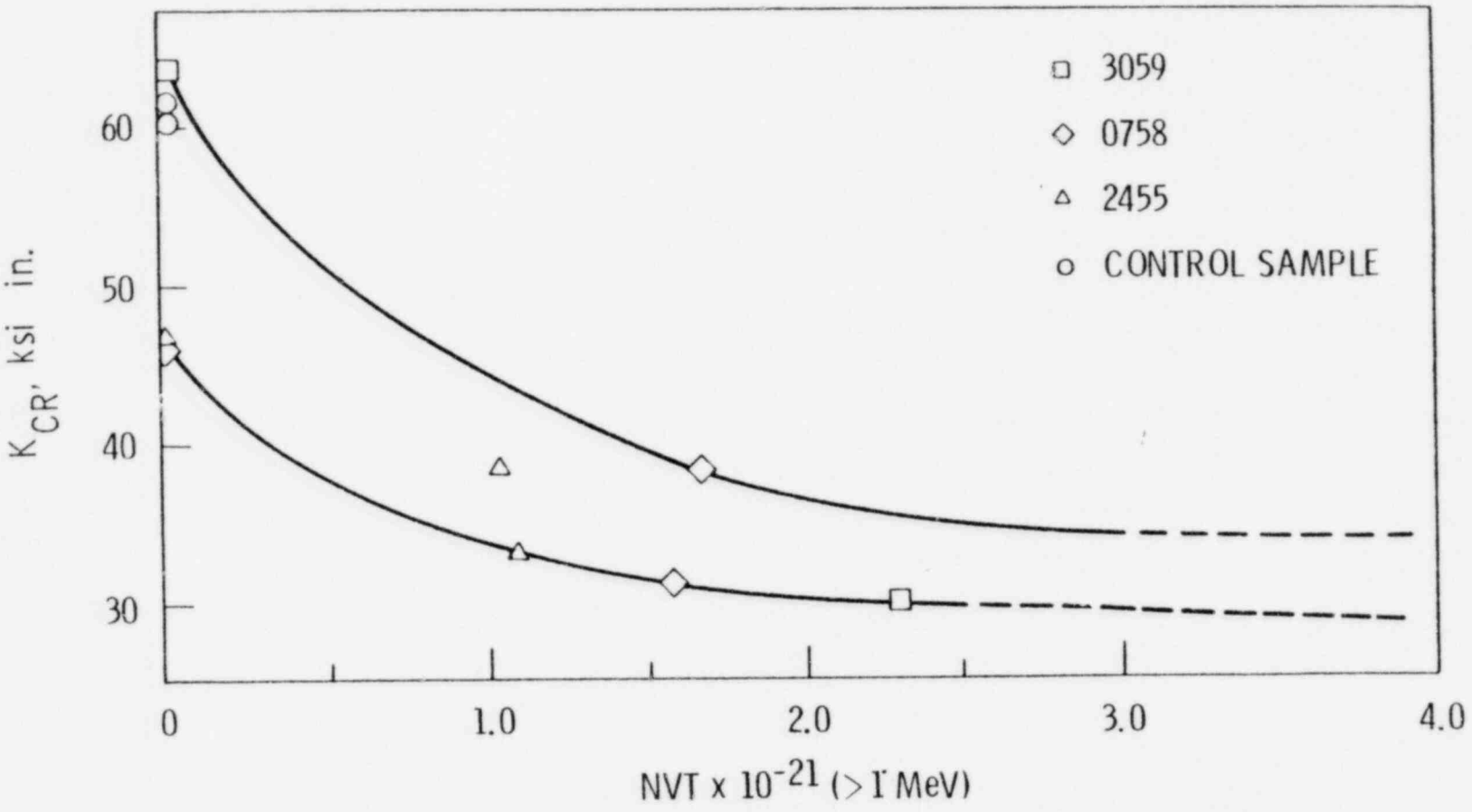

FIGURE 27. Room Temperature Fracture Toughness (K_{CR}) as a Function of Integrated Fast Flux (From Reference 53)

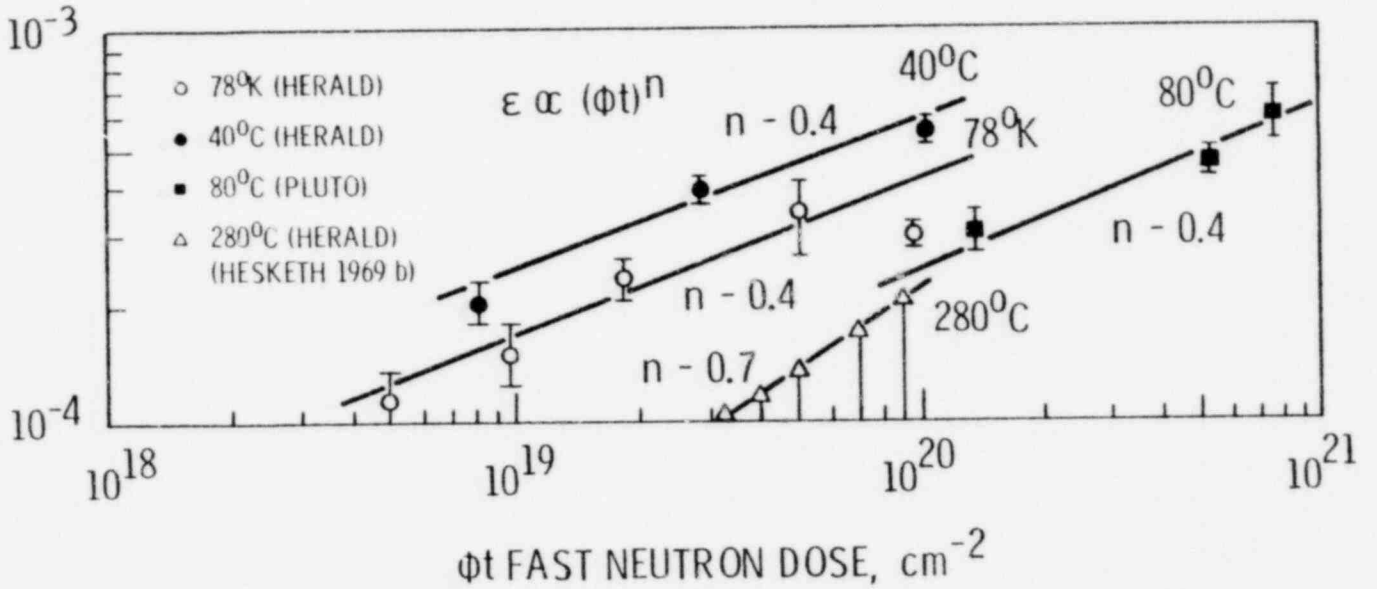

FIGURE 28. Differential Growth Strain as a Function of Dose at Four Different Irradiation Temperatures. The 280°C Data are Derived from Instantaneous Growth Rate Measurements Obtained by a Transducer Technique (From Reference 65)

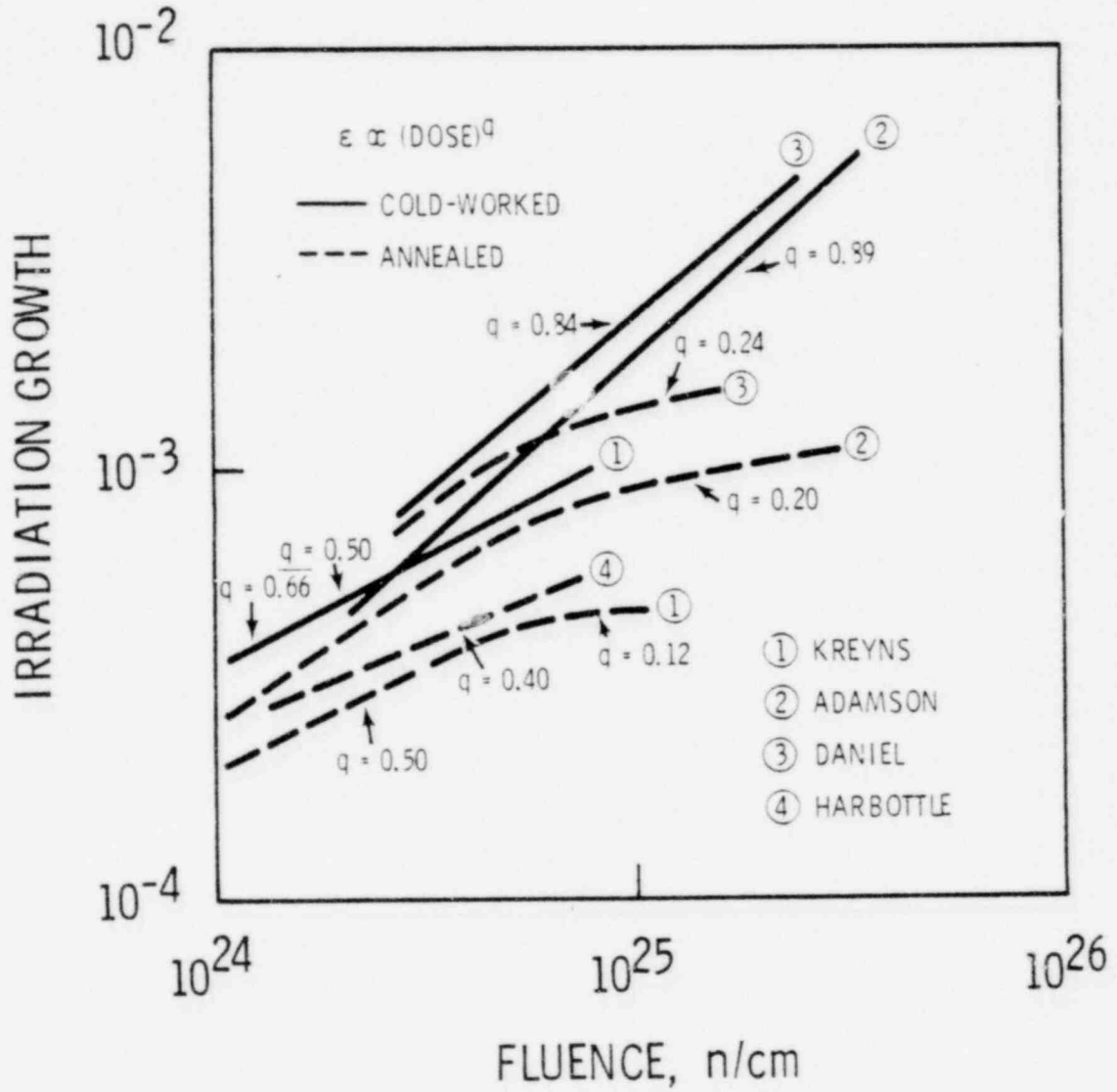

FIGURE 29. The Fluence Dependence of Irradiation Growth of Zircaloy-2 and Zircaloy-4 at About 300°C, Except for Harbottle's Results, Which were Obtained at 80°C (From Reference 30)

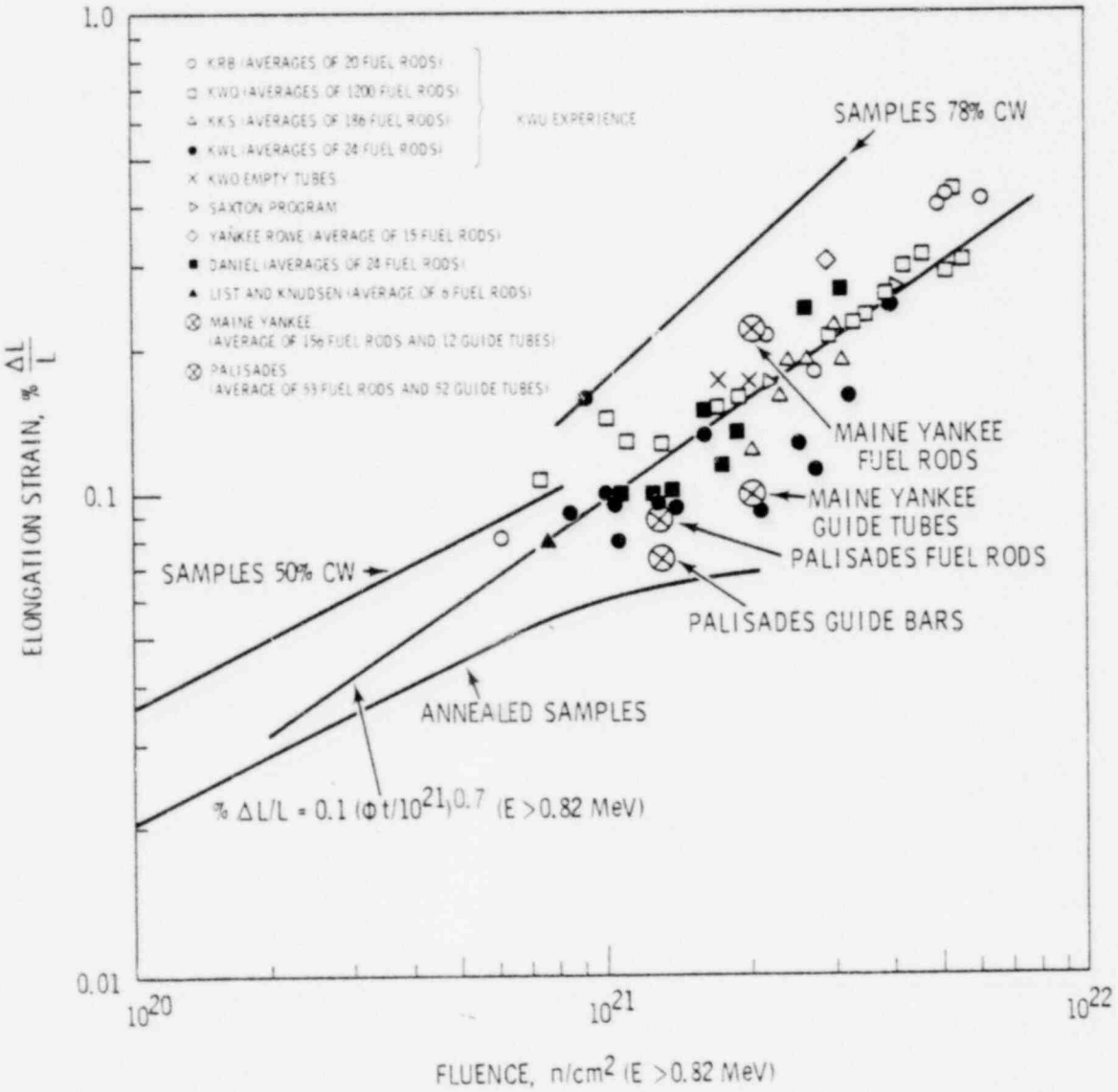

FIGURE 30. Elongation of Zircaloy-4 Fuel Clad Tubing (From Reference 68)

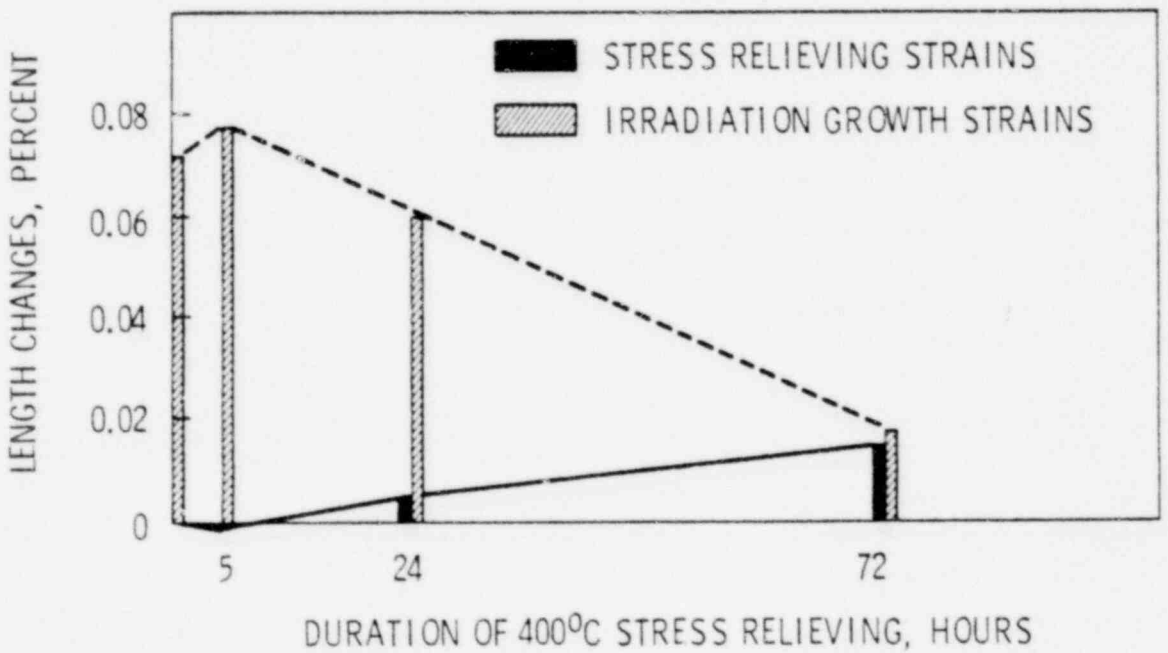

FIGURE 31. Dependence of Irradiation Growth of 40% Cold-Worked Longitudinal Slab Specimens of Zr-2.5 wt% Nb on Duration of Stress-Relieving at 400°C. Specimens Irradiated at About 320°C to a total Dose of 2.3 x E20 n/cm^2 (E>1 MeV) (From Reference 66)

Table 1. Elastic Constants (from Ref. 8)

Material	Measuring Method[a]	Elastic Constant in psi (Top) GN/m^2 (Bottom) (T = °K)	Temperature Range of Measurement - °C
Zr-2	D & S	E = 14.402E6 - 9.195E3 (T - 273) in 10^6 psi = 99.3 - 0.0634 (T - 273) in GN/m^2	20-540
	D & S	Ranging between: E = 14.997E6 - 8.397E3 (T - 273) = 103.4 - 0.0579 (T - 273) and E = 13.793E6 - 8.397E3 (T - 273) = 95.1 - 0.0579 (T - 273)	20-500
	D	E = 14.083E6 - 8.397E3 (T - 273) = 97.1 - 0.0579 (T - 273)	20-500
	D	G = 5.149E6 - 2.871E3 (T - 273) = 35.5 - 0.0198 (T - 273)	
	D	ν = Decrease from 0.367 @ 20°C to 0.330 @ 500°C	
Zr-4	S	ν = Decrease from 0.296 @ 20°C to 0.243 @ 400°C	20-400
Zr-2.5 Nb	D	E = 14.112E6 - 8.702E3 (T - 273) = 96.3 - 0.06 (T - 273)	20-500
	S	E = 14.112 - 8.398E3 (T - 273) = 96.3 - 0.0579 (T - 273)	20-500
	D	Ranging between: G = 5.264E6 - 3.234E3 (T - 273) = 36.3 - 0.0223 (T - 273) and = 4.670E6 - 2.219E3 (T - 273) = 32.2 - 0.0153 (T - 273)	20-500
	D	ν = Decrease from 0.341 @ 20°C to 0.339@ 500°C	

[a] D = dynamic resonant frequency method
S = statis stress - strain method
T = degrees Kelvin

Table 2a. ROOM TEMPERATURE TENSILE PROPERTIES OF UNIRRADIATED AND IRRADIATED ANNEALED ZIRCALOY-2 (From Reference 14)

Irradiation History	Prop. Limit (ksi)	Yield Strength (ksi)	Ultimate Strength (ksi)	Elongation % Uniform	Elongation Total %	f(φt)[a]	f(YS)	f(YS/f(φt)[b]	f(UTS)[c]	f(UTS)/f(φt)
Unirradiated	31.5	36.0	55.2	14	24					
Unirrd.-out pile (280°C)	31.2	34.7	53.4	12	20					
Unirrd.-out pile (380°C)	31.8	35.4	51.3	13	19					
9.1×10^{19} n/cm^2 (50°C)[d]	47.1	50.6	61.3	4	13					
3.6×10^{19} n/cm^2 (220°C)	42.8	46.2	59.8	7	20					
2.7×10^{19} n/cm^2 (280°C)[d]	44.5	46.8	60.5	5	16	.366	.348	.95	.133	.36
2.7×10^{20} n/cm^2 (280°C)	53.2	55.7	64.2	4	13	.498	.602	1.21	.202	.40
9.5×10^{19} n/cm^2 (380°C)	34.7	39.2	53.7	9	18	.385	.109	.28	.095	.11

Results listed represent the average of 6 samples tested in each of the above conditions except where marked as [d]; in which case result is average of 2 samples.

The 280°C irradiation with 2.7×10^{20} n/cm^2 was performed in the X-5 loop; all other irradiations were performed in either low or high-temperature fast-neutron rods.

The out-pile heat treatments were carried out for the same length of time as the corresponding irradiations at the same temperature i.e.: 128 days at 280°C and 41 days at 380°C.

Table 2b. ROOM TEMPERATURE TENSILE PROPERTIES OF UNIRRADIATED AND IRRADIATED COLD-WORK ZIRCALOY-2 (From Reference 14)

Irradiation History	Metallurgical Condition	Prop. Limit (ksi)	Yield Strength (ksi)	Ultimate Strength (ksi)	Elongation % Uniform	Elongation Total %	f(φt)[a]	f(YS)	f(YS/f(φt)[b]	f(UTS)[c]	f(UTS)/f(φt)
Unirradiated	13% C.W.	59.2	62.0	65.3	3	14					
Unirrd.-out pile (280°C)	"	49.5	52.4	59.2	4	12					
Unirrd.-out pile (380°C)	"	41.5	43.8	54.7	8	15					
3.6×10^{19} n/cm^2 (220°C)	"	60.3	63.6	68.0	2	10					
2.7×10^{20} n/cm^2 (280°C)	"	69.0	71.7	73.2	1	9	.498	.369	.74	.236	.47
9.5×10^{19} n/cm^2 (380°C)	"	43.4	47.3	58.2	6	16	.385	.080	.20	.064	.16
Unirradiated	25% C.W. and temp.[d]	51.1	54.2	65.0	6	16					
Unirrd.-out pile (280°C)	"	49.2	53.4	63.3	6	13					
Unirrd.-out pile (380°C)	"	43.8	46.2	57.5	7	11					
3.6×10^{19} n/cm^2 (220°C)	"	58.9	62.0	69.6	3	12					
2.7×10^{20} n/cm^2 (280°C)	"	66.9	69.9	74.4	3	9	.498	.310	.62	.176	.35
9.5×10^{19} n/cm^2 (380°C)	"	44.0	47.6	59.3	5	15	.385	.031	.08	.030	.07

Results listed represent the average of 6 samples tested in each of the above conditions.

The out-pile heat treatments were carried out for the same lengths of time as the corresponding irradiations at the same temperature i.e.: 128 days at 280°C and 41 days at 380°C.

The 280°C irradiation with 2.7×10^{20} n/cm^2 was performed in the X-5 loop; all other irradiations were performed in either low or high-temperature fast-neutron rods.

(a) $f(\phi t) = \sqrt[4]{1-e^{-\beta\phi t}}$ where $\beta = 2.35E\text{-}22$ reciprocal fluence and ϕt = fluence (nv) n/cm^2

(b) $f(YS) = \Delta YS/YS$ where YS = 0.2% offset yield strength and ΔYS = difference in yield strength for the irradiated and non-irradiated condition only.

(c) $f(UTS) = \Delta UTS/UTS$ where UTS = ultimate strength and ΔUTS = difference in irradiated ultimate strength and non-irradiated ultimate strength.

(d) Tempering treatment was 15 minutes at 425°C.

Table 3. EFFECT OF IRRADIATION ON MECHANICAL PROPERTIES OF ZIRCALOY-2
(From Reference 16)

Material Condition[a]	Fluence, n/cm²	Irr. Temp. (°C)	Test Temp. (°C)	Yield Strength ksi		Ultimate Strength ksi		Elongation, percent Uniform		Elongation, percent Total		Reduction in Area, percent		$\varepsilon(\sigma_T)$[b]	$\varepsilon(\sigma_{ys})$[c]	$\varepsilon(\sigma_{ys})/\varepsilon(\sigma_T)$	$\varepsilon(UTS)$[b]	$\varepsilon(UTS)/\varepsilon(\sigma_T)$
				Unirr.	Irr.	Unirr.	Irr.	Unirr.	Irr.	Unirr.	Irr.	Unirr.	Irr.					
A-RD	1.1×10^{20}	60	RT	47.9	72.1	66.0	78.5	16.8	4.2	35.0	19.0	51.0	49.0	0.400	0.505	1.263	0.151	0.379
A-TD	1.1×10^{20}	60	RT	54.4	77.5	63.1	77.5	12.4	0.3	34.4	6.0	55.0		0.400	0.425	2.062	0.228	0.570
10 CW-RD	0.84×10^{19}	60	RT	73.4	85.0	81.6	87.5	2.3	1.5	11.3	6.5	46.0		0.211	0.158	0.750	0.072	0.343
10 CW-TD	0.84×10^{19}	60	RT	69.4	87.9	79.9	87.9	2.7	1.7	11.6	4.3	52.0	50.0	0.211	0.209	0.990	0.100	0.475
10 CW-RD	1.1×10^{20}	60	RT	73.4	92.0	81.6	92.4	2.3	1.1	11.3	4.6	46.0		0.400	0.253	0.634	0.132	0.331
10 CW-TD	1.1×10^{20}	60	RT	69.4	90.9	79.9	9 .2	2.7	1.0	11.6	3.9	52.0	45.0	0.400	0.310	0.774	0.141	0.353
10 CW-RD	1.1×10^{21}	60	RT	73.4	91.0	81.6	91.0	2.3	0.9	11.3	5.2	46.0	41.0	0.691	0.240	0.347	0.115	0.167
10 CW-TD	1.1×10^{21}	60	RT	69.4	92.3	79.9	92.3	2.7	0.9	11.6	4.8	52.0	19.0	0.691	0.330	0.478	0.155	0.224
20 CW-RD	0.84×10^{19}	60	RT	79.2	91.8	88.0	96.4	2.6	1.7	9.6	6.4	42.0		0.211	0.159	0.754	0.095	0.452
20 CW-RD	0.84×10^{19}	60	RT	73.0	88.3	83.9	93.7	2.5	1.2	9.3	4.5	52.0		0.211	0.209	0.993	0.117	0.554
20 CW-RD	1.1×10^{21}	60	RT	79.2	96.2	88.0	96.6	2.6	1.2	9.6	5.8	42.0	40.0	0.400	0.215	0.536	0.098	0.246
20 CW-TD	1.1×10^{21}	60	RT	73.0	98.0	83.9	98.3	2.5	1.0	9.3	5.6	52.0	45.0	0.400	34.2	0.856	0.1.1	0.429
20 CW-RD	1.1×10^{20}	60	RT	79.2	95.9	88.0	97.1	2.6	1.3	9.6	5.3	42.0	36.0	0.691	0.210	0.305	0.103	0.150
20 CW-TD	1.1×10^{20}	60	RT	73.0	94.9	83.9	96.1	2.5	1.2	9.3	5.2	52.0	41.0	0.691	0.293	0.424	0.145	0.210
40 CW-RD	0.84×10^{19}	60	RT	86.0	92.9	96.3	99.7	3.0	2.2	8.7	6.8	39.0	41.0	0.211	0.080	0.380	0.035	0.167
40 CW-TD	0.84×10^{19}	60	RT	80.3	92.0	92.4	98.8	2.5	2.0	8.3	4.9	53.0		0.211	0.145	0.690	0.064	0.328
40 CW-RD	1.1×10^{20}	60	RT	86.0	99.7	96.3	104.0	3.0	1.5	8.7	5.6	39.0	28.0	0.400	0.159	0.398	0.060	0.200
40 CW-TD	1.1×10^{20}	60	RT	80.3	99.6	92.4	103.0	2.5	1.5	8.3	3.0	53.0	32.0	0.400	0.240	0.600	0.115	0.286
40 CW-RD	1.1×10^{21}	60	RT	86.0	98.3	96.3	101.0	3.0	1.8	8.7	5.0	39.0	39.0	0.691	0.165	0.267	0.069	0.071
40 CW-TD	1.1×10^{21}	60	RT	80.3	105.0	92.4	106.0	2.5	1.2	8.3	4.0	53.0	41.0	0.691	0.308	0.445	.147	0.213
70 CW-RD	0.84×10^{19}	60	RT	92.8	103.0	109.0	114.0	3.4	2.6	8.6	4.9	34.0		0.211	0.110	0.521	0.066	0.217
70 CW-TD	0.84×10^{19}	60	RT	85.6	102.0	104.0	112.0	3.6	2.5	7.1	4.7	45.0		0.211	0.151	0.912	0.076	0.192
70 CW-RD	1.1×10^{20}	60	RT	92.8	105.0	109.0	112.0	3.4	2.1	8.6	5.4	34.0	29.0	0.400	0.131	0.329	0.028	0.070
70 CW-TD	1.1×10^{20}	60	RT	85.6	108.0	104.5	116.0	3.6	1.8	7.1	2.7	45.0	21.0	0.400	0.281	0.654	0.110	0.275
70 CW-RD	1.1×10^{21}	60	RT	92.8	104.0	109.0	111.0	3.4	3.5	8.6	6.5	34.0	30.0	0.691	0.171	0.175	0.018	0.027
70 CW-TD	1.1×10^{21}	60	RT	85.6	111.0	104.0	114.0	3.6	1.4	7.1	3.4	45.0	23.0	0.691	0.297	0.429	0.096	0.139

[a] Explanation of designations:

A - annealed

TD - transverse direction

RD - rolling direction

10 CW - 10 percent cold worked

A-650 - annealed at 650°C for 1 hour

A-750 - annealed at 750°C for 1 hour

[b] $\varepsilon(\sigma_T) = \sqrt[4]{1 - e^{-CFT}}$ Where C = 2.35E-22 reciprocal fluence and FT = fluence (NV) n/cm².

[c] $\varepsilon(YS) = \Delta YS/YS$ Where YS = 0.2% offset yield strength and ΔYS = difference in yield strength for the irradiated and non-irradiated condition (°C).

[b] $\varepsilon(UTS) = \Delta UTS/UTS$ Where UTS = ultimate strength and ΔUTS = difference in irradiated ultimate strength and non-irradiated ultimate strength.

Table 4a. TENSILE PROPERTIES OF NPR ZIRCALOY-2 TUBES (From Reference 17)

Material	Working Direction	Material Condition	Test Temp. °C	Yield Strength ksi	Ultimate Strength ksi	Percent Uniform	Strain Necking[i]	Reduction of Area, %	Plastic Work[j] ft-lb
[a](1) Zircaloy-2 NPR (CT-19)[b]	N[c]	As-fab.[d]	RT	57.0	79.5	10.5	12.1	37.8	58.3
(2) Zircaloy-2 NPR (CT-19)	T	As-fab.	RT	60.9	83.3	10.9	5.8	38.2	43.5
(2) Zircaloy-2 NPR (AT-50)	N	As-fab.	RT	70.1	91.5	9.0	10.1	42.6	58.3
(2) Zircaloy-2 NPR (AT-50)	T	As-fab.	RT	67.1	90.4	8.9	9.0	39.1	53.4
(2) Zircaloy-2 NPR (HT-37)	N	As-fab.	RT	61.7	85.5	10.4	7.3	38.6	49.8
(2) Zircaloy-2 NPR (HT-37)	T	As-fab.	RT	63.3	85.3	8.5	2.9	34.7	31.4
(3) Zircaloy-2 NPR (AT-50)	T	Etched[e]	RT	66.9	89.3	9.5	7.1	38.9	47.1
(3) Zircaloy-2 NPR (CT-19)	T	Etched	RT	55.0	80.3	10.7	7.4	37.1	45.7
(3) Zircaloy-2 NPR (HT-37)	T	Etched	RT	64.2	87.8	7.4	2.7	32.5	27.1
(3) Zircaloy-2 NPR (AT-50)	T	Auto.[f]	RT	66.6	86.6	9.6	7.1	39.3	45.7
(3) Zircaloy-2 NPR (CT-19)	T	Auto.[f]	RT	56.8	76.0	9.1	5.1	37.3	37.8
(3) Zircaloy-2 NPR (HT-37)	T	Auto.[f]	RT	63.3	84.6	8.3	3.1	34.5	29.6
(3) Zircaloy-2 NPR (HT-1598)	N	Etched[g]	RT	81.2	89.9	3.3	6.8	38.9	26.9
(4) Zircaloy-2 NPR (HT-1598)	N	Auto.[h]	RT	57.7	80.8	11.2	10.2	44.5	52.6

[a] The number in parenthesis denotes the number of tests performed at each condition.

[b] Tube designation: CT = Chase Tube; AT = Allegheny Tube; HT = Harvey Tube.

[c] T and N refer to an orientation 90° apart with respect to the minor axis of the specimen.

[d] As-fabricated specimens which had previously received a production autoclaving treatment.

[e] Same condition as (d) but with a bright chemical etch.

[f] After fabrication from an autoclaved tube, specimens were etched and reautoclaved.

[g] These specimens were fabricated from a tube which had not been autoclaved previously.

[h] Same condition as (g) but was subsequently given the production autoclaving treatment.

[i] Necking strain is total strain minus uniform strain.

[j] Plastic work is a measure of the total area under the stress-strain curve.

Table 4b. TENSILE PROPERTIES OF NPR ZIRCALOY-2 EXPOSED IN THE OUT-OF-REACTOR LOOP (From Reference 17)

Material	Working Direction[a]	Material Condition[b] %	Test Temp. °C	Yield Strength ksi	Ultimate Strength ksi	Percent Uniform	Percent Strain Necking	Reduction of Area, %	Plastic work ft-lb	Number Tests
Quadrant 116-A (21.2 days)[c] Zircaloy-2 NPR (AT-50)	T	30	RT	68.9	88.4	8.9	9.1	45.0	51.3	2
(AT-50)	N	30	RT	68.5	89.5	9.9	8.0	39.2	50.9	2
(HT-37)	T	28	RT	65.2	88.2	9.5	5.5	34.5	42.0	2
(HT-37)	N	28	RT	64.4	88.4	9.3	6.1	35.2	42.7	2
(CT-19)	T	18	RT	56.7	76.9	10.7	9.1	38.8	39.5	2
(CT-19)	N	18	RT	58.8	79.7	11.9	9.1	38.9	50.5	2
Quadrant 119-A (173.8 days) Zircaloy-2 NPR (AT-50)	T	30	RT	68.0	88.4	9.3	6.9	35.4	45.2	2
(AT-50)	N	30	300°C	42	52.0	4.8	4.3	52.0	14.6	2
(HT-37)	T	28	RT	63.6	86.7	8.6	4.2	33.5	34.2	2
(HT-37)	N	28	300°C	43.6	53.2	3.6	3.0	47.1	10.1	2
(CT-19)	T	18	RT	59.4	79.5	9.0	4.4	36.0	30.5	2
(CT-19)	N	18	300°C	38.0	45.6	4.0	4.2	52.0	10.3	2
Quadrant 120-A (239.2 days) Zircaloy-2 NPR (AT-50)	T & N	30	RT	66.8	91.4	8.0	3.9	40.4	46.2	2
(AT-50)	T & N	30	300°C	44.0	53.4	4.2	4.6	47.6	14.3	2
(HT-37)	T & N	28	RT	64.7	90.9	8.3	3.6	35.0	32.6	2
(HT-37)	T & N	28	300°C	43.6	54.6	3.0	3.2	40.8	9.7	2
(CT-19)	T & N	18	RT	61.1	81.8	9.0	7.3	43.2	38.7	2
(CT-19)	T & N	18	300°C	38.0	45.8	4.0	5.6	48.5	12.4	2
Quadrant 122-A (152.6 days) Zircaloy-2 NPR (AT-50)	T	30	RT	68.8	88.4	8.9	8.1	38.1	48.1	2
(AT-50)	N	30	300°C	43.1	52.7	4.7	5.5	53.4	16.6	1
(HT-37)	T	28	RT	63.8	87.1	8.3	3.2	37.2	30.7	2
(HT-37)	N	28	300°C	42.0	52.1	4.8	4.8	49.0	15.4	2
(CT-19)	T	18	RT	60.3	81.1	9.1	7.1	37.3	39.2	2
(CT-19)	N	18	300°C	36.9	45.3	4.5	6.1	51.0	14.2	2
Quadrant 126-A (57.7 days) Zircaloy-2 NPR (AT-50)	T	30	RT	69.5	90.2	9.7	7.7	38.9	66.8	2
(AT-50)	N	30	RT	67.2	88.3	9.8	7.5	39.6	48.8	2
(HT-37)	T	28	RT	64.8	88.8	12.3	6.7	36.6	53.8	2
(HT-37)	N	28	RT	64.4	87.6	9.5	3.8	35.9	35.6	2
(CT-19)	T	18	RT	62.3	76.0	8.4	4.6	39.6	24.6	2
(CT-19)	N	18	RT	55.4	76.1	10.2	5.9	42.0	38.2	1
Quadrant 141-A (116.8 days) Zircaloy-2 NPR (AT-50)	T	30	RT	69.5	89.8	9.6	8.6	38.8	48.3	2
(AT-50)	N	30	300°C	42.2	51.2	4.9	4.9	53.7	15.6	2
(HT-37)	T	28	RT	67.0	90.1	8.3	3.3	34.2	31.4	2
(HT-37)	N	28	300°C	42.2	53.2	4.7	5.0	49.9	15.5	2
(CT-19)	T	18	RT	61.3	81.9	9.5	7.1	35.7	38.4	2
(CT-19)	N	18	300°C	37.2	46.4	4.4	6.6	54.8	15.0	2

[a] All specimen axes correspond to the tube axes. The designations "T" and "N" refer to the orientation of the width and thickness of the specimens and are 90 deg apart.

[b] The amount of cold reduction prior to any autoclaving treatments.

[c] Number of days exposed at greater than 280°C.

Table 4c. TENSILE PROPERTIES OF NPR ZIRCALOY-2 TUBING IRRADIATED IN THE G-7 HOT WATER LOOP, IRRADIATION TEMPERATURE - 282°C (From Reference 17)

Material	Working Direction[a]	Material Condition[b] %	Test Temp. °C	Yield Strength ksi	Ultimate Strength ksi	Percent Strain Uniform	Percent Strain Necking	Reduction of Area, %	Plastic Work ft-lb	Number Tests	f(z)[c]	f(YS)[d]	f(YS)/f(zt)	f(UTS)[e]	f(UTS)/f(zt)
Quadrant 116 (6.93E19)															
Zircaloy-2 NPR (AT-50)	T	30	RT	93.8	102.4	3.9	4.5	33.3	25.7	3					
(AT-50)	N	30	RT	94.5	101.6	3.8	3.5	33.0	21.6	3					
(HT-37)	T	28	RT	89.5	98.8	3.6	1.8	20.4	16.0	3					
(HT-37)	N	28	RT	89.2	99.6	4.2	1.7	33.4	24.3	3					
(CT-19)	T	18	RT	85.2	92.1	3.1	2.6	32.8	15.3	3					
(CT-19)	N	18	RT	84.3	93.1	4.0	4.0	32.9	22.8	3					
Quadrant 118 (1.11E20)															
Zircaloy-2 NPR (AT-50)	T & N	30	RT	97.2	103.9	3.8	3.8	33.4	24.2	4					
(AT-50)	T & N	30	300°C	59.3	59.3	0.7	4.0	40.6	8.4	2					
(HT-37)	T & N	28	RT	91.8	99.8	3.3	1.0	29.8	15.9	4					
(HT-37)	T & N	28	300°C	58.5	60.1	2.2	3.5	37.8	10.3	2					
(CT-19)	T & N	18	RT	89.9	96.0	4.0	3.5	32.6	21.3	4					
(CT-19)	T & N	18	300°C	53.8	53.9	0.7	3.6	41.1	6.6	2					
Quadrant 119 (1.38E21)															
Zircaloy-2 NPR (AT-50)	T & N	30	RT	110.8	116.4	1.8	1.7	23.0	10.8	3					
(AT-50)	T & N	30	300°C	72.1	74.0	1.3	0.8	31.7	3.5	3					
(HT-37)	T & N	28	RT	109.0	115.6	2.6	1.8	23.8	14.3	3					
(HT-37)	T & N	28	300°C	73.1	78.7	1.2	1.0	24.5	4.2	3					
(CT-19)	T & N	18	RT	107.8	110.4	1.6	1.7	26.8	9.1	3					
(CT-19)	T & N	18	300°C	68.4	72.5	1.0	1.3	32.5	4.3	3					
Quadrant 120 (2.2E21)															
Zircaloy-2 NPR (AT-50)	T & N	30	RT	119.7	120.5	1.4	2.8	29.7	14.4	3					
(AT-50)	T & N	30	300°C	75.4	77.8	1.2	0.8	32.4	3.5	3					
(HT-37)	T & N	29	RT	115.6	116.7	1.7	1.0	26.1	8.8	3					
(HT-37)	T & N	28	300°C	73.0	76.5	1.3	0.8	32.1	3.8	3					
(CT-19)	T & N	18	RT	106.4	107.3	1.3	1.6	35.1	8.1	3					
(CT-19)	T & N	18	300°C	73.9	75.2	1.0	0.9	34.6	3.4	2					
Quadrant 122 (3.5E21)															
Zircaloy-2 NPR (AT-50)	T & N	30	RT	105.8	107.4	2.3	2.6	31.6	15.6	3					
(AT-50)	T & N	30	300°C												
(HT-37)	T & N	28	RT	103.9	107.7	2.0	1.2	28.1	16.6	3					
(HT-37)	T & N	28	300°C												
(CT-19)	T & N	18	RT	101.3	104.2	1.2	3.0	28.1	10.6	3					
(CT-19)	T & N	18	300°C												
Quadrant 124 (1.63E20)															
Zircaloy-2 NPR (AT-50)	T & N	30	RT	101.4	106.4	3.6	3.3	32.7	21.9	3					
(AT-50)	T & N	30	300°C	64.8	66.5	1.1	3.0	39.7	7.4	3					
(HT-37)	T & N	28	RT	97.5	105.1	3.3	2.1	27.2	16.5	3					
(HT-37)	T & N	28	300°C	60.0	62.3	1.7	2.1	27.7	6.6	3					
(CT-19)	T & N	18	RT	93.1	98.4	3.1	3.3	31.5	18.0	3					
(CT-19)	T & N	18	300°C	56.2	57.1	1.0	3.3	36.3	6.2	3					
Quadrant 126 (5.64E20)															
Zircaloy-2 NPR (AT-50)	T & N	30	RT	109.4	113.0	2.4	2.0	32.0	18.7	3	0.594	0.374	0.967	0.253	0.426
(AT-50)	T & N	30	300°C	67.1	69.2	1.3	2.3	40.2	6.2	3	0.594	0.357	0.938	0.313	0.527
(HT-37)	T & N	28	RT	104.6	111.7	2.8	1.9	27.6	15.3	3	0.594	0.614	1.034	0.258	0.434
(HT-37)	T & N	28	300°C	62.5	68.6	1.6	2.3	31.7	7.7	3	0.594	0.488	0.822	0.317	0.534
(CT-19)	T & N	18	RT	104.6	107.0	1.8	2.9	29.3	13.9	3	0.594	0.592	1.503	0.406	0.684
(CT-19)	T & N	18	300°C	63.4	65.3	1.1	1.7	34.3	5.0	3	0.594	0.718	1.206	0.442	0.744
Quadrant 141 (9.49E20)															
Zircaloy-2 NPR (AT-50)	T & N	30	RT	113.6	114.4	2.0	3.1	28.4	17.1	3	0.668	0.634	0.948	0.274	0.410
(AT-50)	T & N	30	300°C								--	--	--	--	--
(HT-37)	T & N	28	RT	110.0	114.1	1.6	1.8	24.1	11.2	4	0.668	0.642	0.960	0.266	0.398
(HT-37)	T & N	28	300°C								--	--	--	--	--
(CT-19)	T & N	18	RT	105.9	109.2	1.4	2.2	26.3	10.0	2	0.668	0.728	1.089	0.333	0.498
(CT-19)	T & N	18	300°C								--	--	--		--

[a] All specimen axes correspond to tube axes. The "N" refers to specimens which have the width direction corresponding to the radial direction of the tubes.

[b] Amount of cold reduction prior to any autoclaving treatments.

[c] Integrated exposure in nvt-1 Mev.

[d] $f(zt) = \sqrt[4]{1 - e^{-\beta zt}}$ where β = 2.35E-22 reciprocal fluence and zt = fluence (nv) c/cm^2

[e] $f(YS) = \Delta YS/YS$ Where YS = 0.2% offset yield strength and ΔYS = difference in yield strength for the irradiated and non-irradiated condition only

[f] $f(UTS) = \Delta UTS/UTS$ Where UTS = ultimate strength and ΔUTS = difference in irradiated ultimate strength and non-irradiated ultimate strength.

Table 4d. TENSILE PROPERTIES OF NPR ZIRACLOY-2 TUBE MATERIALS IRRADIATED IN THE ETR G-6 CORE POSITION, IRRADIATION TEMPERATURE (From Reference 17)

Material	Working[a] Direction	Material[b] Condition %	Test Temp. °C	Yield Strength ksi	Ultimate Strength ksi	Percent Uniform	Strain Necking	Reduction of Area, %	Plastic Work ft-lb	Number Tests	f(φt)[c]	f(YS)[d]	f(YS)/f(φt)	f(UTS)[e]	f(UTS)/f(φt)
Quadrant 663 (1.20E20)[c] Zircaloy-2 NPR (AT-50)	N	30	RT	98.2	103.8	3.8	4.0	36.5	24.1	2	0.408	0.434	1.063	0.174	0.426
(AT-50)	N	30	300°C	59.8	61.1	1.3	2.2	50.1	6.1	2	0.408	0.424	1.038	0.175	0.428
Quadrant 664 (1.06E20) Zircaloy-2 NPR (HT-37)	N	28	RT	90.6	98.4	4.0	4.2	29.0	25.3	2	0.396	0.394	0.995	0.118	0.298
(HT-37)	N	28	300°C	56.6	59.2	2.2	3.1	38.4	9.2	2	0.396	0.341	1.000	0.111	0.280
Quadrant 66 (6.24E19) Zircaloy-2 NPR (CT-19)	N	10	RT	84.8	91.0	4.0	4.6	35.8	24.6	2	0.347	0.467	1.344	0.162	0.466
(CT-19)	N	10	300°C	50.5	51.4	1.2	3.4	46.4	7.2	2	0.347	0.329	0.947	0.127	0.366
Quadrant 666 (9.80E19) Zircaloy-2 NPR (HT-1598)	N	29	RT	94.8	97.9	2.4	4.0	37.6	18.9	2					
(HT-1598)	N	29	300°C	57.0	58.7	1.0	2.8	49.8	6.2	2					

[a] All specimen axes correspond to tube axes. The "N" refers to specimens which have the width direction corresponding to the radial direction of the tubes.

[b] Amount of cold reduction prior to any autoclaving treatments.

[c] Integrated exposure in nvt>1 Mev.

[d] $f(\phi t) = \sqrt[4]{1 - e^{-\beta \phi t}}$ Where β = 2.35E-22 reciprocal fluence and ϕt = fluence (nv) n/cm^2.

[e] $f(YS) = \Delta YS/YS$ Where YS = 0.2% offset yield strength and ΔYS = difference in yield strength for the irradiated and non-irradiated condition only.

[f] $f(UTS) = \Delta UTS/UTS$ Where UTS = ultimate strength and ΔUTS = difference in irradiated ultimate strength and non-irradiated ultimate strength.

Table 5a. BATCH IDENTIFICATION AND FABRICATION DETAILS
(From Reference 19, 20)

Batch Number	Alloy	Vendor	Method and Amount of Final Cold Reduction	Final Stress Relief Heat Treatment
1	Zircaloy 2	Z	15 to 20% cold drawn	None
2	Zircaloy 2	Y	~15% cold drawn	None
7	Zircaloy 2	Z	60% tube reduced	2 h at 495°C
8	Zircaloy 2	X	62% tube reduced	2 h at 427°C
9	Zircaloy 2	X	70% tube reduced	2.5 h at 454°C
11	Zircaloy 2	V	10% cold drawn[a]	None
16	Zircaloy 4	Z	60 to 70% tube reduced	Done, but unknown
17	Zr-2.5Cb	X	42% tube reduced	None
18	Zr-2.5Cb	Y	40% tube reduced	None

[a] Batch 11 was impact extruded at 800°C from small bar stock slugs, then reduced in two draws with an intermediate anneal to finished size. All other batches were conventionally extruded in the high alpha temperature range from prebored or pierced billets, followed by several cold-working and annealing operations to finished size.

IMAGE EVALUATION
TEST TARGET (MT-3)

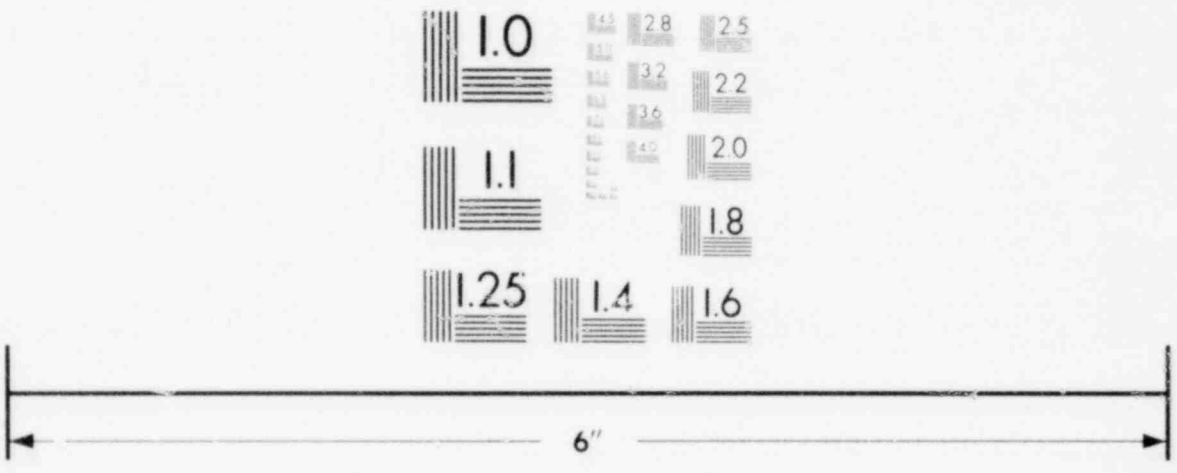

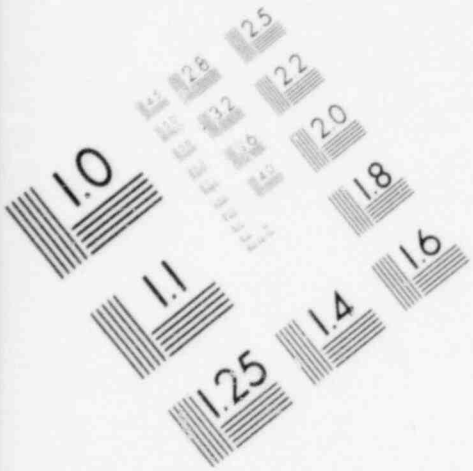

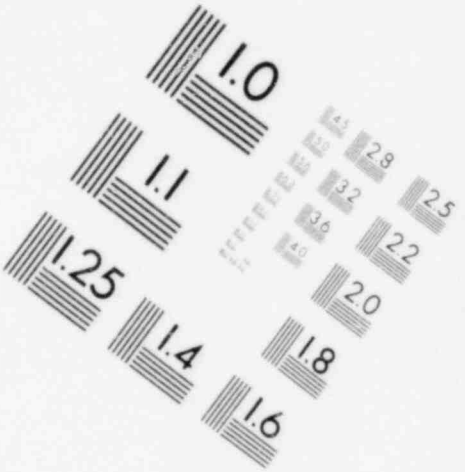

IMAGE EVALUATION TEST TARGET (MT-3)

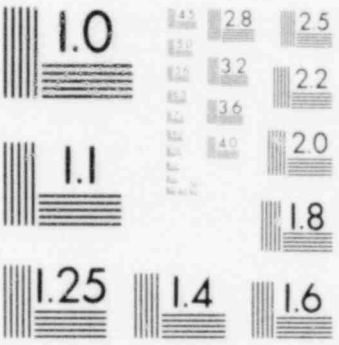

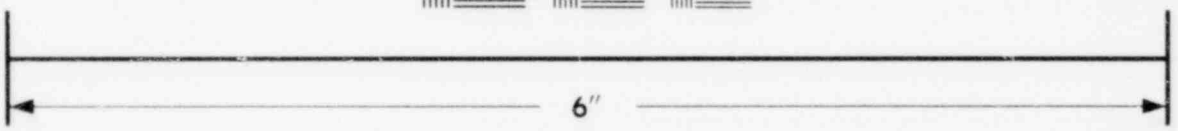

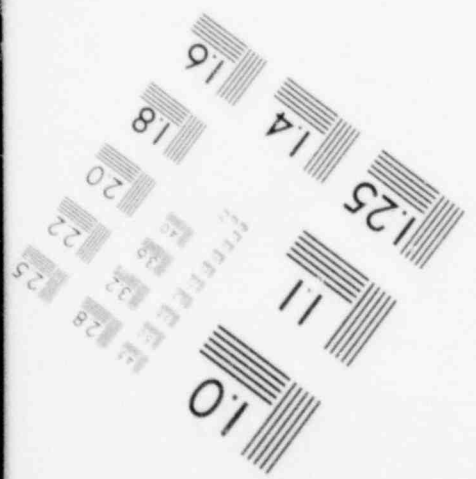

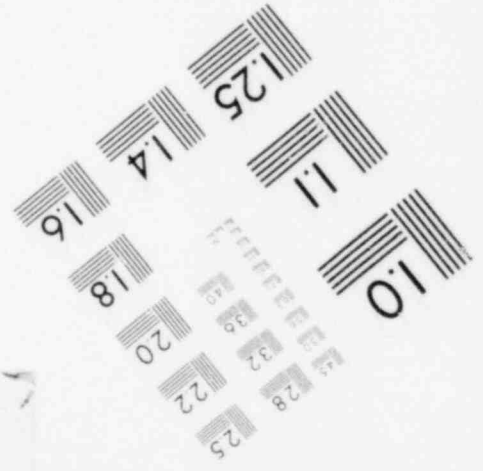

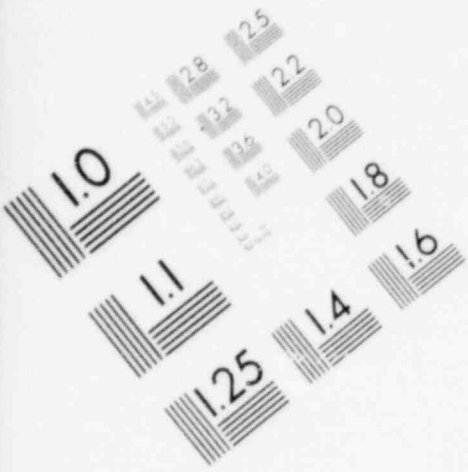

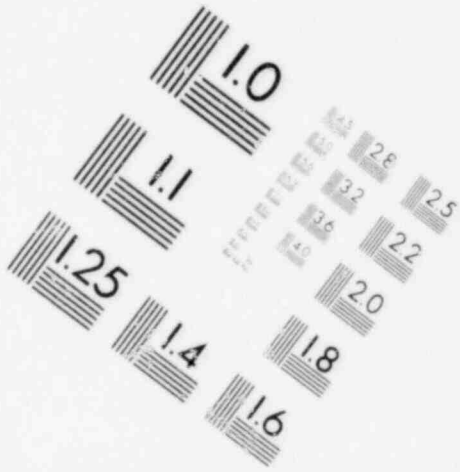

IMAGE EVALUATION TEST TARGET (MT-3)

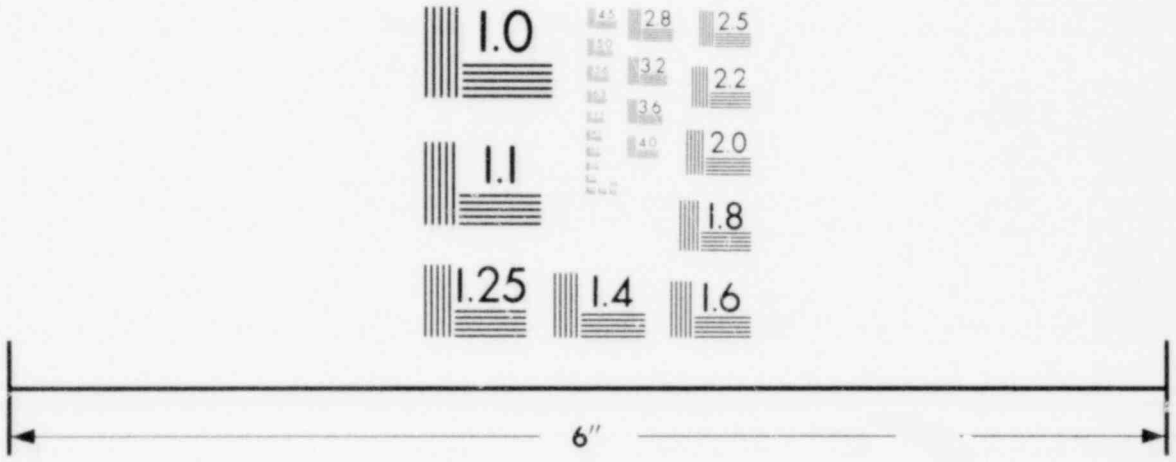

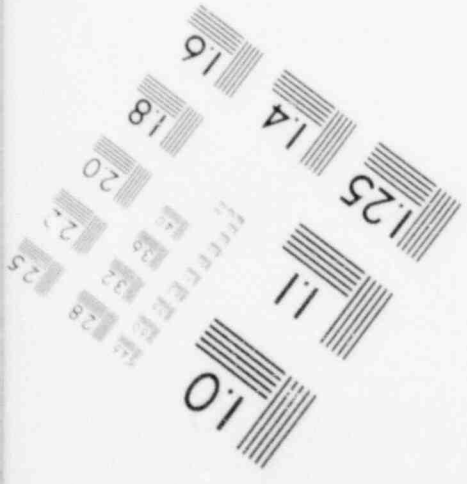

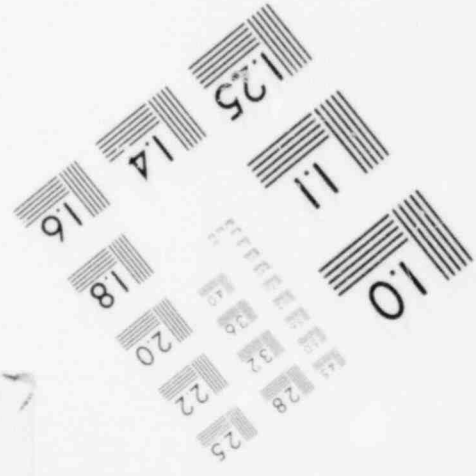

Table 5b. FABRICATION ROUTE AND TEXTURE CHARACTERISTICS OF THE TUBING BATCHES
(From Reference 19, 20)

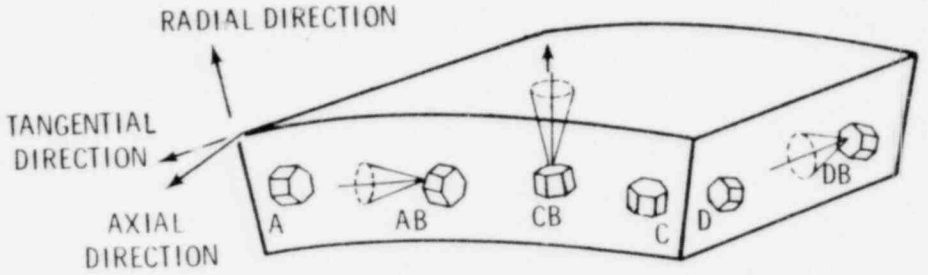

THE IDEALISED ORIENTATIONS

Batch Number and Condition	Alloy	Vendor	Method and Amount of Final Cold Reduction	Final Heat Treatment	<0002>Pole Texture Coefficient				
					A	AB	CB	C	D
7C	Zircaloy-2	Z	60% tube reduced	2 h at 495 C	1.1	1.0	3.7	5.0	0.1
7A	Zircaloy-2	Z	60% tube reduced	as above plus 1 h at 800 C	0.7	0.9	3.0	5.2	0
9C	Zircaloy-2	X	70% tube reduced	2.5 h at 454 C	2.6	1.1	3.0	4.5	0.2
11C	Zircaloy-2	V	~10% cold drawn[a]	none	3.0	1.4	1.4	2.5	0.4
16C	Zircaloy-4	Z	60 to 70% tube reduced	done, but unknown	3.8	1.1	2.4	5.6	0.1

[a] Batch 11 was impact-extruded at 800 C (1472 F) from small bar stock slugs, then reduced in two draws with an intermediate anneal to finished size. All other batches were conventionally extruded in the high alpha temperature range from prebored or pierced billets, followed by several cold-working and annealing operations to finished size.

Table 5c. CLOSED END BURST TEST PROPERTIES (VALUES REPRESENT THE AVERAGE OF TWO OR THREE RESULTS) (From Reference 19, 20)

Batch Number and Condition [a]	Test Temperature deg C	Preirradiation Properties: Yield Strength ksi	Ultimate Strength ksi	Elongation Uniform %	Elongation Total %	Postirradiation Properties: Yield Strength ksi	Ultimate Strength ksi	Elongation Uniform %	Elongation Total %	Fluence E20/n/cm^2	f(at)[c]	f(YS)[d]	f(YS)/f(at)	f(UTS)[e]	f(UTS)/f(at)
1-C [a]	20	106.5	107.6	2.5	14.3	125.7	125.7	0.2	6.0	2.7	0.497	0.191	0.38	0.168	0.33
2-C	20	91.9	97.7	4.5	12.8	122.9	128.0	0.7	4.0	2.1	0.497	0.337	0.67	0.269	0.54
3-C	20	99.9	109.6	4.2	12.1	124.2	129.8	0.7	10.3	2.7	0.497	0.243	0.42	0.182	0.36
6-C	20	96.5	101.0	3.2	17.4	121.3	121.7	0	3.5	2.7	0.497	0.261	0.52	0.205	0.41
9-C	20	111.5	119.5	1.5	4.3	128.1	129.2	0.3	3.5	2.7	0.497	0.137	0.27	0.101	0.16
11-C	20	82.0	85.0	4.7	17.5	108.6	109.0	0.1	21.3	2.7	0.497	0.329	0.65	0.286	0.56
16-C	20	105.8	116.0	4.0	9.0	126.7	138.2	0.9	3.1	2.9	0.506	0.199	0.39	0.149	0.29
17-C	20	125.9	139.9	2.9	15.6	161.9	165.6	0.4	0.5	2.9	0.506	0.311	0.61	0.183	0.36
18-C	20	106.4	115.4	4.0	6.1	154.6	154.6	0.1	1.1	2.9	0.506	0.453	0.90	0.339	0.67
1-A	20	77.5	86.0	10.7	32.5	102.6	104.4	1.0	23.2	2.0	0.462	0.323	0.69	0.214	0.46
7-A	20	90.3	94.7	7.8	23.9	118.4	121.9	0.7	16.4	2.0	0.462	0.440	0.95	0.277	0.60
11-A	20	69.9	80.8	12.8	22.7	87.6	90.1	0.5	23.8	2.0	0.462	0.269	0.58	0.090	0.19
16-A	20	76.0	90.2	8.7	17.0	99.1	106.4	1.1	23.1	2.0	0.462	0.270	0.58	0.207	0.45
1-B	20	64.7	74.9	5.0	14.5	90.1	93.5	0.8	9.2	2.0	0.462	0.445	0.96	0.248	0.53
7-B	20	63.0	75.4	5.5	15.8	91.4	98.2	0.7	11.1	2.0	0.462	0.463	1.00	0.249	0.53
11-B	20	60.0	73.1	6.3	14.5	85.7	86.1	0.1	10.0	2.0	0.462	0.420	0.91	0.174	0.37
16-B	20	61.6	72.6	8.2	18.4	87.2	98.0	1.0	12.5	2.0	0.462	0.435	0.93	0.232	0.45
1-C	800	60.1	60.4	0.5	20.0	76.9	76.9	0.3	0.8	2.7	0.497	0.332	0.62	0.306	0.61
2-C	800	54.1	58.9	1.1	[illegible]	71.1	72.2	0.1	4.0	2.7	0.497	0.267	0.53	0.260	0.54
7-C	800	53.5	65.2	2.2	21.5	85.6	85.8	0.0	2.9	2.7	0.497	0.430	0.86	0.316	0.63
8-C	800	57.8	58.4	1.2	14.8	71.9	72.6	0.7	0.8	2.7	0.497	0.281	0.56	0.243	0.48
9-C	800	63.1	71.6	1.0	4.8	76.2	77.4	1.3	1.9	2.7	0.497	0.102	0.20	0.081	0.16
11-C	800	50.8	51.1	0.7	53.0	...	52.3	0.1	29.0	2.7	0.497	...	...	0.124	0.24
16-C	800	68.2	69.0	2.0	4.9	79.4	82.9	0.7	2.4	2.9	0.506	0.236	0.46	0.180	0.35
17-C	800	92.8	94.2	2.7	8.8	110.6	112.6	0.4	1.9	2.9	0.506	0.340	0.66	0.280	0.55
18-C	800	67.9	73.3	2.3	4.5	98.1	99.3	0.3	1.9	2.9	0.506	0.446	0.88	0.354	0.70
1-A	800	28.5	31.2	12.9	52.9	55.7	55.7	0.1	32.6	2.0	0.462	0.954	2.06	0.765	1.66
7-A	800	28.1	40.0	8.6	50.8	69.9	67.6	1.5	30.7	2.0	0.462	1.303	2.82	0.656	1.42
11-A	800	26.2	38.0	13.2	48.9	46.1	46.7	0.3	32.3	2.0	0.462	0.767	1.65	0.373	0.80
16-A	800	26.3	37.8	11.3	63.5	59.5	61.2	0.8	36.0	2.0	0.462	1.262	2.72	0.672	1.45
1-B	800	27.2	36.1	6.3	23.4	53.8	53.5	0.4	7.7	2.0	0.462	0.963	2.08	0.492	1.06
7-B	800	22.9	35.0	6.9	21.8	53.3	55.4	1.0	17.6	2.0	0.462	0.937	2.03	0.587	1.27
11-B	800	26.6	35.4	10.1	20.2	51.4	52.9	0.1	17.1	2.0	0.462	0.910	2.01	0.434	1.06
16-B	800	26.7	35.9	7.1	26.3	48.2	54.5	0.7	11.0	2.0	0.462	0.805	1.73	0.438	0.93

[a] Metallurgical condition code (see Tables 5a, 5b)
A = alpha annealed. 1 h at 800 C (1472 F).
C = cold worked or cold worked and stress relieved.

[b] Type of specimen code:
I = unirradiated control specimens (Ref 1).
C = unfueled specimens irradiated in a fast neutron facility to fluence of 2 to 3 x 10^{21} n/cm^2 at 125 to 250 C (257 to 482 F)(Ref 1).
F = fueled specimens cut from fuel elements irradiated to average clad fluences of 2.5 to 4.8 x 10^{21} n/cm^2 at 282 to 325 C (540 to 617 F).
FH = similar to F but prehydrided to ~170 ppm hydrogen.
S = unfueled specimens cut from sheaths containing corrosion coupons irradiated in fuel handlet to average fluences of 2.9 to 9.4 x 10^{21} n/cm^2 at 275 to 287 C (527 to 549 F).

[c] $f(at) = \sqrt[3]{1 - e^{-\beta\Phi t}}$ Where β = 2.35E-22 reciprocal fluence and Φt = Fluence (ex) n/cm^2.

[d] $f(YS) = \Delta YS/YS$ Where YS = 0.2% offset yield strength and ΔYS = difference in yield strength for the irradiated and non-irradiated condition only.

[e] $f(UTS) = \Delta UTS/UTS$ Where UTS = ultimate strength and ΔUTS = difference in irradiated ultimate strength and non-irradiated ultimate strength.

Table 5d. CLOSED END BURST TEST PROPERTIES (From Reference 19, 20)

Batch Number and condition[a]	Test Temperature, deg F	Type of Specimen[b]	Number of Results Averaged	Preirradiation Properties: Yield Strength ksi	Preirradiation Properties: Ultimate Strength ksi	Preirradiation Properties: Elongation Uniform Percent	Preirradiation Properties: Elongation Total Percent	Type of Specimen[b]	Number of Results Averaged	Postirradiation Properties: Yield Strength ksi	Postirradiation Properties: Ultimate Strength ksi	Postirradiation Properties: Elongation Uniform %	Postirradiation Properties: Elongation Total %	f(gt)[c]	f(ys)[d]	f(ys)/f(gt)	f(UTS)[e]	f(UTS)/f(gt)
7A	72	T	2	102.2	98.7	7.5	23.9	E	2	118.4	121.6	0.7	16.4	0.462/0.510	0.180	0.961/0.862	0.277	1.606/0.543
								F	5	138.9	142.8	0.6	3.2	0.488/0.571	1.689	1.411/1.202	0.508	1.039/0.889
								F+H	1	--	66.3	0	0					
7C	72	T	3	98.9	109.8	4.2	12.1	E	3	124.2	129.8	0.7	10.3	0.462/0.510	0.242	0.523/0.474	0.182	0.396/0.279
								F	5	142.3	151.9	1.1	2.2	0.488/0.571	0.422	0.864/0.739	0.375	0.767/0.656
								F+H	1	--	118.6	-0.1	-0.1					
9C	72	T	3	113.4	119.5	1.5	4.1	E	2	129.0	129.2	0.3	1.5	0.462/0.510	0.138	0.298/0.270	0.081	0.175/0.159
								F	2	130.8	138.8	0.8	1.0	0.488/0.571	0.153	0.314/0.268	0.161	0.330/0.282
								F+H	2	--	93.3	-0.1	-0.5					
11C	72	T	3	81.9	85.0	4.7	37.5	E	3	108.6	109.0	0.3	21.1	0.462/0.510	0.325	0.703/0.637	0.283	0.612/0.554
								F	2	114.9	117.9	0.9	8.4	0.488/0.571	0.401	0.822/0.703	0.392	0.792/0.677
								F+H	2	--	105.9	-0.1	-0.5					
16C	72	T	3	105.6	116.7	4.0	9.0	E	3	126.6	134.2	0.9	3.1	0.462/0.510	0.200	0.433/0.392	0.149	0.322/0.291
								F	2	127.0	135.4	1.2	1.5	0.488/0.571	0.203	0.416/0.355	0.160	0.328/0.280
								F+H	1	--	82.2	-0.1	-0.5					
7A	300	T	3	76.1	86.8	8.6	50.0	E	3	64.0	67.6	1.5	30.2	0.462/0.510	1.306	2.829/2.555	0.656	1.419/1.286
								F	9	80.2	81.4	0.5	16.2	0.488/0.571	1.854	3.793/3.244	0.995	2.036/1.741
								F+H	1	--	96.6	0.8	0.8					
7C	300	T	3	59.5	65.3	2.2	21.5	E	3	85.6	85.9	0.8	2.9	0.462/0.510	0.439	0.948/0.859	0.315	0.681/0.617
								F	15	82.5	85.9	0.9	1.7	0.488/0.571	0.387	0.793/0.678	0.315	0.645/0.552
								F+H	1	91.8	95.1	0.6	0.7					
9C	300	T	3	69.0	71.6	1.0	1.0	E	1	76.1	77.4	1.0	1.0	0.462/0.510	0.103	0.222/0.201	0.081	0.175/0.159
								F	4	91.2	95.6	0.7	0.8	0.488/0.571	0.321	0.657/0.562	0.314	0.643/0.549
								F+H	1	81.9	88.2	0.45	-0.5					
11C	300	T	3	50.6	51.0	0.7	51.0	E	3	--	57.1	0.1	29.0	0.462/0.510	--	--	0.119	0.257/0.233
								F	4	69.2	71.5	0.3	14.5	0.488/0.571	0.363	0.744/0.637	0.400	0.819/0.701
								F+H	3	69.6	71.4	0.4	6.6					
16A	300	T	3	64.8	69.8	2.0	4.9	E	3	79.3	82.4	0.7	2.4	0.462/0.510	0.223	0.483/0.436	0.160	0.346/0.314
								F	14	77.9	80.9	0.7	0.8	0.488/0.571	0.201	0.412/0.352	0.160	0.327/0.280
								F+H	3	85.4	87.4	0.6	0.9					
								C	4	81.0	82.4	0.5	1.3	0.502/0.560	0.250	0.492/0.446	0.183	0.357/0.323

[a] Metallurgical condition code (see tables 5a, 5b)
A = alpha annealed. 1 h at 800 C (1472 F).
C = cold worked or cold worked and stress relieved.

[b] Type of specimen code:
T = unirradiated control specimens (Ref 1)
E = unfueled specimens irradiated in a fast neutron facility to fluence of 2 to 3 x 10^{21} n/m^2 at 125 to 250 C (257 to 482 F)(Ref 1).
F = fueled specimens cut from fuel elements irradiated to average clad fluences of 2.5 to 4.8 x 10^{21} n/cm^2 at 282 to 325 C (540 to 617 F).
F+H = similar to F but prehydrided to ~120 ppm hydrogen.
C = unfueled specimens cut from sheaths containing corrosion coupons irradiated in fuel bundles to average fluences of 2.9 to 4.4 x 10^{21} n/m^2 at 275 to 287 C (527 to 549 F).

[c] $f(gt) = \sqrt[4]{1 - e^{-\alpha t}}$ Where α = 2.95E-22 reciprocal fluence and t = fluence (ns) n/cm^2.

[d] f(YS) = ΔYS/YS Where YS = 0.2% offset yield strength and ΔYS = difference in yield strength for the irradiated and non-irradiated condition only.

[e] f(UTS) = ΔUTS/UTS Where UTS = ultimate strength and ΔUTS = difference in irradiated ultimate strength and non-irradiated ultimate strength.

Table 5e. AXIAL TUBE TENSILE PROPERTIES (VALUES REPRESENT THE AVERAGE OF TWO OR THREE RESULTS) (From Reference 19, 20)

		Preirradiation Properties				Postirradiation Properties									
Batch Number and Condition	Test Temperature deg C	Yield Strength ksi	Ultimate Strength ksi	Elongation Uniform	Elongation Total	Yield Strength ksi	Ultimate Strength ksi	Elongation Uniform	Elongation Total	Fluence E20 n/cm^2	f(φt)[b]	f(YS)[c]	f(YS)/f(φt)	f(UTS)[d]	f(UTS)/f(φt)
1-C[a]	20	83.2	95.9	5.3	10.5	102.6	107.7	2.3	5.3	2.7	0.497	0.233	0.46	0.123	0.24
2-C	20	76.3	89.7	4.9	13.3	95.2	99.8	2.5	6.6	2.7	0.497	0.247	0.49	0.112	0.22
7-C	20	79.1	99.9	7.5	16.5	103.4	109.1	2.8	9.8	2.7	0.497	0.307	0.61	0.092	0.18
8-C	20	83.8	104.3	5.6	6.3	108.5	115.2	2.5	2.7	2.7	0.497	0.294	0.59	0.104	0.21
9-C	20	88.9	112.7	6.3	12.1	114.3	123.5	3.6	9.0	2.7	0.497	0.285	0.57	0.095	0.19
11-C	20	59.7	74.8	8.7	19.4	88.8	89.9	2.3	9.5	2.7	0.497	0.487	0.97	0.201	0.40
16-C	20	80.9	106.0	8.2	16.7	107.6	119.4	3.4	8.8	2.9	0.506	0.330	0.65	0.194	0.38
17-C[e]	20	80.5	108.5	9.3	22.0	130.9	144.0	3.0	5.7	2.9	0.506	0.626	1.23	0.327	0.64
18-C[e]	20	79.7	103.0	9.5	18.5	125.9	136.0	0.6	0.8	2.9	0.506	0.579	1.14	0.320	0.63
1-A	20	52.3	77.8	14.8	23.9	78.3	87.7	5.3	15.1	2.0	0.462	0.497	1.07	0.127	0.27
7-A	20	53.9	72.8	15.4	25.7	83.0	85.6	3.6	17.7	2.0	0.462	0.539	1.16	0.175	0.37
11-A	20	48.6	71.9	12.9	17.6	68.7	77.7	4.5	11.0	2.0	0.462	0.413	0.89	0.080	0.17
16-A	20	49.1	72.0	17.4	28.3	74.9	81.9	3.8	15.1	2.0	0.462	0.522	1.13	0.137	0.29
1-B	20	57.6	76.5	10.4	16.5	84.1	95.0	2.0	7.1	2.0	0.462	0.460	0.99	0.241	0.52
7-B	20	57.2	77.7	12.4	18.3	82.5	89.2	2.0	5.3	2.0	0.462	0.442	0.95	0.148	0.31
11-B	20	54.6	72.4	10.6	15.8	80.9	86.6	1.6	5.0	2.0	0.462	0.481	1.04	0.196	0.42
16-B	20	54.5	73.7	9.9	13.8	81.1	87.7	1.8	8.0	2.0	0.462	0.488	1.05	0.190	0.41
1-C	300	48.0	54.2	2.7	7.0	67.1	67.1	0.7	2.2	2.9	0.497	0.397	0.79	0.238	0.47
2-C	300	43.1	48.7	2.3	7.4	53.4	53.8	0.9	5.0	2.9	0.497	0.239	0.48	0.101	0.21
7-C	300	51.7	62.3	4.1	11.8	65.8	67.2	1.3	11.3	2.9	0.497	0.272	0.54	0.078	0.15
8-C	300	50.3	63.3	4.8	5.4	66.4	68.1	1.1	1.4	2.9	0.497	0.320	0.64	0.075	0.15
9-C	300	61.1	73.3	4.0	7.4	74.3	80.2	2.7	7.1	2.9	0.497	0.216	0.43	0.094	0.19
11-C	300	35.3	39.8	6.7	15.3	51.3	51.3	0.3	4.8	2.9	0.497	0.453	0.91	0.288	0.58
16-C	300	54.7	67.5	5.6	11.4	71.6	74.7	1.6	6.2	2.9	0.506	0.309	0.51	0.106	0.21
17-C[e]	300	53.5	73.3	4.4	10.6	90.0	97.2	1.9	3.5	2.9	0.506	0.682	1.34	0.326	0.64
18-C[e]	300	49.0	62.0	6.2	17.2	88.1	91.1	0.6	0.8	2.9	0.506	0.798	1.57	0.469	0.92
1-A	300	18.5	32.7	15.3	25.3	46.6	46.6	0.4	7.3	2.0	0.462	0.518	3.28	0.425	0.91
7-A	300	18.0	30.3	22.8	38.2	49.2	49.2	0.2	15.5	2.0	0.462	0.733	3.74	0.623	1.34
11-A	300	18.4	29.6	12.0	23.9	46.6	46.6	0	6.5	2.0	0.462	0.532	3.31	0.574	1.24
16-A	300	18.6	32.3	19.3	32.5	47.8	47.8	0.2	13.8	2.0	0.462	1.569	3.39	0.479	1.03
1-B	300	25.0	37.9	10.2	16.7	55.3	56.6	1.0	6.9	2.0	0.462	1.212	2.61	0.459	0.99
7-B	300	22.5	38.0	12.2	18.9	55.7	56.0	1.2	6.3	2.0	0.462	1.475	3.18	0.473	1.02
11-B	300	25.5	35.7	8.9	13.7	52.2	52.7	0.7	4.5	2.0	0.462	1.047	2.26	0.476	1.02
16-B	300	24.4	35.6	8.3	13.4	53.2	54.1	0.9	5.0	2.0	0.462	1.180	2.54	0.519	1.12

(a) Metallurgical condition code (see Tables 5a, 5b)

(b) $f(\phi t) = \sqrt[4]{1-e^{-\beta\phi t}}$ where β = 2.35E-22 reciprocal fluence and ϕt = fluence (nv) n/cm^2

(c) f(YS) = ΔYS/YS where YS = 0.2% offset yield strength and ΔYS = difference in yield strength for the irradiated and non-irradiated condition only.

(d) f(UTS) = ΔUTS/UTS where UTS = ultimate strength and ΔUTS = difference in irradiated ultimate strength and non-irradiated ultimate strength.

Table 5f. RING TENSILE PROPERTIES (VALUES REPRESENT THE AVERAGE OF TWO OR FOUR RESULTS) (From Reference 19, 20)

Batch Number and Condition[a]	Test Temperature, deg C	Unirradiated Properties: Yield Strength ksi	Unirradiated Properties: Ultimate Strength ksi	Unirradiated Properties: Elongation Uniform %	Unirradiated Properties: Elongation Total %	Postirradiation Properties: Yield Strength ksi	Postirradiation Properties: Ultimate Strength ksi	Postirradiation Properties: Elongation Uniform %	Postirradiation Properties: Elongation Total %	Fluence E20 n/cm^2	f(Φt)[b]	f(YS)[c]	f(YS)/f(Φt)	f(UTS)[d]	f(UTS)/f(Φt)
1-C	20	86.3	103.0	6.6	11.3	113.5	118.5	3.6	8.1	2.7	0.497	0.315	0.633	0.150	0.302
2-C	20	72.4	92.2	9.7	23.5	106.5	109.0	3.0	13.9	2.7	0.497	0.471	0.946	0.182	0.365
7-C	20	78.2	98.0	9.1	21.9	112.5	116.5	3.1	10.5	2.7	0.497	0.438	0.880	0.188	0.379
8-C	20	88.7	109.2	8.4	12.2	111.2	119.5	4.8	11.9	2.7	0.497	0.253	0.509	0.094	0.189
9-C	20	89.8	107.5	6.8	11.4	118.5	124.3	3.4	7.7	2.7	0.497	0.319	0.641	0.156	0.313
11-C	20	60.4	74.2	9.2	32.9	86.5	94.6	4.9	16.8	2.7	0.497	0.432	0.867	0.278	0.552
16-C	20	96.2	108.3	3.7	9.6	130.0	132.0	0.9	3.0	2.9	0.506	0.351	0.694	0.218	0.432
17-C	20	90.5	101.9	3.6	11.0	136.5	139.0	0.9	2.8	2.9	0.506	0.508	1.00	0.364	0.719
18-C	20	84.5	97.1	3.0	8.8	101.2	106.9	1.1	4.5	2.9	0.506	0.1976	0.390	0.100	0.199
1-A	20	64.5	76.4	7.9	20.1	87.6	89.0	1.0	9.2	2.0	0.462	0.358	0.773	0.164	0.356
7-A	20	60.0	71.6	9.5	26.2	82.0	84.9	1.6	17.3	2.0	0.462	0.366	0.792	0.185	0.401
11-A	20	62.0	73.9	9.4	21.5	80.5	82.4	2.0	11.0	2.0	0.462	0.298	0.644	0.115	0.248
16-A	20	59.6	72.1	9.2	26.4	83.0	86.0	1.7	15.9	2.0	0.462	0.392	0.848	0.192	0.416
1-B	20	58.0	73.1	10.6	12.9	69.8	72.7	1.8	6.1	2.0	0.462	0.203	0.439	N.M.	
7-B	20	66.2	82.5	8.1	11.4	79.0	83.0	1.9	6.7	2.0	0.462	0.193	0.417	N.M.	
11-B	20	60.2	75.8	10.7	13.3	79.7	84.1	2.4	6.9	2.0	0.462	0.323	0.699	0.109	0.236
16-B	20	60.9	76.4	8.8	12.2	81.8	86.1	2.1	6.9	2.0	0.462	0.343	0.741	0.127	0.274
1-C	300	49.4	53.8	3.7	13.3	63.4	66.2	3.0	10.4	2.7	0.4979	0.283	0.569	0.230	0.462
2-C	300	44.1	49.1	4.1	22.7	56.5	59.0	2.6	16.1	2.7	0.4979	0.281	0.564	0.150	0.302
7-C	300	50.3	56.6	4.6	19.0	67.2	69.5	2.7	14.9	2.7	0.4979	0.336	0.674	0.227	0.457
8-C	300	50.6	59.5	5.1	11.6	63.7	67.5	4.0	10.9	2.7	0.4979	0.258	0.520	0.134	0.270
9-C	300	59.3	68.8	4.9	10.4	76.2	81.0	3.2	9.8	2.7	0.4979	0.285	0.572	0.177	0.356
11-C	300	29.0	37.4	7.6	43.0	51.7	52.1	2.3	22.1	2.7	0.4979	0.782	1.572	0.393	0.789
16-C	300	53.0	58.3	1.9	10.0	69.1	61.2	0.7	6.4	2.9	0.5060	0.134	0.264	0.049	0.098
17-C	300	63.8	70.6	1.7	11.0	66.5	87.1	1.1	3.3	2.9	0.5060	0.355	0.703	0.233	0.461
18-C	300	59.1	65.4	2.0	9.9	90.8	93.6	0.4	2.8	2.9	0.5060	0.536	1.060	0.431	0.852
1-A	300	28.6	34.2	11.3	32.3	44.1	45.1	0.7	23.0	2.0	0.4629	0.542	1.170	0.318	0.688
7-A	300	24.3	30.5	12.8	43.2	40.0	41.1	0.7	24.5	2.0	0.4629	0.696	1.395	0.347	0.750
11-A	300	24.9	31.0	11.8	30.5	38.0	39.4	2.2	17.3	2.0	0.4629	0.526	1.136	0.277	0.585
16-A	300	25.0	31.0	12.4	39.8	39.0	40.9	1.0	22.8	2.0	0.4629	0.560	1.209	0.319	0.689
1-B	300	38.8	39.7	3.5	10.0	46.8	47.6	1.2	5.3	2.0	0.4629	0.206	0.445	0.199	0.929
7-B	300	31.9	39.1	8.5	11.9	46.6	47.9	1.5	8.0	2.0	0.4629	0.460	0.995	0.225	0.986
11-B	300	31.2	39.4	9.1	12.7	43.6	45.2	1.6	6.8	2.0	0.4629	0.397	0.850	0.147	0.318
16-B	300	30.6	37.7	8.1	12.7	44.5	44.9	1.4	6.3	2.0	0.4629	0.454	0.981	0.191	0.412

(a) Metallurgical condition code (see Tables 5a, 5b)

(b) $f(\phi t) = \sqrt[4]{1-e^{-\beta\phi t}}$ where β = 2.35E-22 reciprocal fluence and ϕt = fluence (nv) n/cm^2

(c) $f(YS) = \Delta YS/YS$ where YS = 0.2% offset yield strength and ΔYS = difference in yield strength for the irradiated and non-irradiated condition only.

(d) $f(UTS) = \Delta UTS/UTS$ where UTS = ultimate strength and ΔUTS = difference in irradiated ultimate strength and non-irradiated ultimate strength.

Table 6. TENSILE TESTS ON LONGITUDINAL COUPON CLADDING SPECIMENS (From Reference 24)

Specimen Identification	Tubing Lot Number	Fluence $1.20\ n/cm^2$	Test Temperature °C	Yield Strength ksi	Ultimate Tensile Strength ksi	Elongation Uniform %	Elongation Total %	f(gt)	f(y%)	f(y%)/f(gt)	f(UTS)	f(UTS)/f(gt)
1	CA-3	0	Room	36.6	73.6	14.4	24.5					
5	CA-2	0		45.0	64.0	14.8	>23.6					
6	CA-2	0		47.0	66.2	17.2	27.4					
13	CA-4	0		51.5	71.8	18.0	31.6					
14	CA-3	0		54.0	74.0	15.8	28.0					
A13-J7	CA-2	3.8		98.4	111.9	1.1	3.0	.876	1.139	1.299	.718	.820
A41-G3	CA-4	3.8		90.3	106.0	0.8	3.2	.876	.753	.859	.476	.543
A41-G2	CA-4	3.8		103.1	112.7	0.8	3.0	.876	1.002	1.142	.569	.649
2	CA-3	0	343	20.6	34.3	11.6	19.6					
7	CA-2	0		22.0	38.5	14.7	22.2					
8	CA-2	0		21.0	35.0	11.0	20.5					
15	CA-4	0		23.5	35.0	15.2	26.8					
A13-B1	CA-2	3.8		57.8	66.0	0.7	1.2	.876	1.688	1.926	.795	.908
A13-B2	CA-2	3.8		66.1	69.7	0.4	1.4	.876	2.074	2.366	.896	1.022
A41-B1	CA-4	3.8		66.3	66.5	0.3	1.2	.876	1.823	2.077	0.980	1.026
A41-B2	CA-4	3.8		55.3*	74.1	1.1*	2.2*	.876	1.353	1.543	1.117	1.274
A46-D1	CA-2	3.4		62.0	67.5	0.3	1.1	.861	2.116	2.457	.836	.971
A46-B2	CA-2	3.4		46.9*	66.2	1.7*	3.0*	.861	1.181	1.371	.801	.930
A46-M3	CA-2	3.2		66.3	68.3	0.2	1.0	.852	2.176	2.552	.858	1.006
B97-E3	CA-2	3.6		75.7	76.2	0.3	1.1	.869	2.520	2.900	1.073	1.234
A46-L2	CA-2	3.2	343	65.9	67.6	0.3	1.2	.852	2.065	2.421	.839	.984
A46-G2	CA-2	3.1	343	68.4	68.4	0.2	1.7	.848	2.171	2.577	.861	1.015
3	CA-3	0	399	20.2	31.0	7.7	18.3					
9	CA-2	0		21.2	29.5	17.0	21.2					
10	CA-2	0		23.0	32.0	14.6	19.5					
17	CA-1	0		25.4	32.2	12.9	19.8					
18	CA-1	0		30.8	38.5	10.8	19.2					
A46-C3	CA-2	3.4		59.6	59.9	0.4	2.0	.861	1.696	1.970	.948	1.101
A46-C2	CA-2	3.4		62.0	62.4	0.3	0.6	.861	1.805	2.096	1.029	1.195
A46-L1	CA-2	3.2		61.6	61.6	0.2	1.9	.852	1.787	2.096	1.003	1.176
4	CA-3	0	454	19.9	28.1	6.8	19.9					
11	CA-2	0		18.5	30.5	12.4	16.6					
12	CA-2	0		18.8	29.8	9.6	16.2					
19	CA-3	0		21.5	31.0	12.2	19.5					
20	CA-3	0		29.3	34.6	7.0	14.2					
A46-J1	CA-2	3.2		38.3	38.8	0.5	12.1	.852	1.053	1.235	.287	.336
A46-J2	CA-2	3.2		45.8	46.8	0.5	5.4	.852	1.455	1.707	.552	.647
A46-M2	CA-2	3.2		35.4	36.4	0.6	9.7	.852	.898	1.053	.207	.243
A46-G1	CA-2	3.1	454	38.7	40.7	0.6	5.0	.848	1.075	1.267	.350	.412

*Accuracy of these values is in doubt. Specimens may have slipped in grips.

†Held at designated test temperature 1 hour prior to testing.

#Held at designated test temperature 16-1/2 hours prior to testing.

NOTE: Unirradiated specimens 1 through 4 were prepared out of cell with a Tensilkut machine and were tested in cell. Specimens 5 through 12 were prepared out of cell with a milling machine and were tested out of cell. Specimens 13 through 15, and 17 through 20 were prepared in cell with a Tensilkut machine and were tested out of cell.

Table 7. TENSILE TEST DATA OBTAINED FROM UNIRRADIATED AND IRRADIATED ZIRCALOY-4 (GROUP A) AND ZIRCALOY-2 (GROUP B) STRIP (From Reference 11)

Specimen Orientation w.r.t. Strip Rolling Direction	Test Temp °F	Fluence, E21 n/cm²	Yield Strength ksi	Ultimate Strength ksi	Fracture Strength ksi	Elongation Uniform %	Elongation Total %	Reduction of Width (Row) %	Reduction of Thickness (Rot) %	Row/Rot	Reduction of Area %	f(φt)[a]	f(ΔYS)[b]	f(ΔYS)/f(φt)	f(ΔUTS)[c]	f(ΔUTS)/f(φt)
	20	--	62.6	71.8	53.8	8.1	29.7	49.7	14.1	3.52	56.8					
	20	--	60.7	72.2	53.1	10.0	32.6	49.2	13.7	3.60	60.6					
	20	0.9	115.6	115.6	86.0	0.0	5.6	19.9	10.7	1.95	28.1	.661	.888	1.344	.605	.915
	20	0.9	116.3	116.3	87.5	0.0	6.4	21.6	10.7	2.02	30.0	.661	.9[illegible]	1.346	.635	.930
	288	--	24.3	30.3	18.6	14.9	50.4	69.0	26.8	2.57	77.3					
	288	--	24.4	30.0	18.9	14.2	50.0	69.7	24.4	2.86	77.3					
A. Transverse	288	--	24.2	29.9	18.5	14.9	49.9	69.2	24.4	2.84	76.7					
	288	--	24.4	30.0	18.3	13.8	51.5	69.9	24.9	2.81	77.3					
	288	0.45	60.0	72.7	--	0.69	14.4	51.8	14.1	3.67	66.1	.563	1.467	2.608	1.433	2.546
	288	0.45	63.4	74.5	--	0.64	15.6	53.5	14.1	3.79	60.1	.563	1.608	2.857	1.463	2.635
	288	0.9	62.6	76.2	--	0.60	12.4	49.1	9.3	5.3	53.9	.661	1.573	2.380	1.552	2.349
	288	0.9	60.9	75.0	--	0.72	10.8	46.2	16.1	2.87	54.9	.661	1.502	2.274	1.514	2.291
	288	1.5	70.2	77.3	44.8	0.65	8.4	18.3	10.7	1.71	27.1	.738	1.888	2.558	1.590	2.154
	288	1.5	65.8	76.4	54.0	0.74	4.8	17.1	16.6	1.03	30.8	.738	1.707	2.313	1.552	2.109
	20	--	52.9	62.6	47.1	9.2	27.2	46.8	16.1	2.91	55.3					
	288	--	20.8	29.4	17.2	11.9	51.5	68.7	25.9	2.65	76.8					
	288	--	19.8	29.2	15.6	9.6	43.7	70.1	29.3	2.39	78.8					
A. Longitudinal	288	0.9	69.7	76.2	47.6	0.56	9.6	31.0	15.6	1.99	41.7	.661	2.438	3.690	1.636	2.492
	288	0.9	63.1	76.6	--	0.88	--	--	--	--	--	.661	2.115	3.201	1.663	2.514
	288	1.5	60.4	76.8	--	0.83	5.6	13.0	15.6	0.83	26.6	.738	1.982	2.685	1.666	2.257
A. Weld Region	20	--	70.5	87.3	74.7	3.9	12.7	20.5	27.5	0.75	42.4					
	288	--	43.6	53.0	39.0	4.4	15.9	40.5	41.2	0.98	65.1					
	288	0.5	72.9	87.2	74.2	1.12	7.6	18.7	19.4	0.96	34.5	.577	.671	1.162	.643	1.115
	288	0.9	83.6	98.7	91.0	1.11	5.6	16.8	21.3	0.79	34.5	.661	.935	1.385	.850	1.302
	288	1.5	85.3	101.9	87.2	1.11	6.0	13.6	14.2	0.96	25.9	.738	.954	1.293	.922	1.249
B. Transverse	327	--	22.5	28.4	--	16.4	30.6	72.6	24.4	2.98	80.0					
	327	1.5	73.8	75.8	--	0.35	5.9	37.1	7.3	5.1	42.0	.738	2.284	3.096	1.700	2.302
	250	1.6	82.0	82.5	--	0.28	5.0	36.8	7.5	4.9	42.0					
	250	2.2	88.6	89.9	--	0.30	5.0	32.0	10.0	3.2	39.0					
B. Transverse (50 ppm oxygen)	250	2.8	83.6	84.5	--	0.40	6.0	29.9	8.4	2.5	28.0					
	327	2.8	80.1	81.9	--	0.50	6.9	23.6	13.9	1.7	34.0	.833	2.575	3.091	1.880	2.256
	327	--	18.6	25.6	--	18.8	27.0	72.2	16.3	4.4	77.0					
B. Beta-Quenched	342	--	35.0	41.1	--	2.4	7.8	25.4	37.3	0.7	53.0					
	342	1.0	69.1	72.0	--	1.7	--	--	--	--	--	.677	.975	1.442	.750	1.110
	342	1.6	77.6	86.2	--	1.2	5.1	13.4	24.4	0.6	34.0	.677	1.219	1.802	1.096	1.621

[a] $f(\phi t) = \sqrt[4]{1 - e^{-\beta\phi t}}$ Where β = 2.35E-22 reciprocal fluence and ϕt = fluence (nv) n/cm².

[b] $f(YS) = \Delta YS/YS$ Where YS = 0.2% offset yield strength and ΔYS = difference in yield strength for the irradiated and non-irradiated condition only.

[c] $f(UTS) = \Delta UTS/UTS$ Where UTS = ultimate strength and ΔUTS = difference in irradiated ultimate strength and non-irradiated ultimate strength

Table 8. TENSILE TEST DATA OF IRRADIATED AND UNIRRADIATED ZIRCONIUM ALLOY SPECIMENS TESTED AT 250°C TO DETERMINE THE EFFECT OF TEXTURE OF STRENGTH AND DUCTILITY (STRAIN RATE 0.05/MIN) (From Reference 12)

Engineering Stress-Strain Data

Specimen[a] No.	Form	Texture (0002 Pole deg)	Fluence E21 n/cm²	Yield Strength ksi	Tensile Strength ksi	Elongation, % Length Uniform	Length Total	Width Total	Thick Total	Reduction of Area %	Ratio, $(W_f W_o)/(t_f/t_o)$	$f(\phi t)$[b]	f(YS)[c]	f(YS)/f(φt)	f(UTS)[d]	f(UTS)/f(φt)
C5-6	T	60-70	No	32.0	36.2	7.9	>14	-63.4	-12.4	70.8	0.42	--	--	--	--	--
E-20-6	T	60-70	No	32.4	35.0	8.9	28.6	-62.9	-31.9	74.0	0.54	--	--	--	--	--
E-38-6	TG	60-70	No	43.7	50.5	<29.8[e]	--	-12.5	-14.4	25.8	1.02	--	--	--	--	--
J-8-6	T	≤30	No	28.4	31.5	11.0	25.0	-63.4	-30.7	77.6	0.53	--	--	--	--	--
C-7-7	T	60-70	1.17	79.0	79.0	0.81	5.6	-32.0	-17.3	44.0	0.82	.700	1.453	2.075	1.219	1.741
C-11-7	TG	60-70	0.64	75.0	91.0	<24.3[e]	--	-7.4	[illegible]	21.6	1.10	.611	0.716	1.171	0.802	1.312
E-29-7	T	60-70	1.90	83.0	83.0	0.86	5.6	-36.5	-10.3	42.5	0.71	.774	1.577	2.036	1.331	1.718
E-43-7	TG	60-70	1.88	92.4	98.4	<14.5[e]	--	-9.7	-4.8	13.5	0.95	.773	1.114	1.441	0.948	1.227
J-10-7	T	≤30	0.83	79.0	79.2	0.83	4.8	-48.8	-15.4	57.0	0.61	.648	1.782	2.746	1.514	2.334
J-12-7	T	≤30	1.33	74.8	74.8	0.81	4.9	-36.0	-17.1	47.6	0.77	.720	1.633	2.269	1.374	1.909
J-15-7	TG	≤30	0.83	78.6	89.1	<23.8[e]	--	-10.4	-14.4	21.2	1.05	.648	1.767	2.724	1.828	2.818
J-16-7	TG	≤30	1.33	69.0	74.8	<29.4[e]	--	-7.8	0	25.5	0.92	.720	1.429	1.986	1.374	1.909
K-7-7	T	≈ 0	1.17	65.0	66.3	0.93	6.3	-26.4	-3.8	29.3	0.77	--	--	--	--	--
K-8-7	RG	≈ 0	1.17	108.0	109.0	<13.2[e]	--	-8.1	-4.8	12.4	0.96	--	--	--	--	--

[a] Specimen form; T = tensile specimen, transverse direction; TG or RG = plane strain grooved specimen with material in transverse or as-rolled directions.

[b] $f(\phi t) = \sqrt[4]{1 - e^{-\beta \phi t}}$ Where β = 2.35E-22 reciprocal fluence and ϕt = fluence (nv) n/cm².

[c] $f(YS) = \Delta YS/YS$ Where YS = 0.2% offset yield strength and ΔYS = difference in yield strength for the irradiated and non-irradiated condition only.

[d] $f(UTS) = \Delta UTS/UTS$ Where UTS = ultimate strength and ΔUTS = difference in irradiated ultimate strength and non-irradiated ultimate strength.

[e] Uniform elongation values for plane strain specimens estimated from RA values and considered to be excessively high.

Table 9. TENSILE TEST RESULTS ON IRRADIATED SAXTON CORE II CLADDING (From Reference 25)

Test Temperature °C	Fluence, E21/n/cm²	0.2% Yield Strength ksi	Ultimate Strength ksi	Elongation Uniform %	Elongation Total %	Reduction of Area %	f(φt)[a]	f(YS)[b]	f(YS)/f(φt)	f(UTS)[c]	f(UTS)/f(φt)
357	3.2	46.2	54.2	3.6	9.3	27	0.850	0.209	0.246	0.093	0.110
357	2.3	54.2	61.7	5.2	9.3	48	0.804	0.419	0.493	0.244	0.303
357	3.1	52.0	59.6	2.5	6.0	44	0.848	0.361	0.426	0.202	0.238
357	2.3	49.1	57.9	6.0	11.3	31	0.804	0.285	0.355	0.167	0.208
357	3.3	48.4	54.6	2.6	8.0	53	0.857	0.267	0.312	0.101	0.118
357	2.3	48.4	58.1	7.1	15.1	50	0.804	0.267	0.337	0.171	0.213
357	3.1	52.5	60.4	4.9	9.8	26	0.848	0.374	0.441	0.218	0.257
357	3.1	51.6	64.8	5.6	18.4	46	0.848	0.350	0.414	0.306	0.361
357	3.1	54.3	65.3	5.7	14.9	56	0.848	0.421	0.497	0.317	0.373
357	2.1	67.0	73.1	2.9	12.2	48	0.790	0.754	0.954	0.474	0.979
357	1.7	40.1	45.9	11.5	13.6	44	0.758	0.050	0.066	-	-
357	2.0	56.9	65.9	6.1	19.5	53	0.783	0.490	0.625	0.329	0.420
357	2.0	48.2	58.2	7.2	19.3	37	0.783	0.262	0.334	0.173	0.221
357	3.2	56.7	67.8	3.6	7.9	37	0.850	0.484	0.570	0.367	0.432
357	2.0	53.2	72.4	7.3	12.5	65	0.783	0.393	0.501	0.460	0.587
357	3.2	42.3	62.0	3.5	11.1	67	0.850	0.107	0.126	0.250	0.294
357	1.5	52.2	61.6	4.0	8.9	49	0.738	0.366	0.497	0.242	0.328
357	1.8	48.3	52.0	3.3	10.4	64	0.766	0.264	0.345	0.048	0.063
357	2.1	49.3	63.3	4.8	8.6	37	0.790	0.290	0.368	0.276	0.350
357	2.1	45.8	59.2	4.1	10.1	58	0.790	0.199	0.252	0.194	0.245
371	3.1	53.8	57.3	4.3	9.0	36	0.848	0.423	0.499	0.169	0.200
371	1.9	44.8	53.8	4.2	18.2	60	0.775	0.185	0.239	0.098	0.126

(a) $f(\phi) = \sqrt[4]{1 - e^{-\beta\phi t}}$ where β = 2.35E-22 reciprocal fluence and ϕt = fluence (nv) n/cm².

(b) f(YS) = ΔYS/YS where YS = 0.2% offset yield strength and ΔYS = difference in yield strength for the irradiated and non-irradiated condition only.

(c) f(UTS) = ΔUTS/UTS where UTS = ultimate strength and ΔUTS = difference in irradiated ultimate strength and non-irradiated ultimate strength.

Table 10. POST IRRADIATION TENSILE PROPERTIES OF ZIRCALOY-2 AND -4
(From Reference 26)

Material[A] Identity	Fluence E21/ncm^2	Test Temperature (°C)	Yield Strength (ksi)	Ultimate Strength (ksi)	Elongation Uniform (%)	Elongation Total (%)	Reduction In Area (%)	F(φT)[B]	F(YS)[C]	F(YS)/F(φT)	F(UTS)[D]	F(UTS)/F(φT)
Zr-4, A	0	Room	48	73	15.0	22.9	41.5					
Zr-4, A	1.0	Room	79	90	3.7	11.4	36.6	0.676	0.655	0.969	0.228	0.337
Zr-4, A	1.4	Room	80	90	3.6	11.4	32.3	0.728	0.677	0.929	0.228	0.337
Zr-2, A	0	Room	45	70	16.7	26.3	39.9					
Zr-2, A	1.0	Room	82	89	3.2	12.3	39.1	0.676	0.810	1.198	0.265	0.392
Zr-2, A	1.4	Room	76	82	3.1	11.8	39.3	0.728	0.678	0.931	0.163	0.224
Zr-4, A	0	150	35	56	13.0	23.9	42.1					
Zr-4, A	1.0	150	67	70	2.8	12.0	39.1	0.676	0.912	1.348	0.253	0.374
Zr-4, A	1.4	150	69	72	2.2	11.6	39.9	0.728	0.965	1.327	0.278	0.382
Zr-4, A	2.5	150	74	76	1.1	9.3	37.2	0.816	1.125	1.379	0.345	0.423
Zr-4, A-E	0	150	53	73	9.3	21.4	50.5					
Zr-4, A-E	1.0	150	82	87	1.5	11.2	49.2	0.676	0.526	0.778	0.186	0.275
Zr-4, A-E	1.4	150	85	88	0.6	9.4	49.7	0.728	0.595	0.817	0.194	0.267
Zr-4, A-E	2.5	150	93	95	0.7	8.8	46.3	0.816	0.743	0.911	0.289	0.354
Zr-4, A-E&H	0	150	55	72	6.9	20.7	45.6					
Zr-4, A-E&H	2.5	150	95	96	0.7	9.1	47.1	0.816	0.699	0.857	0.337	0.413
Zr-4, A&H	0	150	54	54	11.2	24.6	40.3					
Zr-4, A&H	2.5	150	71	74	1.5	10.0	39.1	0.816	1.051	1.288	0.377	0.462
Zr-4, A	0	290	21	40	15.7	27.0	48.0					
Zr-4, A	1.0	290	49	49	0.6	13.7	50.9	0.676	1.320	1.954	0.211	0.313
Zr-4, A	1.4	290	48	49	0.6	12.9	45.1	0.728	1.321	1.814	0.211	0.313
Zr-4, A	2.5	290	59	59	0.2	10.0	42.4	0.816	1.783	2.185	0.453	0.555

[A] Explanation of designations:

A - Annealed

A-E - As extruded

A-E&H - As extruded and hydrided to ~300 ppm

[B] $F(\phi T) = \sqrt[4]{1 - e^{-\theta\phi T}}$ Where θ = 2.35E-22 reciprocal fluence and ϕT = fluence (nv) n/cm^2.

[C] $F(YS) = \Delta YS/YS$ Where YS = 0.2% offset yield strength and ΔYS = difference in yield strength for the irradiated and non-irradiated condition only.

[D] $F(UTS) = \Delta UTS/UTS$ Where UTS = ultimate strength and ΔUTS = difference in irradiated ultimate strength and non-irradiated ultimate strength.

Table 11. IN-FLUX AND POST-IRRADIATION TENSILE DATA FOR ZIRCALOY-4 (From Reference 13)

Test[A] Identity	Test Temperature (°C)	Fluence E>0 n/cm^2	Strain Rate (hr^{-1})	Yield Strength ksi	Ultimate Strength ksi	Elongation Uniform (%)	Elongation Total (%)	Reduction in Area (%)	F(εt)[B]	F(ys)[C]	F(ys)/F(εt)
T-3	315	-	6E-4	21.2	33.7	5.0	8.8	63.5			
T-5	315	-	6E-3	20.3	33.7	9.4	13.5	63.5			
T-11	315	-	6E-2	20.5	33.5	12.3	15.3	65.1			
T-0	315	-	3E0	21.7	32.2	17.0	21.2	67.5			
T-96	282	-	3E0	23.4	31.7	19.8	27.2	68.5			
T-A	282	-	4E-5	21.8	35.5	7.0	9.4	60.2			
TL-99	282	-	3E0	19.5	33.6	18.0	22.9	63.5			
TL-36	282	-	6E-3	16.5	35.5	10.2	14.2	61.2			
TL-39	282	-	1E-5	15.4							
TL-40	282	-	2E-5	12.9							
TL-102	282	-	4E-5	17.8							
TL-104	282	-	4E-5	16.7							
TL-C	282	-	4E-5	16.3	37.5/33.5	6.0	8.8	56.4			
TL-A	282	-	7E-6	14.5	34.2	-	8.8	53.8			
				IN-FLUX TESTS							
TL-32	282	8.2	5E-6	19.0					0.647	0.122	0.188
TL-33	282	1.0	1E-5	22.7					0.390	0.474	1.215
T-4	282	4.0	1E-4	55.2					0.547	1.604	2.932
T-6	282	4.0	5E-5	53.0					0.547	1.431	2.616
T-25	282	1.0	1E-5	38.0					0.390	0.743	1.905
T-14	282	31.8	5E-5	28.0					0.852	0.284	0.334
T-16	282	28.0	5E-5	28.0					0.833	0.284	0.334
				P.I.E. TESTS							
TL-31	282	9.4	5E-6	54.0					0.672	2.724	4.054
TL-56	282	6.0	3E-0	55.4					0.602	1.841	3.058
TL-57	282	6.0	3E-3	46.5					0.602	1.818	3.020

(A) EXPLANATION OF DESIGNATIONS:
T = TRANSVERSE DIRECTION
TL = ROLLING DIRECTION

(B) $F(\varepsilon t) = \Phi \left[1 - e^{-\lambda t}\right]$ WHERE λ = 2.35E-22 RECIPROCAL FLUENCE AND Φt = FLUENCE (NV) N/CM^2.

(C) F(YS) = ΔYS/YS WHERE YS = 0.2% OFFSET YIELD STRENGTH AND ΔYS = DIFFERENCE IN YIELD STRENGTH FOR THE IRRADIATED AND NON-IRRADIATED CONDITION ONLY.

(D) F(UTS) = ΔUTS/UTS WHERE UTS = ULTIMATE STRENGTH AND ΔUTS = DIFFERENCE IN IRRADIATED ULTIMATE STRENGTH AND NON-IRRADIATED ULTIMATE STRENGTH.

Table 12. TENSILE TEST DATA OF IRRADIATED AND UNIRRADIATED ZIRCONIUM-2.5 WT% NIOBIUM (From Reference 23)

Material Condition[a]	Fast Fluence, E20 n/cm^2	Irr. Temp. C	Test Temp. C	Yield Strength ksi		Ultimate Strength ksi		Elongation, % Uniform		Elongation, % Total		Reduction in Area, %		f(σt)[b]	f(YS)[c]	f(YS)/f(σt)	f(UTS)[d]	f(UTS)/f(σt)
				Unirr.	Irr.	Unirr.	Irr.	Unirr.	Irr.	Unirr.	Irr.	Unirr.	Irr.					
Q-B, A-500	3	250-325	RT	113	153	170	160	4	<1	10	1	>25	>5	0.510	0.354	0.694	-	-
Q-B, A-500	1	250	300	85	97	93	102	-	-	14.2	13.3	-	-	0.390	0.141	0.362	0.097	0.248
Q-B, A-500	3	250-325	300	81	114	133	126	3	1.5	12	2	56	<20	0.510	0.407	0.800	-	-
SC-B, 40 CW	3	250-325	RT	97	131	122	152	1	1	-	-	30	26	0.510	0.351	0.687	0.245	0.482
SC-B, 40 CW	3	250-325	300	60	101	90	116	1	1	-	-	34	26	0.510	0.683	1.340	0.289	0.566
Q-B, A-500	1	250	RT	-	136	-	142	-	-	-	10.5	-	-	-	-	-	-	-
SC-(A + B)	3	250-325	RT	61	107	132	150	12	3.0	-	-	56	37	0.510	0.754	1.478	0.136	0.267
SC-(A + B)	3	250-325	300	32	80	100	120	18	2.0	30	11	72	60	0.510	1.500	2.941	0.200	0.392
SC-B	3	250-325	RT	73	100	130	123	9	10	-	-	44	13	0.510	0.370	0.725	-	-
SC-B	3	250-325	300	34	68	92	120	5	4	12	9	67	40	0.510	1.000	1.960	0.304	0.596
Q-(A + B)	3	250-325	RT	109	142	194	210	4	1	-	-	60	55	0.510	0.303	0.594	0.082	0.162
A-500	3	250-325	300	85	116	167	175	3	<1	12	11	70	65	0.510	0.365	0.715	0.048	0.094
Q-B	1	250	300	77	108	87	115	-	-	14.5	11.3	-	-	0.390	0.403	1.032	0.322	0.825

(a) Explanation of designations:

SC - slow cooled — Q - quenched

(A+B) - from (alpha + beta) phase — A-500 - annealed at 500°C

B - from beta phase

Table 13. TENSILE PROPERTIES OF THE Zr-2.5 WT% Nb ALLOY IN VARIOUS METALLURGICAL CONDITIONS (From Reference 23)

Metallurgical Condition	Irradiation[a] History	Test Temp °C	Yield Strength ksi	Ultimate Strength ksi	Elong. Uniform %	Reduction in Area %	$f(\phi t)$[b]	$f(YS)$[c]	$\frac{f(YS)}{f(\phi t)}$	$f(UTS)$[d]	$\frac{f(UTS)}{f(\phi t)}$
Slow cooled from (α + β) phase	Unirradiated	RT	61	132	12	56	--	--	--	--	--
	Irradiated	RT	117	150	3	37	0.510	0.754	1.476	0.136	0.267
	Unirradiated	300	72	100	18	72		--	--	--	--
	Irradiated	300	80	120	2	60		1.500	2.937	0.167	0.326
Slow cooled from β-phase	Unirradiated	RT	73	130	9	44		--	--	--	--
	Irradiated	RT	100	123	10	13		0.370	0.724	--	--
	Unirradiated	300	34	92	5	67		--	--	--	--
	Irradiated	300	68	120	4	40		1.000	1.958	0.304	0.596
Quenched from (α + β) phase and aged 24 hr at 500°C	Unirradiated	RT	109	194	4	60		--	--	--	--
	Irradiated	RT	142	210	1	55		0.303	0.592	0.083	0.161
	Unirradiated	300	85	167	3	70		--	--	--	--
	Irradiated	300	116	175	<1	65		0.365	0.714	0.058	0.114
Quenched from β-phase and aged 24 hr at 500°C	Unirradiated	RT	113	170	4	>25		--	--	--	--
	Irradiated	RT	153	160	<1	< 5		0.354	0.693	--	--
	Unirradiated	300	81	133	3	55		--	--	--	--
	Irradiated	300	114	126	1.5	<20		0.407	0.798	--	--
Cold drawn 40% after slow cooling from (α + β) phase	Unirradiated	RT	97	122	1	30		--	--	--	--
	Irradiated	RT	131	152	1	26		0.351	0.686	0.246	0.481
	Unirradiated	300	60	90	1	34		--	--	--	--
	Irradiated	300	101	116	1	26		0.683	1.338	0.289	0.566

(a) AW Material. Irradiated specimens were at 250° - 325°C during irradiation to 3 x 10^{20} n/cm^2

(b) $f(\phi t) = \sqrt[4]{1 - e^{-\beta\phi t}}$ where β = 2.35E-22 reciprocal fluence and ϕt = fluence (nv) n/cm^2.

(c) $f(YS) = \Delta YS/YS$ where YS = 0.2% offset yield strength and ΔYS = difference in yield strength for the irradiated and non-irradiated condition only.

(d) $f(UTS) = \Delta UTS/UTS$ where UTS = ultimate strength and ΔUTS = difference in irradiated ultimate strength and non-irradiated ultimate strength.

Table 14a. ROOM TEMPERATURE TENSILE DATA FOR Zr ALLOYS IRRADIATED TO ~4E19 n/cm^2

Material Identity[a]	Testing Direction	Irradiation Temperature °C	Yield Strength ksi	Ultimate Strength ksi	Elongation Uniform %	Elongation Total %	Reduction of Area %	Strain Hardenability du/dε	f(YS)[c]	f(YS)/ΔT	f(UTS)[d]	f(UTS)/ΔT
CN, Zr	L	U[b]	12.0	27.0	29	35	62	0.09	--	--	--	--
		50-100	33.0	34.1	1	11	62	0.16	1.750	5.62	0.259	0.83
		300	24.9	33.1	11	17	54	0.11	1.075	3.46	0.226	0.73
	T	U	20.0	29.0	18	22	68	0.09	--	--	--	--
		50-100	41.5	41.5	0	8	67	--	1.075	5.62	0.431	1.39
		300	33.1	33.1	5	13	66	0.	0.655	2.11	0.141	0.46
CA, Zr-0.55n	L	U	14.9	33.1	32	43	62	0.10	--	--	--	--
		50-100	35.1	38.0	3	25	62	0.14	1.356	4.36	0.148	0.48
		300	38.0	40.0	2	23	63	0.15	1.550	4.98	0.208	0.67
	T	U	30.0	40.2	21	32	78	0.10	--	--	--	--
		50-100	49.0	48.0	0	11	70	--	0.633	2.04	0.194	0.62
		300	42.1	43.1	4	21	73	0.07	0.403	1.30	0.072	0.23
BZ, Zr-0.14Nb	L	U	14.9	32.2	35	43	66	0.09	--	--	--	--
		50-100	41.2	42.1	4	16	58	0.21	1.765	5.67	0.307	0.99
		300	39.6	48.0	3	12	57	0.35	1.658	5.33	0.491	1.58
	T	U	26.5	36.4	24	38	74	0.09	--	--	--	--
		50-100	47.0	47.0	0	9	69	--	0.774	2.49	0.291	0.94
		300	41.0	47.0	11	22	66	0.11	0.547	1.76	0.291	0.94
BY, Zr-0.6Nb	L	U	16.0	37.0	20	26	64	0.16	--	--	--	--
		50-100	46.0	50.0	3	6	47	0.20	1.875	6.03	0.351	1.13
		300	55.8	68.3	4	8	44	0.40	2.488	8.00	0.838	2.69
	T	U	36.0	46.7	21	39	69	0.16	--	--	--	--
		50-100	59.0	67.0	3	9	57	0.17	0.639	2.054	0.434	1.40
		300	51.0	65.0	5	10	46	0.41	0.417	1.341	0.820	2.64
BX, Zr-2.35Nb	L	U	24.9	46.7	21	39	69	0.16	--	--	--	--
		50-100	64.1	67.0	3	9	57	0.17	1.574	5.06	0.435	1.40
		300	69.9	85.0	5	10	46	0.41	1.807	5.81	0.820	2.64
	T	U	43.8	62.5	5	10	43	0.23	--	--	--	--
		50-100	81.0	81.0	0	5	53	--	0.849	2.73	0.543	1.75
		300	79.0	85.1	4	9	32	0.25	0.804	2.59	0.621	2.00
BS, Zr	L	U	12.5	27.6	33	41	57	0.08	--	--	--	--
		50-100	24.8	27.8	10	25	58	0.06	0.984	3.16	--	--
		300	23.1	27.8	9	30	61	0.06	0.848	2.73	--	--
	T	U	18.4	31.2	24	34	65	0.09	--	--	--	--
		50-100	33.5	35.0	12	27	69	0.05	0.821	2.64	0.122	0.39
		300	27.6	34.4	19	32	69	0.08	0.600	1.93	0.103	0.33
BU, Zr-2	L	U	48.4	69.9	13	24	41	0.25	--	--	--	--
		50-100	68.6	78.6	4	16	35	0.35	0.417	1.34	0.124	0.40
		300	61.1	75.4	6	19	44	0.33	0.262	0.84	0.079	0.25
	T	U	68.7	74.4	9	19	46	0.14	--	--	--	--
		50-100	89.6	89.6	0	8	50	--	0.304	0.98	0.205	0.66
		300	80.2	80.1	0.5	13	46	--	0.167	0.54	0.076	0.24
BT Zr-2.5NB	L	U	56.1	73.0	14	28	60	0.21	--	--	--	--
		50-100	86.0	91.5	3	14	51	0.24	0.533	1.71	0.254	0.82
		300	97.0	102.1	6	13	35	0.37	0.551	1.77	0.399	1.29
	T	U	76.3	80.6	7	16	47	0.16	--	--	--	--
		50-100	107.0	107.0	0.5	6	40	--	0.403	1.30	0.328	1.05
		300	108.1	110.1	6	11	35	0.18	0.415	1.33	0.366	1.17

(a) Material Identity.

Alloy Designation	Alloy Composition Atomic Weight Percent	Oxygen Concentration Atomic Weight Percent	Annealing Treatment Time, hr.	Annealing Treatment Temperature, °C	Grain Size μm
BS	zirconium	0.028	0.1	700	40
CN	zirconium	0.014	1	600	21
CA	Zr-0.55n	0.048	1	600	18
BZ	Zr-0.14Nb	0.048	1	600	23
BY	Zr-0.6Nb	0.091	24	600	19
BX	Zr-2.35Nb	0.065	24	800	14
BU	commercial Zircaloy-2	0.60	1	800	15
BT	commercial Zr-2.5Nb	0.51	1	800	4

(b) U = Unirradiated

(c) f(YS) = ΔYS/YS where YS = 0.2% offset yield strength and ΔYS = difference in yield strength for the irradiated and the non-irradiated condition only.

(d) f(UTS) = ΔUTS/UTS where UTS = ultimate strength and ΔUTS = difference in ultimate strength for the irradiated and non-irradiated condition only.

Table 14b. 300°C TENSILE DATA FOR Zr ALLOYS IRRADIATED TO ~4E19 n/cm^2 (From Reference 27)

Material Identity[a]	Testing Direction	Irradiation Temperature °C	Yield Strength ksi	Ultimate Strength ksi	Elongation Uniform %	Elongation Total %	Reduction of Area %	Strain Hardenability dσ/dε	f(YS)[c]	f(YS)/f(ε_u)	f(UTS)[d]	f(UTS)/f(ε_t)
CN, Zr	L	U[b]	7.3	15.7			86	0.07	--	--	--	--
		300	20.0	20.7			85	0.08	1.740	5.59	0.318	1.02
	T	U	9.9	16.7	8.5	18	83	0.09	--	--	--	--
		300	22.5	22.5	0	10	84	--	1.273	4.09	0.433	1.39
CA, Zr-0.5Sn	L	U	8.6	19.0	29	41	86	0.06	--	--	--	--
		300	23.4	27.0	0	14	83	--	1.720	5.53	0.421	1.35
	T	U	14.9	21.0	10	22	86	0.08	--	--	--	--
		300	30.5	30.9	0	11	88	--	1.047	3.37	0.471	1.52
BZ, Zr-0.14Nb	L	U	6.8	16.7	27	41	87	0.06	--	--	--	--
		300	27.7	31.2	2	11	86	0.27	3.07	9.88	0.868	2.79
	T	U	10.7	17.5	13	25	90	0.07	--	--	--	--
		300	31.1	31.6	0.5	10	88	0.14	1.906	6.13	0.805	2.59
BY, Zr-0.6Nb	L	U	9.3	20.6	25	34	80	0.07	--	--	--	--
		300	42.1	49.2	3	10	76	0.03	3.527	11.3	1.388	4.46
	T	U	16.1	21.5	7	16	78	0.10	--	--	--	--
		300	42.5	46.2	6	14	80	0.50	1.640	5.27	1.149	3.69
BX, Zr-2.35Nb	L	U	14.8	31.8	20	17	90	0.13	--	--	--	--
		300	35.1	64.5	3.5	9	75	0.31	1.372	4.41	1.028	3.30
	T	U	19.9	32.5	7	16	87	0.20	--	--	--	--
		300	61.5	66.4	2	9	78	0.29	2.090	6.72	1.043	3.35
BS Zr	L	U	5.1	14.2	29	44	89	0.05	--	--	--	--
		300	13.6	15.1	11	28	86	0.03	1.667	5.36	0.063	0.20
	T	U	8.8	14.9	11.5	26	89	0.07	--	--	--	--
		300	18.9	20.3	0	15	92	--	1.148	3.69	0.362	1.16
BU Zr-2	L	U	17.4	30.3	21	42	71	0.10	--	--	--	--
		300	30.0	36.1	4	27	65	0.20	0.724	2.33	0.191	0.62
	T	U	27.6	32.1	16	30	71	0.07	--	--	--	--
		300	36.8	36.8	0	20	73	0.39	0.333	1.07	0.145	0.47
BT, Zr-2.5Nb	L	U	28.3	42.2	19	33	68	0.11	--	--	--	--
		300	60.6	75.7	5	14	57	0.39	1.141	3.67	0.794	2.55
	T	U	33.6	40.0	5.5	17	69	0.16	--	--	--	--
		300	72.2	75.4	3	9	59	0.19	1.149	3.69	0.885	2.85

(a) Material Identity.

Alloy Designation	Alloy Composition Atomic Weight Percent	Oxygen Concentration Atomic Weight Percent	Annealing Treatment Time, hr.	Annealing Treatment Temperature, °C	Grain Size μm
BS	zirconium	0.023	0.1	700	40
CN	zirconium	0.014	1	600	21
CA	Zr-0.5Sn	0.048	1	670	18
BZ	Zr-0.14Nb	0.048	1	600	23
BY	Zr-0.6Nb	0.091	24	800	19
BX	Zr-2.35Nb	0.065	24	800	14
BU	commercial Zircaloy-2	0.60	1	800	15
BT	commercial Zr-2.5Nb	0.51	1	800	4

(b) U = Unirradiated

(c) f(YS) = ΔYS/YS where YS = 0.2% offset yield strength and ΔYS = difference in yield strength for the irradiated and non-irradiated condition only.

(d) f(UTS) = ΔUTS/UTS where UTS = ultimate strength and ΔUTS = difference in ultimate strength for the irradiated and non-irradiated condition only.

Table 15a. THE HEAT TREATMENT, HARDNESS AND TENSILE PROPERTIES OF ZIRCONIUM ALLOYS TESTED FOR CREEP IN-REACTOR (From Reference 31)

Material (code no.)	Material	Heat Treatment	Hardness on Transv. Section (VHN)	Tensile Properties (Longitudinal Sections)								In-Reactor Creep Test No.	Average Grain Size μm
				Room Temperature				300°C					
				0.2% Y.S. ksi	UTS ksi	Total* Eln. %	R.A. %	0.2% Y.S. ksi	UTS ksi	Total* Eln. %	R.A. %		
9	Zircaloy-2 Rod	20% cold-worked stress-relieved 72 h at 400°C	230	71.0	87.3	12	30	51.0	53.0	7	58	R-2	7
11	Zircaloy-2 Tube	19% cold-worked, autoclaved 72 h at 400°C	191	67.0	87.0	19		46.9	56.0	20		R-8, R-9	7
18	Zircaloy-2 Rod	20% cold-worked, stress-relieved 72 h at 400°C	227	89.0	99.0	18	39	45.3	50.0	20	47	R-4, Rx-20	8
25	Zircaloy-2 Tube	16% cold-worked, autoclaved 72 h at 400°C	193	71.0	86.0	13	34	44.9	51.0	12	45	R-6, Rx-14, Rx-21	7
27	Zr-2.5 wt % Nb Rod	Water quenched from 850°C aged 24 h at 500°C	268	108.9	120.0	14	60	82.0	93.0	15	80	Rx-7, Ru-6, Ru-7	
33	Zirconium Rod	Annealed	66	30	28.0	50	72	11.9	20.5	36	92	Rx-19	98
34	Zr-2.5 wt % Nb Tube	21% cold-worked, autoclaved 72 h at 400°C	214	77.9	110.9	14	44	53.0	73.9	14	56	R-11, R-12 Rx-17	
36	Zr-2.5 wt % Nb Rod	Water quenched from 875°C, cold-drawn 30% aged 24 24 h at 500°C	247	86.0	117.0	19	53	67.0	75.9	19	68	Rx-13, Ru-1	
37	Zr-2.5 wt % Nb Tube	Water quenched from 880°C cold-drawn 22% aged 24 h at 500°C	252	86.0	105.9	23	54	58.0	74.9	20	61	Rx-16	
39	Zr-2.5 wt % Nb Tube	Water quenched from 880°C, cold-drawn 5%, aged 24 h at 500°C	255	96.0	115.0	19	52	60.0	82.0	19	62	Rx-18	
42	Zricaloy-2 Tube	19% cold-worked, autoclaved 72 h at 400°C	205	81.0	87.3		36	45.9	56.0	17		Rx-15	8
50	Zr-2.5 wt % Nb Tube	Water quenched from 870°C cold-drawn 16%, aged 24 h at 500°C	262	97.0	122.0	20	51	73.9	88.0	17	65	Rx-22	
51	Zr-2.5 wt % Nb Tube	Water quenched from 870°C, cold-drawn 5%, aged 24 h at 500°C	261	98.0	120.0	18	55	72.0	84.0	17	53	Rx-24	
52	Zr-2.5 wt % Nb tube	Water quenched from 870°C, cold-drawn 11% aged 24 h at 500°C	274	97.0	121.0	18	47	76.9	88.0	18	51	Rx-23, Ru-5	

* 2.5 cm gauge length.

Table 15b. UNIAXIAL IN-REACTOR CREEP DATA AT 300°C (From Reference 31)

Test No.	Material	Test Conditions: Direction of Testing	Stress ksi	Flux E13 n/cm²-sec	Duration hr	Creep Rate Near End of Test E7 hr^{-1}	Comments	Creep Rate of Unirradiated Test After Same Time as In-Reactor Test E7-hr^{-1}
						$hr^{-1} \times 10^{7}$		
R-6	Zircaloy-2, tube 84 stress	L	20	0.6	5700	*3.5±10%	Rx-14 specimen preirradiated	0.2
Rx-14	relieved 72 h at 400°C	L	20	0.7	2000	*3.0±30%	to 3×10^{20} n/cm^2	0.8
Rx-48	(material 1, Table I)	T	20	0.6	1800[a]	1.5±50%	at 300°C. Its out-of-flux creep rate after 2000 h = 0.4×10^{-7} h^{-1}	1.0
Rx-40		L	40	0.8	4000	*4.7±10%		
Ru-20		L	40	2.0	1300	*14.0±15%		4.0
Rx-44		L	65	0.7	640	12.0±10%	Specimen ruptured because of accidental overload	20
Ru-25	Zr-2.5 wt % Nb, tube 603,	L	65	2.8	2900[a]	*45.0±15%	Specimen stress relieved	130
	stress relieved 3 h at						24 h at 400°C	75
Rx-41, part I	400°C (material 3, Table I)	T	40	1.0	3600	*2.7±20%	Estimated creep rate in Rx-40 flux = 2.15×10^{-7} h^{-1}	1.5
Rx-41, part II		T	65	0.9	2300[a] (total 5900)	*9.0±10%	Estimated creep rate in Rx-44 flux = 7.0×10^{-7} h^{-1}	13
Rx-42		T	65	1.1	1600	*5.0±20%	Estimated creep rate in Rx-44 flux = 3.2×10^{-7} h^{-1}	19
R-11	Zr-2.5 wt % Nb, tube 411	L	23	0.7	3200	*2.0±15%		0.4
R-12	stress relieved 72 h at	L	16.5	0.6	2800	*0.7±10%		0.3
	300°C (material 2, Table I							
Rx-17	As above, tube 412	L	20	0.7	2100	1.0±40%		1.5
Rx-43		L	20	0.8	550	8.5±10%		3.0
Ru-15	Zircaloy-2 slab, as received	L	20	2.6	3600	*10.0±10%		0.4
Ru-14	(material 5, Table I)	S-T	20	2.5	1950	*8.0±20%	Test was at 316°C; estimated creep rate at 300°C = 6×10^{-7} h^{-1}	2.0
Ru-17		S-T	20	2.3	4300	*5.5±30%		0.6

[a] Test still in progress. Creep rate steady. L Longitudinal (axial). T Transverse. S-T Short transverse

Table 15c. IN-REACTOR CREEP TESTS ON ZIRCALOY-2
(From Reference 31)

Test No.	Material (code no., see Table)	Test conditions: Temperature °C	Stress ksi	Flux (E>1 MeV) n/cm²-sec	Loading strain %	Total test time hr	Properties at given test conditions: Duration hr	Total strain near end of test %	Creep rate near end of test hr⁻¹	Creep rate of laboratory control test after same total time as in-reactor test hr⁻¹
R-2	9	300	30.0	5.0	0.185	2000	2000	0.605	$1.6 \times 10^{-6} \pm 30\%$	$0.2 \times 10^{-6} \pm 30\%$
R-2	9	300	30.0	6.6	0.185	2100	300	0.765	$1.5 \times 10^{-6} \pm 10\%$	0.2×10^{-6}
R-4	18	300	20.0	5.9	0.220	260	260	0.275	$6 \times 10^{-7} \pm 30\%$	$6 \times 10^{-7} \pm 20\%$
R-4	18	300	20.0	0	0.250	880	620	0.305	$0.8 \times 10^{-7} \pm 30\%$	$0.9 \times 10^{-7} \pm 20\%$
R-4	18	300	20.0	5.8	0.310	1280	400	0.350	$3.5 \times 10^{-5} \pm 30\%$	$0.4 \times 10^{-7} \pm 40\%$
R-4	18	300	30.0	0	0.370	1900	620	0.450	$4.0 \times 10^{-7} \pm 20\%$	$4.0 \times 10^{-7} \pm 20\%$
R-4	18	300	30.0	3.6	0.460	3230	1330	0.620	$8.0 \times 10^{-7} \pm 10\%$	$2.0 \times 10^{-7} \pm 30\%$
R-4	18	300	30.0	0	0.585	5950	271	0.640	$0.4 \times 10^{-7} \pm 100\%$	$0.3 \times 10^{-7} \pm 100\%$
R-4	18	300	30.0	4.2	0.655	6920	970	0.715	$7.0 \times 10^{-7} \pm 20\%$	-
R-6	25	300	20.0	5.4	0.210	3600	3600	0.360	$3.5 \times 10^{-7} \pm 10\%$	$0.4 \times 10^{-7} \pm 20\%$
R-6	25	100	20.0	0	0.210	3850	250	0.363	$0.5 \times 10^{-7} \pm 10\%$	$0.4 \times 10^{-7} \pm 20\%$
R-6	25	100	20.0	6.0	0.210	5735	1885	0.405	$2\text{-}3.5 \times 10^{-7}$	$0.2 \times 10^{-7} \pm 50\%$
R-6	25	100	20.0	6.0	0.400	5783	48	0.405	-	-
R-6	25	350	20.0	6.0	0.400	5882	99	0.420	$1.3 \times 10^{-6} \pm 100\%$	$1.1 \times 10^{-6} \pm 10\%$
R-6	25	375	20.0	6.0	0.410	5930	48	0.455	$1.0 \times 10^{-5} \pm 10\%$	$6.4 \times 10^{-5} \pm 20\%$
R-6	25	390	20.0	6.0	0.450	5985	55	0.56	$2.0 \times 10^{-5} \pm 20\%$	$1.6 \times 10^{-5} \pm 10\%$
R-8	11	300	16.5	0	0.148	35,040	35,040	0.240	$5 \times 10^{-9} \pm 50\%$	-
R-8	11	300	15.7	6.0	0.228	35,440	400	0.255	$4 \times 10^{-7} \pm 50\%$	-
R-9	11	300	19.0	0	0.173	10,000	10,000	0.241	$3 \times 10^{-8} \pm 75\%$	-
R-9	11	300	11.0	6.1	0.105	12,140	2,140	0.117	$5 \times 10^{-8} \pm 60\%$	-
R-9	11	300	18.0	5.8	0.179	13,620	1,480	0.245	$3 \times 10^{-7} \pm 20\%$	-
Rx-14	25	30	20.0	7.3	0.205	650	650	0.280	$5 \times 10^{-7} \pm 20\%$	$1.4 \times 10^{-7} \pm 10\%$
Rx-14	25	300	20.0	6.4	0.205	2,000	1,150	0.310	$3 \times 10^{-7} \pm 30\%$	$0.8 \times 10^{-7} \pm 20\%$
Rx-14	25	320	20.0	6.8	0.310	2,270	270	0.327	$5 \times 10^{-7} \pm 20\%$	-
Rx-14	25	350	20.0	6.8	0.335	2,480	210	0.360	$1.4 \times 10^{-6} \pm 20\%$	(see test R-6 control)
Rx-14	25	375	20.0	6.8	0.367	2,573	33	0.403	$1.0 \times 10^{-5} \pm 10\%$	(see test R-6 control)
Rx-14	25	400	20.0	6.8	0.408	2,543	30	0.508	$2.7 \times 10^{-5} \pm 10\%$	
Rx-14	25	400	20.0	0	0.508	2,576	33	0.553	$1.3 \times 10^{-5} \pm 10\%$	
Rx-15	42	220	30.0	9.6	0.272	2,130	2,130	0.365	$1.5 \times 10^{-7} \pm 30\%$	$<1 \times 10^{-8}$
Rx-15	42	290	30.0	9.3	0.384	3,010	880	0.420	$5.0 \times 10^{-7} \pm 40\%$	$4 \times 10^{-8} \pm 30\%$
Rx-15	42	300	30.0	9.4	0.420	4,300	1,290	0.500	$8 \times 10^{-7} \pm 30\%$	$7 \times 10^{-8} \pm 30\%$
Rx-15	42	350	30.0	9.4	0.500	4,826	526	0.66	$3.2 \times 10^{-6} \pm 10\%$	$1.5 \times 10^{-6} \pm 10\%$
Rx-15	42	350	30.0	0	0.500	4,450	120	0.530	$1.4 \times 10^{-6} \pm 20\%$	-
Rx-15	42	375	30.0	0	0.70	4,880	54	0.76	$1.3 \times 10^{-5} \pm 10\%$	$8 \times 10^{-6} \pm 20\%$
Rx-15	42	300	30.0	9.4	0.76	4,948	68	0.77	-	-
Rx-15	42	375	30.0	9.4	0.82	4,977	29	0.87	$2 \times 10^{-5} \pm 10\%$	$8 \times 10^{-6} \pm 20\%$
Rx-15	42	400	30.0	9.4	0.90	4,985	8	0.95	$7 \times 10^{-5} \pm 10\%$	$2 \times 10^{-5} \pm 20\%$
Rx-20	18	350	45.0	11.6	0.58	8.4	4.4	2.37	$5.0 \times 10^{-3} \pm 10\%$	Failed on loading
Rx-20	18	350	30.0	11.6	2.13	382	280	2.58	$6.0 \times 10^{-6} \pm 10\%$	
Rx-21	25	300	45.0	0.6	0.43	305	305	0.67	$1.0 \times 10^{-5} \pm 20\%$	9×10^{-5}* (ruptured after approx. 200 h - mean of three tests)
Rx-21	25	300	45.0	8.4	0.86	1,085	780	1.56	$1.2 \times 10\text{-}5 \pm 10\%$	
Rx-21	25	300	45.0	0	0.86	660	100	1.18	$0.3 \times 10^{-5} \pm 10\%$	
Rx-21	25	170-180	45.0	8.4	0.86	1,250	160	1.55	$0.14 \times 10^{-5} \pm 30\%$	
Rx-21	25	300	45.0	8.4	1.52	1,590	290	1.93	$1.2 \times 10^{-5} \pm 10\%$	
Rx-21	25	300	40.0	8.4	1.92	1,655	65	1.95	$3.5 \times 10^{-6} \pm 50\%$	

Table 15d. IN-REACTOR CREEP OF Zr-2.5 WT% Nb ALLOYS (From Reference 31)

Test No.	Material Code No. (See Table)	Test Conditions: Temperature °C	Stress ksi	Flux E12 n/cm²-sec	Loading Strain %	Total Test Time hr	Properties at Given Test Conditions: Duration hr	Total Strain Near End of Test %	Creep Rate Near End of Test hr^{-1}	Creep Rate of Laboratory Control Test After Same Total Time as In-reactor Test hr^{-1}
R-7	27	300	30.0	6.2	0.240	835	835	0.293	1.0×10^{-7} ±30%	1.7×10^{-7}
R-7	27	300	30.0	6.2	0.275	2650	1210	0.301	0.8×10^{-7} ±30%	2.0×10^{-7}
R-11	34	300	23.0	7.0	0.254	3200	3200	0.355	2.0×10^{-7} ±15%	4.0×10^{-8}
R-12	34	300	16.5	5.6	0.102	2800	2800	0.157	7.0×10^{-8} ±10%	5.0×10^{-8}
Rx-13	36	300	23.0	5.7	0.226	2569	2569	0.420	2.0×10^{-7} ±15%	3.5×10^{-7}
Rx-13	36	350	23.0	5.7	0.424	2612	43	0.439	1.5×10^{-6} ±10%	7.0×10^{-6}
Rx-13	36	400	23.0	5.7	0.450	2629	17	0.520	4.3×10^{-5} ±10%	1.3×10^{-4}
Rx-16	37	300	23.0	5.7	0.288	295	295	-	-	-
Rx-16	37	300	36.5	5.7	0.375	1750	1455	0.478	1.5×10^{-7} ±30%	6.0×10^{-7}
Rx-16	37	350	45.0	5.7	0.558	2980	1230	0.628	2.0×10^{-7} ±30%	6.0×10^{-7}
Rx-16	37	320	45.0	5.7	0.628	3130	150	0.635	-	-
Rx-16	37	300	16.0	5.7	0.388	5540	2410	0.358	9.5×10^{-8} ±30%	7.0×10^{-8}
Rx-17	34	300	20.0	6.8	0.249	2125	2125	0.340	1.05×10^{-7} ±40%	1.5×10^{-7}
Rx-18	39	300	16.0	5.3	0.232	2100	2100	0.295	0.80×10^{-7} ±40%	0.9×10^{-7}
Rx-22	50	300	16.0	5.8	0.184	4900	4900	0.308	9.0×10^{-8} ±20%	1×10^{-8}
Rx-23	52	260	20.0	5.3	0.195	5300	5300	0.27	1.05×10^{-7} ±15%	2×10^{-8}
Rx-23	52	300	20.0	5.3	0.27	6250	950	0.30	4×10^{-7} ±20%	7×10^{-8}
Rx-23	52	350	20.0	5.3	0.31	6620	370	0.35	1.3×10^{-6} ±20%	1.4×10^{-6}
Rx-24	51	300	60.0	8.9	0.568	930	930	0.755	8.0×10^{-7} ±15%	2×10^{-6}
Ru-1	36	300	23.0	24	0.218	2560	2560	0.648	1.4×10^{-6} ±20%	1.3×10^{-7}
Ru-5	52	300	16.0	22	0.266	1120	1120	0.420	1.15×10^{-6} ±15%	7.0×10^{-8}
Ru-6	27	300	16.0	24	0.182	1400	1400	1.260	8.0×10^{-7} ±50%	0.5×10^{-7}
Ru-7	27	300	16.0	21	0.210	3140	3140	0.440	1.8×10^{-7} ±50%	$<0.5\times10^{-7}$

Table 16. IN-REACTOR CREEP TESTS OF ANNEALED ZIRCONIUM (From Reference 31)

Test Conditions									
Temp. (°C)	Stress	Flux, ($\times 10^{12}$ n/cm^2-sec)	Lagging Strain %	Total Strain %	Duration at any Given Condition hr	Accumulated Test Time hr	Creep Rate Near End of Test hr^{-1}	Creep Rate of Laboratory Test After Same Total Time as In-reactor Test hr^{-1}	Remarks
200	10.0	6.7	0.17	0.23	2100	2100	$5-10\times10^{-8}$	1.5×10^{-7}	Large scatter of test data beyond 1700 h. Machine removed from reactor for repairs and returned for test at higher stress and temperature on the same specimen
220	20.0	6.1	0.35	0.78	1500	3600	4.0×10^{-7}	3×10^{-7}	Suffered large temperature cycles in the early part of 220 °C test
220	20.0	0 (during shutdown)		0.77	100	3400	$4-5\times10^{-7}$		
260	20.0	6.1	0.80	0.98	300	3950	4×10^{-6}	6×10^{-5}	Creep rate steady
260	15.0	6.1	0.92	0.96	300	4250	1.6×10^{-6}	1.4×10^{-6}	Creep rate steady
260	15.0	(during shutdown)		0.93	150	4100	1.6×10^{-6}		
300	15.0	"	0.97	1.02	35	4275	2.2×10^{-5}		
300	15.0	6.1		1.14	25	4300	2.2×10^{-5}	--	
300	10.0	6.1	1.105	1.12	60	4360	2.7×10^{-6}	--	

Table 17a. FATIGUE CRACK PROPAGATION DATA FOR IRRADIATED AND UNIRRADIATED ZIRCALOY-2 TUBING AT 20°C
(From References 52, 53 & 54)

Ultimate Strengths @20°C = 110 ksi unirradiated
= 130 ksi irradiated

Material Condition	Fluence E20 n/cm^2	Failure Stress ksi	Critical Crack Length (2a) inches	R/t	$\frac{a}{\sqrt{Rt}}$	K_c ksi $\sqrt{in.}$
CW ~45% R.A.	-	38.0	1.0	10	0.98	67.7
	-	28.0	1.5	10	1.47	67.5
	-	18.0	2.0	10	1.97	56.4
	-	15.0	2.5	10	2.46	61.0
	~1-4	22.0	1.0	10	0.98	35.3
	~1-4	20.0	1.12	10	1.10	35.1
CW ~45% R.A., ~300 ppm H_2	-	20.0	1.0	10	0.98	36.6
	-	14.0	1.1	10	1.08	27.6
	-	12.0	1.2	10	1.18	30.1
	-	14.0	1.25	10	1.23	31.7
	-	15.0	1.3	10	1.28	35.6
	-	12.0	1.3	10	1.28	28.2
CW ~30% R.A.	-	30.0	1.5	5	1.17	59.1
	-	20.0	1.8	5	1.41	60.6
	-	19.0	2.25	5	1.76	72.5
CW ~30% R.A., ~300 ppm H_2	-	21.0	1.25	5	0.98	39.9
	-	19.0	1.12	5	0.88	31.8
	-	17.0	1.4	5	1.10	33.9
CW ~30% R.A.	9.5	27.0	0.97	5	0.76	39.9
	10.2	22.0	1.07	5	0.84	34.4
	12.0	38.0	0.6	5	0.47	43.3
	19.0	22.0	1.0	5	0.78	32.6

Table 17b. EFFECT OF IRRADIATION ON THE FRACTURE TOUGHNESS OF IRRADIATED ZIRCALOY-4 (From Reference 54)

Specimen No.	Description	Valid	Estimated Fluence E20 n/cm²	Measured Fluence E20 n/cm²	Test Temperature °C	K_{IC} secant ksi $\sqrt{in.}$	K_{IC} popin ksi $\sqrt{in.}$	K_{IC} max. ksi $\sqrt{in.}$
82-5044	FT-1 unhydrided	yes	5.6	7.7	20	--	45.9	45.9
-5046	α-annealed Zr-4	yes	5.6	7.95	80	43.0	--	55.0
-5048	Ingot R-59	no	5.3	7.66	315	21.8	--	41.6
-5050	TW orientation	no	5.3	7.51	204	31.2	--	48.6
-5052		yes	4.9	7.17	20	45.6	--	--
-5053		yes	4.9	7.07	-18	23.9(c)	--	23.9(c)
-5688		yes	5.1		-73	--	34.2	34.2
-5689		yes	5.1		0	--	28.5	42.0
-5045		yes	15.3		20	--	43.2	50.8
-5047		yes	15.3		93	53.5	--	61.0
-5042		yes	15.1		20	48.5	--	48.5
-5049		yes	15.1		20	--	51.6	51.6
82-5613	FT-2 hydrided to	yes	5.1		20	20.1	--	20.1
-5615	250 ppm	yes	5.1		80	33.4	--	33.4
-5758	α-annealed Zr-4	yes	9.6	10.35	20	23.0	--	23.0
-5765	Ingot WC377671Q	yes	9.6	9.6	-73	16.7	--	16.7
-5617	TW orientation	yes	13.5		20	22.0	--	22.0
-5620		yes	13.5		80	20.0(c)	--	20.0(c)
-5618		yes	20.8		150	31.4(d)	--	31.4
-5759		yes	20.8		150	--	--	--
-5763		yes	20.8		230	40.7	--	40.7
-5628		yes	20.8		230	41.2	--	43.0
-5764		yes	20.8		315	42.5	--	42.5
-5716		yes	20.8		315	45.4	--	45.4
82-5737	FT-3 hydrided to	yes	4.9		20	26.2	--	26.2
-5738	250 ppm	yes	4.9		80	26.0	--	26.0
-5767	α-annealed Zr-4	yes	9.2	9.4	80	27.8	--	27.8
-5746	Ingot WC377671Q	yes	9.2	10.0	20	25.0	--	25.0
-5739	WT orientation	yes	12.8		20	26.9	--	26.9
-5740		yes	12.8		150	65.0	--	65.0
-5744		yes	20.5		20	24.6	--	24.6
-5745		no(e)	20.5		230	43.6	--	47.4
82-5602	FT-4 unhydrided	yes	2.4		20	38.2	(b)	(b)
-5606	α-annealed Zr-4	yes	2.4		-18	(b)	41.5	(b)
-5611	Ingot WC377671Q	yes	5.0		-18	--	40.3	40.3
-5614	TW orientation	yes	5.0		20	42.1	(b)	(b)
-5761		yes	9.8	9.6	80	46.2	--	59.2
-5760		yes	9.8	10.13	-73	27.4	--	27.4
-5612		yes	9.8		-73	(b)	35.7	(b)
-5619		yes	9.8		20	--	40.8	46.5
-5754		yes	18.9		-73	--	32.8	32.8
-5755		yes	18.9		-73	(b)	38.7	--
-5753		yes	19.0		-18	--	32.5	32.5
-5756		yes	19.0		-18	52.0(c)	--	72.5(c)
-5751		yes	19.1		20	52.4	(b)	(b)
-5752		yes	19.1		20	54.5	--	54.5
-5749		yes	19.0		93	55.2	(b)	(b)
-5750		yes	19.0		93	54.6	--	63.5
-5747		no	19.0		93	46.8	--	59.0
-5748		(a)	19.0		93 (a)	--	--	58.5
82-5741	FT-5 unhydrided	yes	9.8		20	--	37.4	52.8
-5743	α-annealed Zr-4 Ingot WC377671Q WT orientation	yes	9.8		80	48.0	--	55.8
82-5773	FT-6 unhydrided	yes	5.2		-78	--	32.0	34.6
-5776	α-annealed Zr-4 Ingot WC377671Q RT orientation	yes	5.2		80	49.9	--	49.9
82-5772	FT-7 unhydrided	yes	10.2	10.35	20	--	39.9	39.9
-5782	β-quenched Zr-4 Ingot WC377671Q WT orientation	yes	10.2	10.9	80	55.6	--	58.3
82-5777	FT-8 hydrided to	yes	10.1	10.35	20	25.2	--	25.2
-5779	250 ppm	yes	10.1	10.75	80	25.6	--	25.6
-5780	β-quenched Zr-4	yes	20.4		20	24.6	--	24.6
-5781	Ingot WC377671Q WT orientation	no(e)	20.4		260	47.7	--	47.7

(a) Validity impossible to determine due to strain gage failure.
(b) Specimens unloaded rapidly after $K_{IC\ secant}$ or $K_{IC\ popin}$ for sectioning to allow for plastic zone size determination.
(c) Validity highly questionable due to excessively long fatigue crack.
(d) Specimen improperly loaded.
(e) Thickness required for ASTM valid test ~0.6 in.

Table 18. MILLED SLOT FRACTURE DATA FOR IRRADIATED AND UNIRRADIATED 17% - 23% COLD WORKED ZIRCALOY-2 TUBING
(From Reference 52, 55)

Test Temperature °C	Fluence n/cm^2	Failure Stress ksi	Critical Crack Length 2a - in.	R/t	$\frac{a}{\sqrt{RT}}$	K_c (1) ksi $\sqrt{in.}$
300	1.2×10^{21}	17.6	3	10	2.78	62.1
20	1.2×10^{21}	28.6	2	10	1.85	106.8
20	8.0×10^{20}	16.3	4	10	3.70	156.9
20	1.2×10^{21}	17.2	3	10	2.78	110.4
300	1.0×10^{21}	24.0	2.5	10	2.32	120.1
20	8.0×10^{20}	21.3	2.5	10	2.32	106.6
300	8.0×10^{20}	34.2	2	10	1.85	127.7
300	0	24.8	2	10	1.85	92.6
20	0	34.4	2	10	1.85	128.4
300	0	19.0	3	10	2.78	121.9
20	0	20.4	3	10	2.78	130.9
300	0	21.1	2.5	10	2.32	105.6
20	0	23.0	2.5	10	2.32	115.1
300	0	18.7	3	10	2.78	120.0
300	7.0×10^{20}	16.0	3.5	11	3.24	127.4
300	2.0×10^{20}	16.8	3	11	2.78	107.8
300	Out of flux	15.0	3	11	2.78	96.3
300	2.6×10^{20}	44.0	1.5	11	1.39	115.7
300	2.6×10^{20}	21.9	3	11	2.78	140.5
300	2.6×10^{20}	38.6	1.5	11	1.39	101.5
300	2.6×10^{20}	18.0	3	11	2.78	115.5
300	Out of flux	39.2	1.5	11	1.39	103.1
300	Out of flux	16.2	3	11	2.78	104.0
300	1.6×10^{20}	25.2	2.25	14	1.98	69.1

(1) Value uncorrected for plasticity effects where:

$$C_p = \cos \sigma_2 \left(\frac{\sigma_{flawed}}{\sigma_{unflawed}} \right).$$

Table 19. MILLED SLOT FRACTURE DATA FOR IRRADIATED AND UNIRRADIATED 30% COLD WORKED ZIRCALOY-2 TUBING (From Reference 52, 54)

Sample	Fluence n/cm^2	Slot Length in.	$\frac{a}{\sqrt{Rt}}$	Ultimate Hoop Stress - ksi	K_c ksi $\sqrt{in.}$
1756-1	0	0.81	6.64	83.5	103.3
1756-2	0	3.00	2.36	30.8	98.7
1756-3	0.82×10^{21}	0.81	0.64	81.7	105.9
1756-4	0.82×10^{21}	3.00	2.36	28.6	91.6
1756-5	0	0.81	0.64	83.5	108.1
1756-6	0	3.00	2.36	29.7	95.1
2455-1	0.82×10^{21}	0.35	0.27	135.0	106.7
2455-2	1.10×10^{21}	3.00	2.36	35.7	114.4
2455-3	1.11×10^{21}	0.81	0.64	86.0	111.4
2455-4	1.01×10^{21}	1.50	1.18	65.0	125.8
0758-1	1.75×10^{21}	1.50	1.18	45.0	87.1

Table 20. EFFECT OF IRRADIATION ON THE FATIGUE CRACK PROPAGATION RATE OF ZIRCALOY-4
(From Reference 56)

Specimen No.	Specimen Description	Fluence E20 n/cm^2	Test Temperature °F	K ave ksi$\sqrt{in.}$	$\Delta a/\Delta n$ μin./cycle
82-5052	FT-1 unhydrided	7.1	RT	20.8	12.0
-5053	α-annealed, R-59	7.0	RT	22.0	13.0
-5047	TW orientation	15.3	RT	16.4	23.0
82-5758	FT-2 hydrided	10.3	RT	13.0	6.2
-5765	α-annealed, 71Q	9.5	RT	15.1	8.7
-5613	TW orientation	5.1	RT	17.1	16.7
-5617		13.5	RT	14.7	8.3
-5620		13.5	RT	17.5	16.7
-5628		20.8	RT	15.1	83.0
-5716		20.8	RT	20.9	78.0
-5759		20.8	RT	13.0	11.0
82-5767	FT-3 hydrided	9.2	RT	10.7	none
-5737	α-annealed, 71Q, WT	4.9	RT	13.3	12.5
82-5611	FT-4 unhydrided	5.0	RT	17.4	5.0
-5619	α-annealed	9.8	RT	18.4	38.3
-5761	Zr-4, 71Q, TW	9.8	RT	17.1	60.0
-5754		18.9	RT	13.6	none
-5753		19.0	RT	13.4	none
82-5741	FT-5 unhydrided	9.8	RT	11.6	none
-5743	α-annealed, 71Q, WT	9.8	RT	14.4	none
82-5772	FT-7 unhydrided β-quenched, 71Q, TW	10.2	RT	15.5	5.3
82-5779	FT-8 hydrided β-quenched, 71Q,TW	10.1	RT	18.0	13.6

Table 21. FATIGUE CRACK GROWTH AND PROPAGATION DATA FOR UNIRRADIATED Zr-2.5 WT% Nb ALLOY TUBING AT 20°C (From Reference 57)

Material Condition	Nominal Peak Hoop Stress ksi	$\Delta\sigma$ ksi	Critical Crack Length 2a - in.	Cycles to Initiate Cracking	Cycles to Leak	Leak Crack Length in.	Cycles to Failure	Cycle Rate per sec	R/t	$\frac{a}{\sqrt{Rt}}$	K_c ksi$\sqrt{in.}$
Heat Treated	23.0	21.5	1.37	~5,000	9,695	0.43	10,628	400	7	1.60	35.8
+ 15% CW											
+ Aged											
	23.0	21.5	1.31	~10,000	17,400	0.42	24,960	400	7	1.53	35.7
	23.0	21.5	1.08	~15,000	28,400	0.41	35,554	400	7	1.26	31.9
	23.0	21.5	0.95	~22,000	80,550	0.41	47,199	400	7	1.11	29.6
	23.0	21.5	1.05	~94,000	114,900	0.38	121,550	80	6	1.16	31.2
	20.0	19.5	2.05	---	~14,600	0.32 (EDM slot to ID surface)	31,131	400	7	2.40	41.4
	26.5	26.0	0.95	~2,000	~3,760	0.38	9,550	400	6	1.11	33.2
	27.0	26.5	1.5	---	---	---	1,550	400	7	1.76	38.6
	28.0	26.5	1.25	---	2,250	0.33	10,000	400	6	1.38	42.5
	27.0	25.5	1.21	~6,600	10,600	0.47	15,520	400	7	1.42	40.3
	25.0	23.5	1.05	~4,700	5,000	0.43	13,420	400	7	1.23	34.2
	25.5	24.0	0.97	~4,000	6,250	0.38	24,300	400	7	1.08	32.4
	34.0	32.5	0.85	90,000	179,000	0.46	Static Failure		7	1.00	42.4
30% CW	56.0	22.0	0.60/0.41	---	---	---	Static Failure	400	7	0.80/0.50	72.6/57.1
30% CW Irradiated	31.0	30.0	1/2	---	1,350	---	1,428	400	7	0.59	29.0
	19.0	18.0	1-1/2	---	1,543	---	2,468	400	7	1.76	31.9
Heat Treated + 15% CW + Aged and Hydrided	15.0	15.0	0.25		(Failed in first few cycles)			3,000	7	0.29	9.5
	14.0	12.5	0.46	~13,000	73,000	---	25,830	3,000	7	0.54	12.0
	12.5	11.0	1.61	~635,000	---	---	665,040	3,000	10	1.49	21.0
	11.5	11.0	1.68	~50,000	170,000 (Estimated)	---	176,000	10,000	10	1.55	19.9
Heat Treated + Aged + Hydrided	17.4	16.0	1.2	~15,000	50,100	---	79,120	400	7	1.41	25.4
	20.0	19.5	0.76	~10,000	18,500	---	49,680	400	7	0.99	27.7
	26.0	23.5	0.42	~3,700	6,470	---	6,522	400	7	0.49	21.9
30% CW and Hydrided	17.0	14.5	3.05	~40,000	53,050	---	---	400	7	3.57	48.3
30% CW and Hydrided	21.0	17.5	2.6	~40,000	57,900	---	67,000	400	7	3.04	52.4
30% CW and Hydrided	21.0	20.0	---	~15,000	23,300	---	---	400	7	---	---
30% CW + Hydrided and Irradiated	15.0	14.5	0.5*	384	---	---	10,101	400	7	0.59	13.5
	12.0	11.5	1.5*	---	---	---	5	400	7	1.76	19.9
Heat Treated + 15% CW + Hydrided	25	24	0.83	---	---	---	---	1,000	20	0.93	30.0
	30	285	0.38	---	---	---	---	1,000	20	0.42	24.2

Table 22. MILLED SLOT FRACTURE DATA FOR IRRADIATED AND UNIRRADIATED Zr-Nb PRESSURE TUBES (From Reference 5, 57)

Ultimate Strengths - 20°C = 122 ksi, 300°C = 80 ksi unirradiated
20°C = 152 ksi, 300°C = 110 ksi irradiated

Material Condition	Fluence E20 n/cm^2	Test Temp.	Failure Stress ksi	Critical Crack Length(2a) inches	R/t	$\frac{a}{\sqrt{Rt}}$	K_c ksi $\sqrt{in.}$
CW ~20% R.A., 25 ppm H_2	-	20°C	54	2.0	21	2.27	181.0
	-	20°C	37	2.5	21	2.84	164.4
	-	20°C	30.5	3.0	21	3.41	172.7
	-	300°C	18.5	2.5	21	2.84	82.2
	-	300°C	17.0	3.0	21	3.41	96.3
	-	300°C	34	2.0	21	2.27	114.0
	-	300°C	26	2.75	21	3.12	131.0
	-	300°C	21	3.25	21	3.69	132.6
CW ~20% R.A., 300 ppm H_2	-	20°C	31	2.0	21	2.27	103.9
	-	300°C	31	2.0	21	2.27	103.9
CW ~20% R.A., 25 ppm H_2	~1.5-8	300°C	27	2.0	21	2.27	90.5
	~1.5-8	300°C	26	2.5	21	2.84	115.5
	~1.5-8	300°C	26	3.0	21	3.41	147.3
	~1.5-8	300°C	19	4.0	21	4.54	151.8
	-	300°C	25.0	3.0	21	3.41	141.7
	-	300°C	24.0	3.0	21	3.41	136.0
	-	300°C	23.0	3.0	21	3.41	130.0
CW ~30% R.A., 50 ppm H_2	~1.5-8	20°C	40.0	2.0	11	1.96	121.5
	~1.5-8	300°C	20.0	3.0	11	2.95	100.5
	-	300°C	27.0	3.25	11	3.20	85.1
	~1.5-8	20°C	39.0	2.0	11	1.96	118.5
	~1.5-8	300°C	22.0	3.5	11	3.45	76.6

Table 23. POSTIRRADIATION BURST TESTS OF ZIRCALOY-2 PRTR PRESSURE TUBES (From Reference 63)

Tube	Specimen	Microstructure	Test Temperature °C	Fluence, nvt	Hoop Strength, ksi	Hoop Elongation, %	Remarks
6103	1 B	Annealed	20	$1.6 - 3.3 \times 10^{16}$	86.2	9	No apparent cause for low strength.
	1 C	Annealed	20	$1.25 - 1.35 \times 10^{19}$	86.7	0	Burst started at 0.002 in. deep crack in 0.002 in. deep hydride layer over a fret mark.
6061	2 C	Annealed	20	$5.2 \times 10^{17} - 1.1 \times 10^{18}$	106.2	20	-
	2 D	Annealed	300	$4.7 - 5.4 \times 10^{19}$	58.2	Not Measured	-
5529	3 2	Annealed	20	$6.8 \times 10^{17} - 1.35 \times 10^{18}$	97.0	17	-
	3 3	Annealed	20	$3.6 - 6.3 \times 10^{19}$	111.0	15	-
5679	4 B	Annealed	288	$1.3 - 2.4 \times 10^{18}$	47.2	36	-
	4 C	Annealed	282	$3.8 - 7 \times 10^{19}$	61.2	48	-
	4 F	Cold Worked	296	$6.2 \times 10^{19} - 1.2 \times 10^{20}$	70.5	Not Measured	-
5702	5 B	Annealed	20	$3.3 - 6.2 \times 10^{18}$	107.0	Not Measured	Test Specimen continued 0.009 - 0.011 in. deep fret marks which had no apparent effect on burst.
	5 C	Annealed	96	$1.35 - 1.8 \times 10^{20}$	111.0	Not Measured	-
	5 E	Cold Worked	20	$2.1 - 2.25 \times 10^{20}$	130.0	3.3	Burst started at 0.017 in. deep fret mark.
	5 G	Cold Worked	290	$6.8 \times 10^{18} - 1.7 \times 10^{19}$	74.0	Not Measured	-
5540	6 B	Annealed	295	$1.4 - 2.8 \times 10^{19}$	56.9	Not Measured	Test was stopped before burst.
	6 C	Annealed	277	$2.9 - 3.2 \times 10^{20}$	78.1	16	"Pinhole" failure.
	6 E	Cold Worked	20	$1.3 - 2.2 \times 10^{20}$	129.0	0	Burst started at 0.014 in. deep fret mark.
	6 C	Second Test	20	$2.9 - 3.2 \times 10^{20}$	125.8	0	Elongation of zero probably due to first burst test.
	6 D	Undetermined	288	4.2×10^{20}	78.4	20	"Pinhole" failure.
0720	8 B	Annealed	97	1×10^{16}	75.0	Not Measured	-
	8 C	Annealed	210	$3.2 - 6.2 \times 10^{17}$	58.0	Not Measured	-
	8 F	Cold Worked	210	$1.2 - 1.7 \times 10^{18}$	84.5	Not Measured	-
5683	9 B	Annealed	20	$3.5 - 6.5 \times 10^{18}$	104.8	7.5	-
	9 H	Cold Worked	20	$1.6 - 2.6 \times 10^{20}$	134.2	7	-
5682	10 C	Annealed	20	$2.7 - 3.5 \times 10^{20}$	129.0	15	-
	10 G	Cold Worked	20	$3.2 - 4.1 \times 10^{20}$	134.8	9	-
6115	11 C	Annealed	20	$1.45 - 2.0 \times 10^{20}$	97.5*	Less than 0.2%	*Based on average ID and wall; no allowance for stress concentration. Burst started by 0.016 - 0.020 in. deep mark at the onset of uniform plastic strain.
6079	12 A	Annealed	20	1.9×10^{19}	112.8	12	
	12 E	Cold Worked	20	3.3×10^{20}	123.7	7	
6084	14 D	Undertermined	20	1.8×10^{21}	142.6	6	

Table 24. IRRADIATION GROWTH MEASUREMENTS ON ZIRCALOY-2
(From Reference 64)

Irradiation Temperature	Fluence n/cm^2	Measured Differential Growth Strain	Growth Coefficient: Instantaneous $G_{t_2-t_1}$	Growth Coefficient: Average $G_{t_2-t_1}$	Number of Specimens	Reactor
-195°C	4.9×10^{18}	$1.2 \pm 0.2\times10^{-4}$	8.0 ±1.0	18.0 ±4.0	3	Herald
	9.7	1.5 0.3	5.0 1.0	11.6 2.3	4	
	1.9×10^{19}	2.3 0.3	3.5 0.5	9.5 1.1	3	
	5.0	3.5 0.5	2.0 0.3	5.2 0.7	3	
	9.8	3.0 0.1	1.5 0.2	2.3 0.1	4	
40°C	8.2×10^{18}	2.1 0.2	8.0 1.0	19.0 1.0	7	
	2.9×10^{19}	4.0 0.2	3.6 0.3	10.2 0.4	7	
	1.0×10^{20}	5.6 0.4	1.7 0.2	4.0 0.3	7	
80°C	1.3×10^{20}	3.1 0.4	0.6 0.1	1.7 0.2	4	Pluto
	5.4	4.7 0.4	0.30 0.03	0.7 0.1	7	
	7.7	6.3 1.0	0.20 0.02	0.6 0.1	4	
280°C	2.2×10^{17}		9		1	Herald
	1.0×10^{18}		5		1	
	1.0×10^{19}		3		1	
	3.0		1.5		1	